ENDOLYN SORTING AND FUNCTION DURING KIDNEY DEVELOPMENT

by

Di Mo

BS in biology, Zhejiang University, 2007

Submitted to the Graduate Faculty of

School of Medicine in partial fulfillment

of the requirements for the degree of

Doctor of Philosophy

University of Pittsburgh

2012

UNIVERSITY OF PITTSBURGH

SCHOOL OF MEDICINE

This dissertation was presented

by

Di Mo

It was defended on

April 17, 2012

and approved by

Gerard Apodaca, PhD, Department of Cell Biology and Physiology

Jeffrey Hildebrand, PhD, Department of Biological Sciences

Rebecca Hughey, PhD, Department of Cell Biology and Physiology

Neil Hukriede, PhD, Department of Developmental Biology

Dissertation Advisor: Ora Weisz, PhD, Department of Cell Biology and Physiology

ENDOLYN SORTING AND FUNCTION DURING KIDNEY DEVELOPMENT

Di Mo

University of Pittsburgh, 2012

The polarity of epithelial cells is critical for proper function. Maintenance of polarity requires sustained proper sorting of proteins and lipids to either apical or basolateral membranes using distinct sorting signals. Compared to basolateral sorting signals, apical signals are not well characterized and can be present within the lumenal, transmembrane, or cytosolic regions of the protein. N-glycosylation has been identified as one of the apical sorting signals. The sialomucin endolyn (CD164) is a transmembrane protein that contains an apical sorting signal (N-glycans) in the lumenal domain and a lysosomal/basolateral targeting signal (YXXØ motif) in its cytoplasmic tail. It cycles between the apical surface and lysosomes of renal epithelial cells and is expressed in embryonic and adult kidney. The first objective of this research was to dissect the specific determinant on N-glycosylation for endolyn apical sorting using a lipofectamine-mediated RNAi approach. The results demonstrated that sialylation but not branching of N-glycans is required for endolyn proper delivery. Futher, knockdown of galectin-9 (but not galectins 3, 4 or 8) selectively disrupted endolyn polarity suggesting that interaction between endolyn and galectin-9 is critical for endolyn apical delivery. Next, the function of endolyn in pronephric kidney was investigated during development using zebrafish as a model system. Knockdown of zebrafish endolyn using a translational inhibiting morpholino resulted in pericardial edema, hydrocephaly, and body curvature, suggesting a possible osmoregulation defect. Although the pronephric kidney appeared normal morphologically, clearance of fluorescent dextran was delayed, indicating an imbalance in water regulation in morphant embryos. Rescue experiments using rat endolyn mRNA revealed that both apical sorting and endocytic/lysosomal targeting are required for endolyn function during development of the zebrafish pronephric kidney. This work broadens our understanding of apical sorting mechanisms in polarized cells as well as its significance on kidney function and development.

TABLE OF CONTENTS

LIST OF TABLES

LIST OF FIGURES

PREFACE

It has been an amazying journey for the last five years…

I would like to thank…

my mentor, Dr. Ora Weisz. She has been a great advisor for my graduate training.

all my "team lab" past and present members, especially Jennifer Bruns, Simone Costa, Dr. Anatalia Labilloy, Dr. Polly Mattila, Christina Szalinski, Venkatesan Raghavan, Youssef Rbaibi, Dr. Robert Youker, Dr. Beth Potter. GO TEAM LAB!

my dissertation committee, Dr. Gerard Apodaca, Dr. Jeffrey Hildebrand, Dr. Neil Hukriede, Dr. Rebecca Hughey, for their help and suggestions throughout my entire training.

all those who helped me along the way including Dr. Eric de Groh, Dr. Lisa Antoszewski, Dr. Chiara Cianciolo Cosentino, Dr.Gudrun Ihrke, Lauren Brilli.

my parents and my husband, for their unconditional love and support.

1.0 INTRODUCTION

1.1 PHYSIOLOGICAL STRUCTURE AND FUNCTION OF KIDNEY

1.1.1 The anatomy of kidney

The kidneys in humans are bean-shaped organs located just below the rib cage with one on each side of the body [1]. The size of each kidney is similar to that of a fist. The kidneys are complex organs that filter approximately 200 liters of blood daily [2]. The waste and excess water processed by kidneys are delivered to the urinary bladder to become urine. The kidney contains two distinctive regions: the medulla, a discontinous layer shaped like a pyramid, and the cortex, a continous layer surrouding the medulla and extending to the outer portion of the kidney [3] (Fig.1D).

1.1.2 The nephron

The nephron is the basic structural and functional unit of the kidney. Each nephron is composed of a glomerulus and a renal tubule. In humans, the glomerulus is surrounded by Bowman's capsule and consists of endothelial cells, glomerular basement membrane and podocytes. The renal tubule comprises the proximal tubule, the loop of Henle and the distal tubule [1]. The glomerulus receives its blood supply from an afferent arteriole through the fenestrated

endothelium. The filtration takes place at the glomerular basement membrane and slit-diaphragm [4]. The blood pressure within the glomerulus serves as the driving force for filtration of water and solutes from the blood and into Bowman's capsule [5]. This filtration is based on molecular weight, size, shape and electrical charge of the molecule such that large and negatively charged macromolecules are retained and those small and positively charged pass through into the filtrate [5]. The filtrate then enters the renal tubule, where most of the water and some electrolytes are reabsorbed. Following refinement, the filtrate continues to the collecting duct system, where most wastes are concentrated for excretion in the urine [3]. The number of nephrons in a fully functional kidney varies between vertebrates based on their requriments for kidney function [2]. For example, an adult human kidney consists of approximately 800,000-1.2 million nephrons, as compared to the mouse kidney, which contains ~11,000 nephrons [3,6] . The kidneys of some amphibians and fish contain only a few nephrons [7].

1.2 VERTEBRATE KIDNEY DEVELOPMENT

Three stages are involved in vertebrate kidney development: the pronephros, the mesonephros and the metanephros as shown in Fig.1 [6,8]. In the following sections, the processes of kidney development are discussed in details.

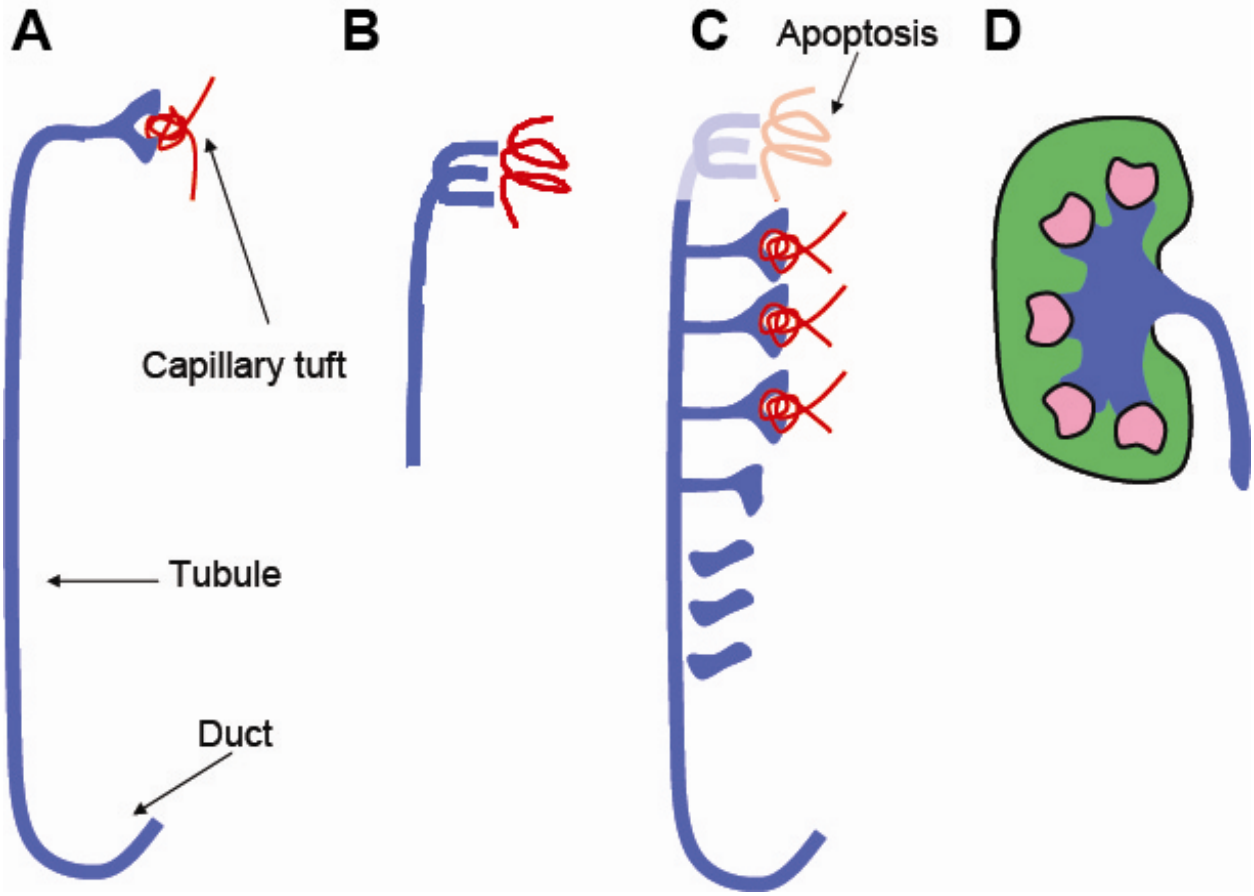

Figure 1. Stages of kidney development

Three stages of kidney development arising from the intermediate mesoderm which are the pronephros (A and B), the mesonephros (C) and the metonephros (D) are shown. An active pronephros is shown in A while an inactive pronephros is shown in B. Adapted from [6,8].

1.2.1 The pronephros

The pronephros is derived from the intermediate mesoderm, a layer between the paraxial and lateral-plate mesoderm within the embryonic trunk [9]. The function and composition of the pronephros varies depending on the requirements for this early kidney during development and the surrounding environment [9]. For example, the pronephros is a fully functional kidney for

some vertebrate larvae living in fresh water. These require a complex renal system to constantly remove excess water and reabsorb ions [2]. Remarkably, these active and simple pronephros contains typical cell types and tubule segmentations in *Xenopus* or zebrafish larvae, which make them an ideal model system to study kidney function and developmental events [9,10]. The program of morphogenesis and epithelialization of pronephros is highly conserved in all vertebrates and occurs in four common steps [11]. In the case of zebrafish, (i) the intermediate mesoderm differentiates mesenchymal cells to enter the nephric fate around 12 hours post fertilization (hpf); (ii) a mesenchymal-to-epithelial transition is mediated by further signals to form the pronephric duct by 24 hpf; (iii) additional differentiation and patterning of the nephron primordia takes place to form the glomerulus and renal tubules between 30 hpf and 40 phf; (iv) a functional glomerulus is formed when the capillary loop finishes its fusion with the glomerular capsule by 48 hpf. In vertebrates like mammals and birds, the pronephros is rudimentary. Cells in the pronephros undergo apoptosis soon after forming; and, this process sets the stage for the formation of the mesonephros and metanephros as confirmed by a detailed study which documented the involvement of apopltosis in the regression of rat pronephric kidneys [12].

1.2.2 The mesonephros

Mesonephros, the second stage of kidney development, functions as an active temporary kidney for vertebrates such as birds and mammals. However, little is known about its function and significance because of its transient existence [6]. The development of the mesonephros initiates with the formation of renal vesicles from the condensations of nephrogenic cord cells which come from the mesenchymal tissue surrounding the nephric duct or tubule. The nephrogenic cord cells undergo a mesenchymal-to-epithelial transition followed by the elongation of the renal

vesicles into the S-shaped body, before transitioning into the mesonephros [13,14]. The timing of mesonephros development varies among species. For example, in mice, the degeneration of the mesonephroes begins at E14.5 and most tubules disappear secondary to apoptosis within 24 hours [15]. In humans, the degeneration of tubules starts at about the fifth week and completes by the fourth month [3]. Interestingly, the degree of degeneration is sex-dependent. Most tubules regress in female mice while some posterior tubules remain in male mice, ultimately contributing to the epididymal ducts of the testis in male mice [6]. The similar sex-dependent differentiation is also observed in humans [3].

Conversely, the mesonephros functions as the terminal adult kidney in vertebrates like fish and amphibians. The formation of this mesonephros is similar to that of mammals and birds. However, the number of nephrons is much greater because a terminal adult kidney requires more complex composition for proper function. For example, the adult zebrafish mesonephros contains approximately 200 nephrons. The number of nephrons is dependent on age and body mass [16]. Typically, pronephros degeneration of the pronephros is followed by the formation of mesonephros. However, in some fish, the pronephros becomes integrated into the mesonephros, forming the head kidney, also known as the lymphoid organ [17].

1.2.3 The metanephros

The third stage of kidney development, formation of the metanephros, is the most complex. This stage is the terminal form of the kidney for mammals, birds, and reptiles. Experimental results have clarified how kidney development progresses [18]. The process begins with a blastoma of metanephric mesenchyme cells, usually a few thousand, established in the caudal region of each intermediate mesoderm. The ureteric bud is subsequently induced to branch off from the

posterior nephric duct and invades to the metanephric mesenchyme through reciprocal interactions [19]. Constant signal transduction triggers the bud to divide to form the collecting ducts of the metanephros. In the meantime, small condensations of the metanephric mesenchyme are formed by the duct tips and these condensations rapidly epithelialize to form renal vesicles [19]. The primitive nephrons proceed through the comma- and S-shaped body stages. The existing nephrons start to spread to the medulla to develop the loop of Henle, while neonephrogenesis continues at the duct tips [20]. In mice, the population of nephrons becomes stable approximately two weeks after their birth [6]. In humans, stable and functional kidney formation is completed approximately six weeks before birth [3]. Several key factors have been revealed to mediate kidney morphogenesis. For example, *Wnt (Wilms' tumor suppressor)* gene family is involved in tubule formation [21]. *Paired-box transcription factor* (*Pax)-2* and *Lhx-1* are involved in initiation of kidney morphogesis and early patterning of the kidney [22,23].

As the metanephros becomes functional, the mesonephros begins to degenerate through an apoptotic mechanism [12]. Most portions of the mesonephros degenerate while some portions are incorporated into the reproductive tract [6]. The formation of the adrenal glands and gonads is partially from the migration of mesonephric cells to the neighboring primordium [6]. At this point, a fully developed metanephros functions and neonephrogenesis ceases. The number of nephrons remains unchanged as the metonephros matures and the nephrons change in cell density and size to respond to any future damage [24].

1.3 POLARIZED EPITHELIAL CELLS

Polarized epithelial cells line the surface of several internal organs including kidney as shown in Fig.2. The asymmetrical distribution of cellular components defines their polarity [25,26,27]. The plasma membrane of the poliarized cells is delineated by tight junctions into two asymmetric compartments: an apical domain and a basolateral domain [25]. The apical domain of kidney tubules faces towards the lumen of organs and is enriched in a layer of glycocalyx which provides protection from the environment [25]. Microvilli, small membrane protrusion that expands the cell surface, are commonly observed on the apical domain of absorptive polarized epithelial cells [28]. In addition, the presence of a primary cilium is a distinguishing feature of the apical domain [29]. Conversely, the basolateral domain composed of basal and lateral membranes, connects with neighboring cells and provides contact with the blood supply [25]. This apical-basolateral polarity is conserved in both simple epithelia, such as cells in the kidney and intestine, and stratified epithelia, including the epidermis [28]. This polarity ensures that epithelial cells serve as a barrier against pathogens. Additionally, they regulate ions and metabolites, allowing fluid to flow within or between the external and internal surroundings [28].

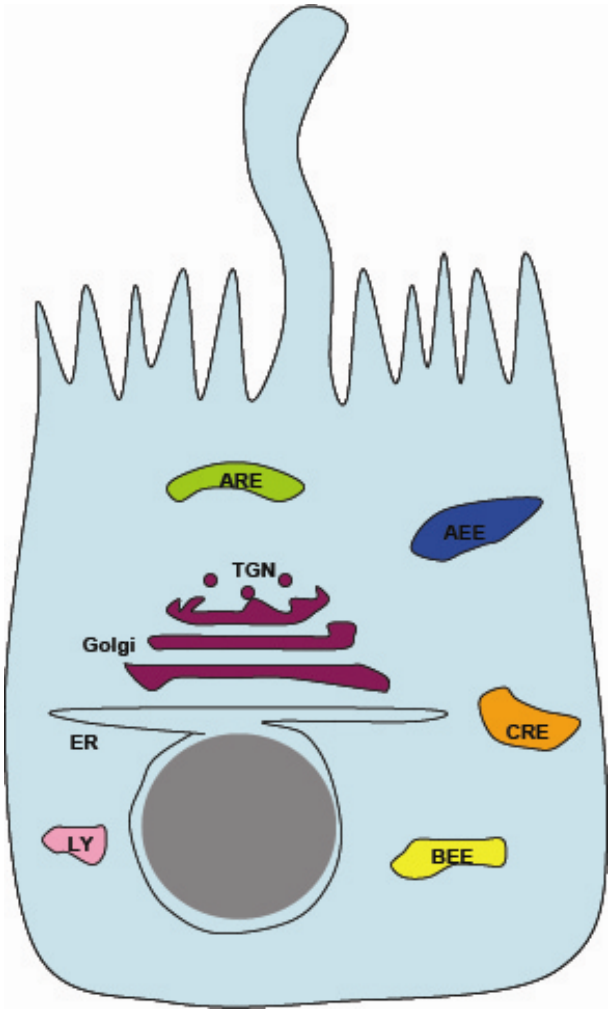

Figure 2. Polarized epithelial cells

The plasma membrane of polarized cells is devided into two domains: the apical domain and the basolateral domain. The major organelles are indicated in the diagram. ARE: apical recycling endosome; AEE: apical early endosome; CRE; common recycling endosome; BEE: basolateral early endosome; LY: lysosome; ER: endoplasmic reticulum; TGN: *trans*-Golgi network. Adapted from [30].

Cell epithelization is regulated during development by cell adhesion complexes and epithelial cell polarity complexes [31]. The formation and maintenance of the apical-basolateral polarity depends on two major cell adhesion complexes, termed adherens junctions and tight

junctions [32,33]. The major components of the adherens junctions are complexes of the cadherin-catenin and the nectin-afadin [34]. The interaction between cadherins and catenins connects cells to each other and also binds to the actin cytoskeleton [34]. The tight junctions are multiprotein complexes that form a contiguous structure around the cell, and distribute apically to adherens juctions in polarized cells [35]. Further, tight junctions present a physical barrier to restrict the diffusion of apical and basolateral proteins and lipids. The junctions also function as a dynamic gate for the space between neighboring cells to regulate ions and water transport [36]. The core of tight junctions consists of transmembrane proteins, such as occludin, claudin, tricellulin and junctional adhesion molecule, and cytosolic scaffolding proteins, such as ZO1-3, multi-PDZ domain protein 1 and cingulin [36].

Studies from yeast, worms, and flies have revealed three major protein complexes that regulate the establishment of polarity [33]. These complexes include the PAR complex, (PAR3/aPKC/PAR6/CDC42), the CRUMBS complex (Crumbs3/PALS1/PATJ), and the SCRIB complex (Scrib/mDIg/mLgl) [33]. The PAR complex mediates the formation of the apical-basolateral border. The CRUMBS complex regulates the development of the apical membrane, and the SCRIB complex defines the basolateral domain [37]. The establishment of polarity initiates from the cell-cell contact through the basal surface [38]. The interaction between PAR3 and afadin recruits E-cadherin and junctional adhesion molecule A to the primordial adhesions where adherens junction and tight junction associated proteins are both localized [39,40]. This is followed by the separation of the adherens junction and tight junction proteins along the basolateral domain [41]. The maturation of the belt-like adhesion junctions and tight junctions is mediated by the exclusion of PAR3 from the PAR and CRUMBS complexes [42]. This defines the apical-lateral boundary, thus marking the establishment of the apical domain. Meanwhile, the

SCRIB complex antagonizes the PAR and CRUMBS complexes to promote the basolateral domain identity by inhibiting the expansion of the apical membrane [43,44].

The maintenance of cell polarity requires the continuous expression and efficient activity of junction-associated proteins. Evidence suggests that the loss of junctions disrupts the polarity, interferes with coordinated signaling events, and up-regulates proliferation [45,46]. Depolarization is believed to be associated with numerous pathophysiological conditions, including tumor development and progression [46]. Therefore, the integrity of cell polarity is critical for normal physiological function.

1.4 PROTEIN SORTING IN POLARIZED EPITHELIAL CELLS

Once cell polarity is developed, sustained proper sorting of proteins and lipids to the designated membranes along the biosynthetic and postendocytic pathways is critical. The mechanisms that recognize different sorting signals and transport proteins to either apical or basolateral domains are highly regulated within cells. Disruption of such regulation may cause disease due to the mislocalization and malfunction of proteins [47]. For example, the mis-sorting of sucrose-isomaltase (SI) from the apical to basolateral domain in intestinal epithelial cells results in sucrose intolerance type IV, an autosomal recessive intestinal disorder that causes sugar malabsorption [48].

Madin-Darby canine kidney (MDCK) cells have been used as a model system to study the underlying mechanisms of protein sorting in polarized epithelial cells [49,50,51,52,53]. MDCK cells grown on polycarbonate filter support establish a tight polarized monolayer. An advantage of this system is that the apical and basolateral surface of the cells can be selectively

accessed [54]. In this dissertation, MDCK cells are used to study how newly-synthesized proteins are delivered to the apical surface. In the following sections, I will discuss in detail regarding the distinct sorting signals and underlying mechanisms.

1.4.1 Basolateral Sorting Signals

Numerous sorting signals have been identified to mediate proper sorting of proteins and lipids to either apical or basolateral domains in polarized epithelial cells. In the following section, I will discuss different classes of sorting signals in detail.

Basolateral sorting signals are identified as amino acid motifs in the cytoplasmic portion of various proteins [55]. For example, the basolateral signal of the polymeric immunoglobulin receptor (pIgR) resides in its cyplamic tail [56]. Evidence suggested that the addition of the pIgR cytoplasmic region to a normally apical targeted protein re-routed it to the basolateral membrane [57]. Certain features can be found within the basolateral signals despite the diversity and heterogeneity. Specifically, a tyrosine-based motif YXXØ, where X can be any amino acid and Ø is required to be a bulky hydrophobic residue, is shared by several basolateral proteins for example low-density lipoprotein (LDL) receptor and vesicular stomatitis virus G (VSV-G) protein [58,59]. Evidence demonstrated that the tyrosine-based motif on LDL receptor re-routed an apical targeted protein to the basolateral membrane [60]. Alternatively, Hunziker et al., revealed that dileucine/hydrophobic residues rather than a critical tyrosine residue is crucial for Fc receptors possessive basolateral sorting behavior [61]. Similar studies have shown that such a motif is critical for other basolateral sorting proteins including E-cadherin and melanoma cell adhesion molecule-1 [62,63].

The frequent finding that these sorting motifs are similar to those endocytic and lysosomal determinants has led to the suggestion that some common essentials are shared between these machineries [63]. Precisely, the recognition of both signals relies on adaptor protein (AP) complexes, called adaptins. AP-1, AP-2, AP-3, AP-4, and AP-5 are the five adaptins identified so far [64,65]. Among them, AP-5 is not associated with clatherin and considered to be an evolutionarily ancient complex [65]. AP-2 is the key module of clathrin-coated vesicles budding exclusively from the plasma membrane [66]. The remaining adaptins are involved in clathrin-coated pits originating from the TGN and endosomal compartments [66]. All the adaptins consist of one large subunit (γ, α, δ, ε), one lange β subunit, one medium subunit (μ1and μ2) and one small subunit (σ1 and σ2) [66]. Two subtypes of AP-1 have been identified. AP-1A contains a μ1 subunit whereas AP-1B contains a μ2 subunit [67]. Early studies using epithelial cell lines lacking μ1B subunit of the AP-1 demonstrated that basolateral proteins were re-routed to the apical membrane, suggesting that the interaction between basolateral signals and adaptins is essential [68]. Additional observations propose a role for AP-2 and AP-4 in basolateral sorting pathways by linking the cargo proteins to a clathrin coat [66,69]. Interestingly, some unusual basolateral signals have been described including bipartite basolateral sorting motifs and PDZ-binding motifs which are not believed to be AP complex-dependent [70,71].

1.4.2 Apical sorting signals

Apical sorting signals are more diverse and heterogeneous compared to basolateral sorting signals. Apical sorting sequences have been identified in the cytoplasmic tails, transmembrane regions, or lumenal domains of apically sorted proteins. In addition to signals in the primary

amino acid sequence, post-translational modifications such as N- and O-linked glycosylation and lipidation can also be required for the apical sorting of proteins. Outlined below is a general overview describing the structure/function of these apical sorting signals and the adaptor machinery that decode them.

1.4.2.1 Associations with Lipid Rafts

The first apical sorting signal identified was the glycosylphophatidylinositol, GPI-lipid anchor. Two groups showed that the addition of a GPI anchor attachment sequence to certain proteins led to apical delivery of these chimeric proteins [72,73]. This is supported by the fact that the apical membrane is enriched with glycosphingolipids. These lipids can form small transient aggregates in the *trans*-Golgi Network (TGN) often called "lipid rafts". They are thought to assist protein apical delivery. GPI-anchored apical proteins are demonstrated to be insoluble in cold non-ionic detergent Triton X-100, which is one of the hallmark for lipid-raft association [74]. Lipid rafts are microdomains enriched in glycosphingolipid and cholesterol and are found in plasma and Golgi complex membranes leading to the model that lipid rafts act as sorting platforms to ferry GPI-anchored proteins from the TGN to the cell surface [75]. Such lipid rafts are formed in the Golgi apparatus and may integrate GPI-associated proteins through a long saturated acyl chain and subsequently move past the plasma membrane bilayer [76]. Further studies have indicated that influenza hemagglutinin (HA) is also associated with lipid rafts and depletion of glycosphingolipids or cholesterol leads to the mis-sorting of HA [77]. Additional studies revealed that a sequence of ten residues within the transmembrane region is critical for its incorporation to the lipid rafts and apical trafficking, as the detergent insolubility of HA is reduced in mutants lacking the ten amino acids [78,79,80]. Recently, it has been shown that an HA mutant which lacks its raft targeting signal is retained in the Golgi complex [81]. Other

evidence suggests that cysteine-palmitoylation at cytoplasmic and transmembrane regions may also be required for association between HA and lipid rafts [82,83]. However, HA trafficking is not retarded within the Golgi complex when the acylation is perturbed [81].

It has been proposed that lipid rafts sort apical proteins by promoting their incorporation into vesicles that are destined for the apical membrane [84]. Previous studies have suggested that oligomerization and "clustering" is critical in the sorting of GPI-anchored proteins, and lipid rafts function as an apical sorting platforms [85]. This provides a plausible explanation for the general sorting of GPI-anchored proteins. Paladino et al. demonstrated that the addition of a GPI anchor to green fluorescent protein (GFP) results in the apical delivery of this protein. However, this is disrupted by mutations that disturb the oligomerization of GPI-tagged GFP [86]. Additionally, a high molecular weight cluster was observed only when GPI-associated proteins which are designated to the apical surface, were incorporated into the lipid rafts. Subsequently, disruption of clustering leads to mis-sorting to the basolateral membrane [86]. One explanation is that clustering stabilizes the apical sorting platforms formed by the lipid rafts. The conjunction of smaller rafts into larger rafts through oligomerization could increase the curvature of a budding vesicle at the TGN, thereby aiding its delivery towards the apical surface [86]. However, discrepant results exist. For example, association into lipid rafts does not correlate exclusively with apical sorting of GPI-anchored proteins, as some basolateral proteins are associated with raft-like domains in Fischer rat thyroid (FRT) cells [87]. A possible explanation was provided by work from Meiss and coworkers using a mutant MDCK cell line resistant to concanavalin A (conA) lectin which results in defects in N-glycan core structure [88]. GPI-linked proteins are missorted to the basolateral membrane in ConA-resistant MDCK cells due to their inability to oligomerize into immobile aggregates, suggesting that clustering of GPI-anchored proteins

before their arrival to the membrane is essential [89]. An alternative explanation came from work by Kinoshita and coworkers, demonstrating that an event of remodeling of fatty-acid chains on GPI anchors occurs upon their addtion to proteins [90]. The GPI-anchored proteins that are usually found in lipid rafts contain two saturated fatty chains wherease GPI-anchored proteins that are usually excluded from rafts contain unsaturated fatty chains. A remodeling event likely occurs in the Golgi complex to generate saturated fatty chains [90]. Such a remodeling event is required for association of GPI-anchored proteins with lipid rafts, thus suggesting that specific lipid structure is important for proper apical targeting of GPI-anchored proteins [91]. To summarize, lipid raft association by itself is a necessary but not sufficient apical sorting signal.

Several molecules have been identified as candidates for mediating lipid raft clustering, for example VIP17/MAL (myelin and lymphocyte protein). A putative role of MAL has been implied whereby VIP17/MAL escorts proteins to the apical surface through interaction with lipid rafts, maintaining the stability of the apical surface [92]. MAL1 cycles between the Golgi and the apical membrane where it regulates apical transport of multiple proteins including influenza HA, secreted gp80 and GPI-anchored proteins [93,94,95]. MAL2 traffics between the apical recycling endosome and the apical surface in liver hepatocytes where it mediates transytosis of several proteins including GPI-anchored proteins and single-pass transmembrane apical proteins [96,97]. Interestingly, vectorial delivery instead of transytosis of these proteins is promoted when MAL1 is overexpressed in WIF-B cells, liver hepatocytes which normally lack MAL1, suggesting that both MAL1 and 2 are involved in regulation of direct and indirect routes to the apical surface [98]. Another candidate of raft clustering mediator is the phosphatidylinositol 4-phosphate adaptor protein 2 (FAPP2). Depletion of FAPP2 results in disrupted apical delivery of YFP-GPI

and Forsmann antigen, an apical glycolipid [99,100]. A third potential clustering agent is galectin-4, which will be discussed in detail in section 1.4.2.4.

1.4.2.2 Transmembrane and Cytoplasmic Tail Apical Determinants

Another group of apical sorting signal relies on the cytoplasmic domain or transmembrane region of certain proteins. The first sequence that has been identified is in the cytosolic tail of rhodopsin [101]. Deletion of the cytosolic tail leads to the mis-sorting of the protein [102]. The introduction of rhodopsin's cytosolic tail to another non-apical protein results in the apical delivery of this chimeric protein. Megalin is another protein that relies on its cytosolic tail for apical trafficking [103,104]. Additionally, the receptor guanylate cyclases M_2 muscarinic receptors are also delivered to the apical surface due to sequences on the cytoplasmic domains [105]. Although no consensus sequence has been identified that is responsible for their apical delivery, research suggests that conformational changes are critical for these signals. For example, the fourth transmembrane spanning domain is responsible for delivery of the gastric H,K-ATPase to the apical surface by inducing a conformational sorting motif [106]. Additionally, Carmosino et al., identified two motifs within the cytoplasmic tail of the renal Na-K-Cl cotransporter type 2 that mediate the apical delivery by a conformational cross-talk event between the sorting sequences and their surrounding environment [107].

1.4.2.3 Glycosylation

A third group of apical sorting signals involves in glycosylation, a ubiquitous post-translational modification of numerous proteins. This process is believed to aid protein folding, stabilization, and protein-protein interactions. The earliest evidence that indicates an involvement of glycosylation in apical sorting arose from studies using specific glycosylation inhibitors in

MDCK cells. In the next few sections, the synthesis and modification of glycosylation, especially N-glycans, will be reviewed. Additionally, the involvement of N-glycosylation in apical sorting and proposed mechanisms will be addressed.

(a) O-glycosylation

The biosynthesis of serine/threonine (O)-linked glycans is initiated by the addition of an N-acetylgalactosamine (GalNAc) residue to serine or threonine residues [108]. This process is catalyzed by a polypeptide GalNAc transferase (GalNAcT). Next, galactose or N-acetylglucosamine (GlcNAc) is added to form one of the four subtypes of the core structure that are based on various monosaccharide linkage reactions. The glycan structure can be further elongated by addition of N-acetyllactosamine, sialic acid, fucose, galactose, GlcNAc, GalNAc, and sulfate [108]. The different combinations of sugar structures are regulated by specific expression levels of various glycosyltransferases that participate in O-glycan biosynthesis [108].

O-linked glycans are proposed to play a role in apical delivery. The neurotrophin receptor p75 (p75NTR) contains an O-glycan-rich stalk proximal to the transmembrane domain [109]. Deletion of this region leads to nonpolarized distribution of this protein. Similar studies were performed on sucrose isomaltase (SI), an intestinal brush-border membrane protein, and MUC1 [110,111]. Evidence suggests that introduction of the heavily O-glycosylated stalk domains of SI to rat growth hormone, a secreted protein which usually secretes in a non-polarized manner, cause it to be delivered to the apical domain [112]. Recent work from Kinlough and coworker demonstrated that the apical sorting signal of MUC1 is the heavily O-glycosylated mucin-like domain. Transfer of this domain to the interleukin-2 receptor α subunit (Tac) enhanced its apical expression [111].

Other indications for an involvement of O-glycosylation in apical sorting came from studies using glycosylation inhibitors. For example, a compound commonly used is GalNAcα-O-benzyl (BGN), an efficient acceptor for galactosyltransferases and sialyltransferases. BGN treatment results in truncated O-glycans. It has been shown that treatment with this compound disrupts O-glycosylation and thus perturbs the apical delivery of proteins including dipeptidylpeptidase IV (DPPIV) and MUC1 in HT-29, Caco-2, and MDCK cells [113,114,115]. However, the effect of this compound on N-glycans complicates the results. It has been reported that BGN blocks terminal processing of N-glycans in some cell lines, which leads to misorting of glycoproteins [116,117]. Data from our lab suggest that the apical delivery of endolyn, an N-glycan dependent protein, is also disrupted in BGN-treated cells.

(b) N-glycosylation

A lipid-linked oligosaccharide precursor is transferred to asparagine residues on newly synthesized protein in the endoplasmic reticulum (ER) membrane of eukaryotes (Fig.3) [118]. The minimal consensus sequence for N glycosylation is Asn-X-Thr/Ser (where X is any residue except proline) [119]. Asn-X-Cys is used as a recognizable sequence in some rare cases [108]. This oligosaccharide precursor consists of a core glycan structure of $Glc_3Man_9GlcNAc_2$, where Glc represents glucose, Man represents mannose, and GlcNAc represents N-acetylglucosamine. The following steps are conserved among all eukaryotic cells and are thought to play critical roles in regulating glycoprotein folding. First, the sequential removal of all three glucoses is mediated by Glucosidases I and II in the lumen of the ER. One mannose is further trimmed by α-mannosidase I. Other α-mannosidase enzymes located in the Golgi complex further process the N-glycans thereby comprising the high content of mannose. The core structure before leaving the

ER is $Man_3GlcNAc_2$-Asn. The contents of mature N-glycans are diverse on vertebrate glycoproteins and are classified into high-mannose, hybrid, and complex subtypes [108]. Structures that contain between five to nine mannose units are defined as high mannose. Structures with high mannose content and substitution with GlcNAc on a single nonreducing mannose are termed hybrid. Complex N-glycans are formed when both mannose residues (α3- and α6-linked) are elongated with GlcNAc moieties. Two or more GlcNAc-bearing branches may exist on vertebrate glycoprotein hybrid and complex subtypes. Up to five of these branches, referred to as antennae, have been observed on certain vertebrate glycoproteins. Furthermore, the addition of fucose or sialic acid complicates the heterogeneity of N-glycosylation in eukaryotic cells [119]. Indeed, the production of antennae and extension by fucose and sialic acid are considered terminal processing of N-glycans (Fig. 4).

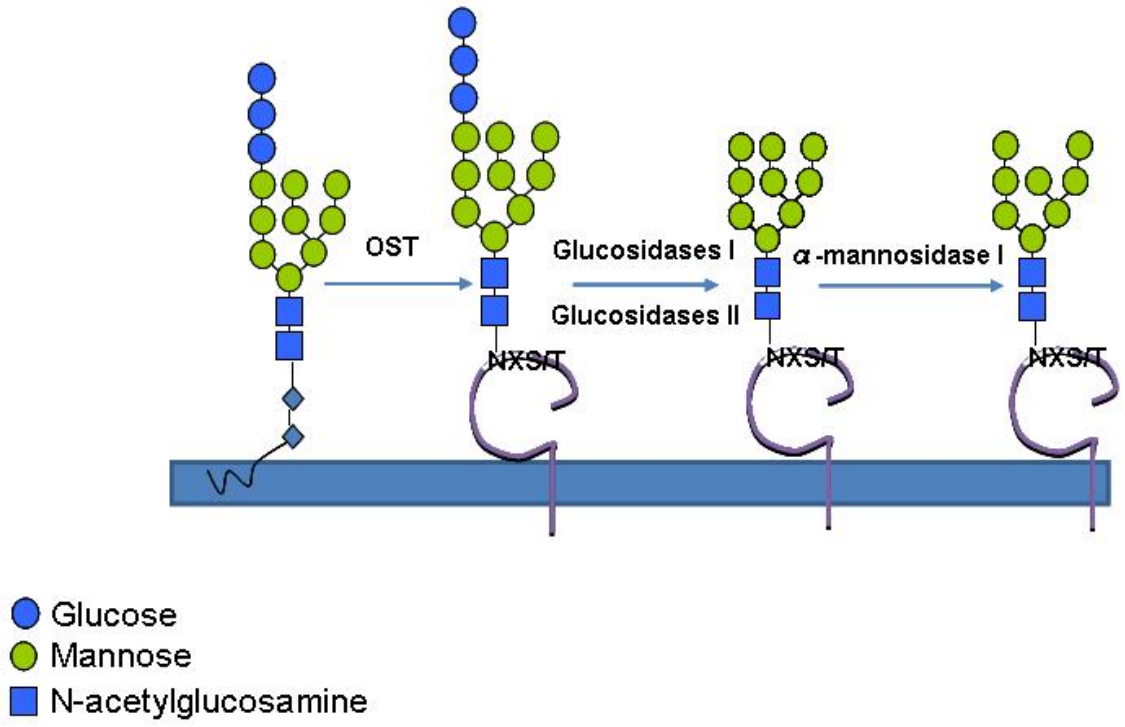

Figure 3. N-glycosylation in ER

The synthesis of the core structure $Glc_3Man_9GlcNAc_2$ on dolichol pyrophosphate initiates the generation of N-glycans within the ER. This core structure is subsequently transferred by the OST complex to an asparagine residue within the NXS/T motif. Glucose and mannose residues are trimmed sequentially by Glucosidases I, II and α-mannosidase I before the glycoprotein exits the ER. Adapted from [118].

Terminal processing of N-glycans in the Golgi initiates with the action of GlcNAcT-I on high mannose structures in the *medial*-Golgi [108]. Subsequently, α-Mannosidase II removes two external mannose residues to generate the substrate for GlcNAcT-II. Sequentially, GlcNAcT-III transfers GlcNAc to the β-linked mannose at the core position and thus making a bisecting branch which prevents further branching and elongation. Conversely, GlcNAcT-IV and -V transfer a GlcNAc to β4 or β6-linked mannose thereby generating more branches [108]. The addition of galactose, poly-N-acetyllactosamine, sialic acid and fucose to each branch greatly increases the diversity of N-glycan structures. Poly-N-acetyllactosamine (polylactosamine or PL) chains are linear polymers comprising repearting units of GlcNAc and galactose. PLs have been reported to be preferentially added onto ß1,6 branch of multiantennary N-glycans, whose synthesis is regulated by GlcNAcT-V [108]. Sialic acids (a.k.a neuraminic acid) are 9-carbon monosaccharides which are commonly found on glycoproteins and gangliosides as terminal components [120]. The C2 can be conjugated to several positions of the penultimate sugar residue. Of these, the most common are to the C3 or C6 of galactose and the 6-position of GalNAc. Sialic acid is found in α2-3 linkages on many, and perhaps all, cells and tissues in vertebrates [108,121]. Members of a family of at least five different α2-3 sialyltransferases (ST3Gal-I-V) are responsible for synthesis of these structures. Studies of the expression patterns of these genes indicate that ST3Gal-III and ST3Gal-IV are expressed in most tissues and cells in

adult mammals. They are also responsible for the addition of sialic acids onto the two most common N-glycan terminal chains. In contrast, ST6Gal-I is solely responsible for the addition of α2-6 sialic acid on N-glycans [108].

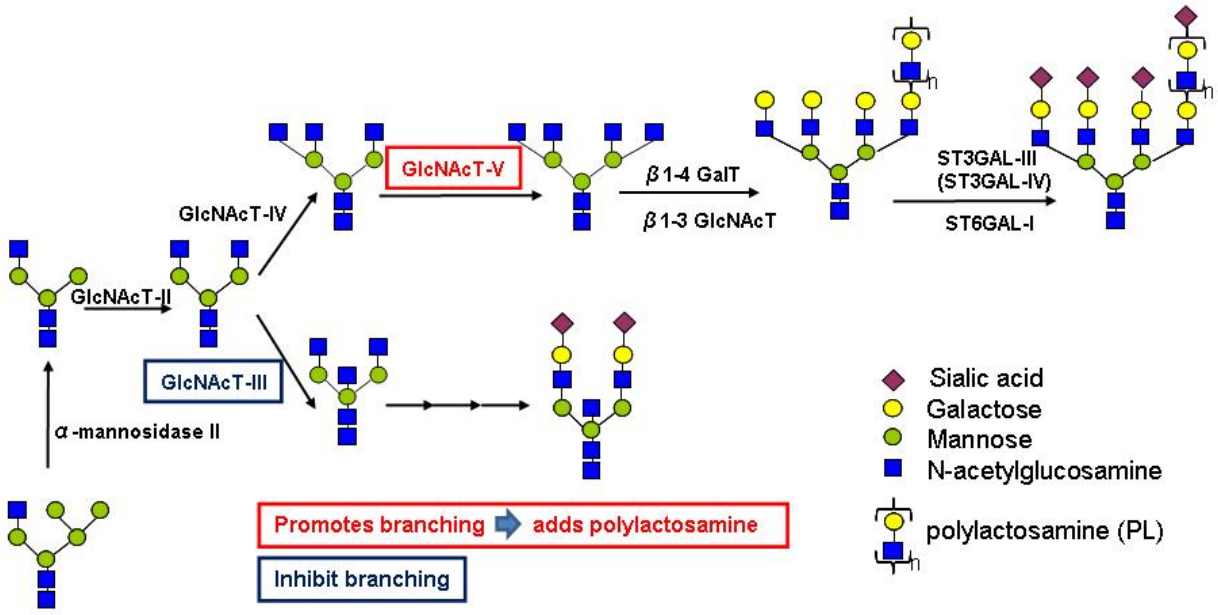

Figure 4. Terminal processing of N-glycans

Upon entering the Golgi apparatus, more mannose residues can be trimmed by α-Mannosidase II to generate the substrate for GlcNAcT-II. Sequentially, GlcNAcT-III transfers GlcNAc to the β-linked mannose and thus inhibits further branching. Conversely, GlcNAcT-IV and V can add GlcNAc to β4 or β6-linked mannose to thereby generate additional branches. Addition of galactose, poly-N-acetyllactosamine repeatedly generates long polylactosamine chains in the hybrid or complex structures. Furthermore, addition of sialic acid mediated by ST3Gal-III and ST3Gal-IV for α2,3 linkages and ST6Gal-I for α2,6 linkages to each branch, greatly increases the diversity of the N-glycan structures. Adapted from [108].

The early evidence for involvement of N-glycans in apical sorting mostly came from specific drug inhibitors and mutant cell lines that are inefficient in N-glycosylation processing. The first indication for an N-glycan being an apical sorting signal came from work of Scheiffele and coworkers. They demonstrated that an addition of two N-glycans to rat growth hormone converted its nonpolarized secretion to apical delivery suggesting that N-glycans are indeed a kind of apical sorting signal [122] . Further, apical delivery of gp80 (clusterin) in MDCK cells treated with tunicamycin (a GlcNAc analogue) abolishes the initial step of N-glycosylation, and thus causes the seretion of gp80 to be non-polarized [123]. Additionally, removal of N-glycans from gastric H^+/K^+-ATPase β subunit prohibits its apical delivery resulting in a defect of delivery to the surface by accumulating intracellularly [124]. Addition of N-glycans onto proteins that are normally not glycosylated mediates their apical targeting and transport [125]. The reporter proteins accumulate in the Golgi apparatus in the absence of N-glycans [125]. Interestingly, evidence indicates that the specific structure and number of N-lycans are necessary for proper apical delivery. For instance, two out of eight N-glycans are important for apical delivery of the sialomucin endolyn [126]. One out of three N-glycans is critical for erythropoietin apical delivery [127]. Another case in point is that three out of four N-glycans are essential for the apical delivery of the neuronal glycine transporter GLYT2 [128].

Recent work has shown that the terminal processing, rather than the core structure, is critical for apical sorting of some proteins. For example, Potter et al., demonstrated that sialomucin endolyn apical delivery was disrupted by kifunensine (KIF) and deoxymannojirimycin (DMJ), compounds that inhibit terminal processing of N-glycosylation [126]. The fact that apical delivery of endolyn was not affected by deoxynojirimycin (DNJ), an inhibitor for ER glucosidase I that affects the formation of the N-glycan core structure, indicates

the terminal processing is important for proper trafficking of endolyn. Other evidence also suggests a role of terminal process on glycoprotein surface delivery: studies by Dennis and colleagues have demonstrated that addition of polylactosamine can selectively modulate surface expression levels of a variety of cellular receptors [129]. Additionally, sialic acids have previously been implicated in glycosylation dependent apical sorting. When MDCK cells were treated with GalNac-alpha-O-benzyl (BGN), a competitive inhibitor of sialylation, the apical secretion of mouse soluble dipeptidyl peptidase IV was decreased [117]. In chapter 3, we investigated whether terminal processing is critical for endolyn apical sorting by testing whether polylactosmamine chains or addition of sialic acids has an effect on endolyn trafficking. However, the heterogeneity of glycans presents a significant challenge to dissect glycan terminal processing at a molecular level. Glycans are extremely diverse in nature, including various composition of monosaccaride, diverse positions where sugar chains are linked, and the different stereocheminal nature of the linkages (α is equatorial whereas ß is axial) [130]. This heterogeneity is highly regulated by differential expression of specific glycosyltransferases and glycosidases, as well as their availability to substrates in a cell-type- and developmental stage-specific manner [131,132]. To overcome this problem, I used an RNAi knocksown approach that I optimized in Chapter 2 to specifically knock down glycosyltrasferases that are responsible for addition of polylactosamine and sialic acids on N-glycans. Further, I utilized lectin-binding assay as a sensitive approach to measure the change in glycan profiles after knockdown [133,134].

1.4.2.4 Proposed Mechanism for Glycan-mediated Protein Sorting

Abundant evidence indicates a role for both N- and O-glycans in the apical sorting of glycoproteins. However, unlike the lipid raft dependent model, where the unifying hypothesis is that proteins develop interactions with lipid rafts at TGN, the glycan-dependent model lacks a

universal theory. Notably, no obvious difference in glycan structures has been identified in apical and basolateral sorted glycoproteins, indicating that no consensus sugar structure accounts for the apical sorting signal. Two prevalent mechanisms have been proposed for glycan-dependent apical sorting [135].

One hypothesis postulates that a group of receptors or binding partners exists to interact with glycans for apical sorting. A group of proteins that naturally recognize glycans are termed lectins, which are proteins containing carbohydrate recognition domain(s) that recognize distinct glycans in order to mediate particular physiological or pathological processes. Early indications for an involvement of lectins in apical sorting came from studies on vesicular integral protein 36 (VIP36). VIP36 was initially isolated from lipid rafts and is localized to the Golgi complex, apical membrane and endosomal compartments [136,137]. However, recent evidence suggests a contradictary role of VIP36 in apical sorting [137]. High resolution confocal microscopy revealed that VIP36 is localized in ER-Golgi intermediate compartment rather than the TGN, indicating a role of VIP36 in the early glycoprotein transport but not apical sorting [137].

Interestingly, recent work implicates a role of the galectin family in apical sorting. Galectins are lectins that have high affinity for β-galactose glycoconjugates and are conserved in their carbohydrate recognition domains [108]. They are widely expressed in all organisms [138]. Using RNAi approaches, galectin-4 has been shown to play a role in lipid rafts mediated apical targeting. Depletion of galectin-4 in enterocyte-like HT-29 cells disrupts the lipid raft formation and therefore impairs apical delivery [139,140]. Work from Huet and coworkers suggests a model in which the interaction between galectin-4 and raft-associated proteins within the endosomal compartment is required for apical sortini8g [141]. Galectin-4 has high affinity for both glycosphingolipids, a component of lipid rafts, and complex N-glycans with

polylactosamine chains [138,140]. Galectin-3, another galectin that is widely expressed, has been identified to be involved in raft-independent apical sorting in MDCK cells. A direct interaction between galectin-3 and lactase-phlorizin hydrolase (LPH), p75NTR, and the gp114 has been observed. Depletion of galectin-3 by RNAi results in mis-localization of these proteins [142]. More recently, the intracellular trafficking defects of LPH and dipeptidylpeptidase IV (DPPIV) on intestinal brush border in galectin-3 null mice have been reported [143]. Schneider et al., reported in 2010 that galectin-3 localizes in Rab11-positive apical recycling endosomes [144]. This provides a possibility that galectin-3 mediates apical sorting through interaction with glycoproteins within early endocytic compartments. Recent work suggests that some galectins like galectin-3 and galectin-9 are involved in general establishment of apical-basolateral polarity in polarized epithelial cells [145,146]. Knockdown of galectin-3 in MDCK cells leads to abnormal epithelial cyst formation in 3D and perturbs ciliogenesis [145,147]. Knockdown of galectin-9 in MDCK cells results in severe loss of epithelial polarity [146].

Another feasible model for raft-independent apical sorting is that a transport-competent conformation is required for further progress along the apical sorting pathway. It is conceivable that oligomerization is involved in this process. In support of this model, it has been reported that inhibition of glycosylation of some apical sorted glycoproteins causes retention of these proteins in the TGN in both MDCK and CHO cells [125]. However, the diversity in requirements utilized by numerous proteins, argues against a uniform protein conformation required for all glycan-dependent sorting events.

Clustering of cargo proteins is a model that is possibly shared by both raft dependent and independent proteins. As mentioned in Section 1.4.2.1, clustering is required by several GPI-anchored proteins for their apical delivery [85]. For correct apical delivery of glycan-dependent

proteins, galectin-3, as a candidate, is capable of oligomerizing through its N-terminal domain to pentamers and thus clusters glycoproteins into multimeric lattices in raft-independent specific carriers [142]. It has been reported that a high molecular weight cluster is formed during p75 NTR apical sorting, indicating that clustering events are important for the apical sorting in both raft-dependent and raft-independent ways [148].

1.5 SIALOMUCIN ENDOLYN

1.5.1 The structure and sorting of endolyn

Sialomucin endolyn has been studied extensively in our laboratory as an N-glycan dependent apical targeted protein. The focus of this dissertatioin is to determine the requirement(s) on glycan structure which is essential for its apical delivery. Further, the possible mechanism of N-glycan apical sorting is studied using endolyn as a model protein. Finally, the function of endolyn during kidney development is also studied in this dissertation.

Rat endolyn is a type I transmembrane protein comprising 173 amino acids with a molecular weight of 78 KDa [149]. It is defined as a mucin due to the two mucin-like motifs in the ectodomain (Fig.5). A putitve globular domain hinged by disulfide bonds is flanked by the two mucin domains. There are many putative sites for O-glycosylation (40 of Ser-Thr) and N-glcosylation (8 of Asn-x-Ser/Thr) within the lumenal domain. The transmembrane domain and short cytoplasmic tail are highly conserved among species. A FIGGI sequence of unknown function in the transmembrane region is conserved among species. A tyrosine motif YXXØ

motif in the short carboxy terminal cytosolic tail is responsible for its delivery to lysosomes and also serves as a potential basolateral targeting signal [149].

Endolyn has been identified in many species, including zebrafish (Fig.5). Zebrafish endolyn contains only one mucin domain. However, it retains many potential O-glycosylation (twenty-eight) and N-glycosylation (nine) sites in the lumenal domain with a few conserved with rat endolyn. The lumenal domain also contains a proposed globular domain with disulfide bond linkage. Moreover, the transmembrane domain and cytoplasmic region are identical with that of rat endolyn. This 43% consensus sequence with critical conserved regions makes it possible to use rat endolyn in the zebrafish model system. The advantage of this approach is that reagents and techniques available for rat endolyn may be used. More significantly, a conserved protein function can be revealed.

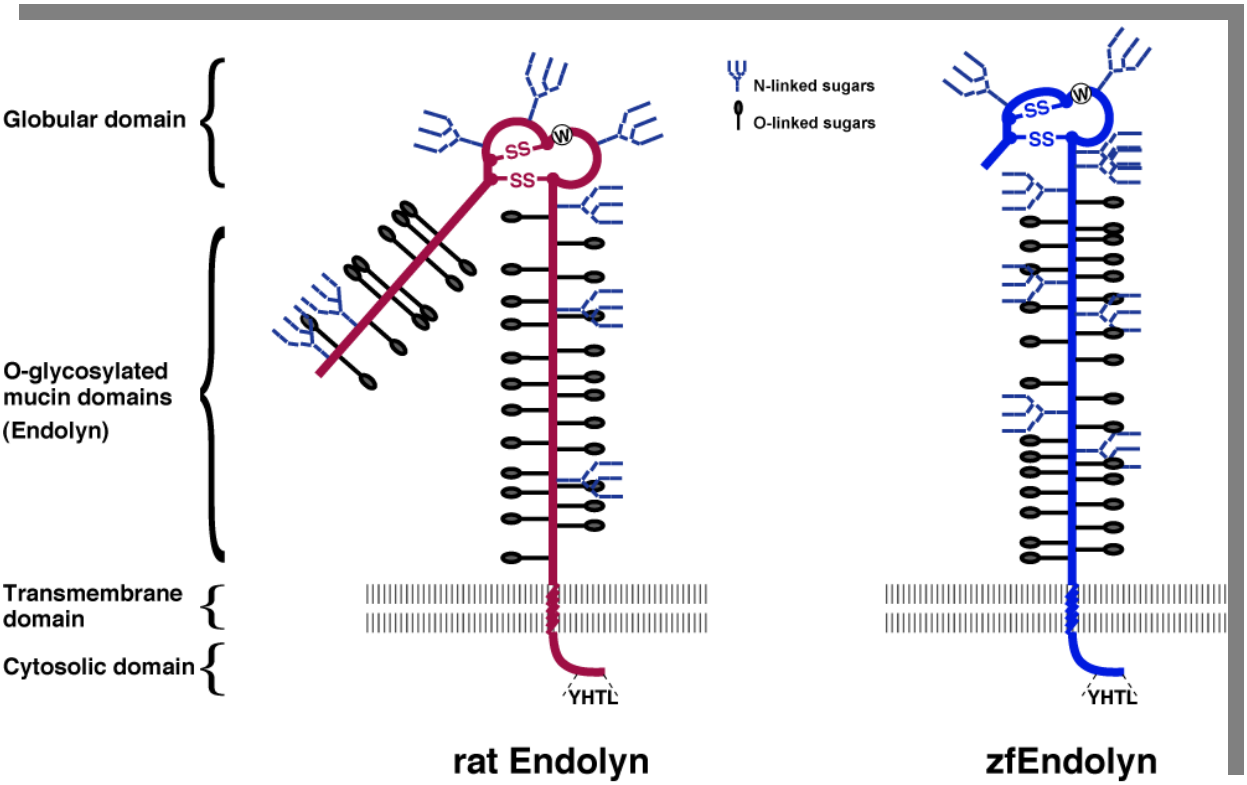

Figure 5. Structure of rat vs. zebrafish endolyn

A schematic diagram of rat and zebrafish endolyn. The transmembrane and cytosolic domains of zebrafish and rat endolyn are identical. Unlike rat endolyn, zfEndolyn has only one mucin region and a proposed globular region linked by disulfide bonds. ZfEndolyn contains nine potential N-glycosylation sites, two within the globular region and seven between this domain and the transmembrane domain. Of the serines and threonines, 28 of 40 residues in the luminal domain are potential O-glycosylation sites as determined using the NetOglyc3.1 program. Figure provided by Dr. G. Ihrke.

Endolyn is primarily localized in lysosomes at steady state, with a small fraction localized on the plasma membrane. Unlike typical lysosomally targeted proteins which take a route directly from the *trans*-Golgi network (TGN) to lysosomes via early/late endosomes, endolyn exploits an unconventional pathway from the TGN to the plasma membrane, where it is endocytosed, and delivered to lysosomes [150,151,152,153]. One explanation for the indirect lysosomal pathway of endolyn (via the cell surface) is that its YXXØ motif is not proceded by a glycine residue. This residue has been demonstrated to be essential for efficient direct lysosomal transport of typical lysosomal membrane proteins (e.g. Lamp-1 and Lamp-2) [154,155].

The indirect pathway for lysosomal proteins includes via either the apical surface or the basolateral membrane before delivery to lysosomes in polarized cells [60,152]. Evidence suggests that endolyn likely takes the route via the apical surface. Endolyn was found in a subapical compartment before moving to the lysosomes in polarized hepatocyte cells [149]. Consistent with this, antibodies against endolyn were internalized from the apical surface in MDCK cells [152]. AP-3 has been shown to be involved in the sorting of endolyn from both the TGN and early endosomes in both 3T3 and NRK cells [155]. Interestingly, a small portion of

endolyn recycled back to the apical surface while the bulk remained in lysosomes after endocytosed from the apical membrane [155].

Data from our laboratory demonstrated that the apical delivery of endolyn is N-glycosylation dependent in MDCK cells: (1) Its solubility in Triton X-100 at 4°C indicates that its apical sorting is independent of lipid rafts [152]. (2) Regardless of the large quantity of O-glycosylation sites within the lumenal domain of endolyn, its apical sorting is disrupted upon tunicamycin treatment [152]. (3) Potter et al., have shown that two out of eight N-glycans within the globular region are critical for endolyn apical delivery since mutations on these two N-glycosylation sites attenuated its apical trafficking [100]. (4) Moreover, apical delivery of endolyn was restored when these two glycans were reintroduced into mutated endolyn which lacks all N-glycosylation consensus sequences [100]. (5) The apical sorting of endolyn along the postendocytic pathway is also N-glycan dependent and simlar to that on newly synthesized endolyn [156]. As discussed in Section 1.4.2.3(b), evience suggests that terminal glycosylation processing is important for endolyn trafficking such that its apical delivery is disupted in MDCK cells treated with compounds that perturb N-glycan terminal processing [100]. Notably, endolyn contains both an apical targeting motif (N-glycans) and a basolateral/lysosomal signal (YXXØ motif). Futhre studies should investigate how its apical sorting signal is dominant over its basolateral/lysosomal signal.

1.5.2 The function of endolyn

Work from Watt and colleagues suggests a novel role for the human ortholog of endolyn, CD164, in adhesion and proliferation of hematopoietic progenitor cells as an adhesion receptor [157]. Endolyn has been identified on primitive hematopoietic $CD34^{+}$ cells and has been

reported to regulate adherence of hematopoietic cells to stromal cells, by negatively regulating their differentiation [158]. Further evidence suggests that the role of endolyn in adhesion and survival is through its interaction with CXCR4, a key chemokine receptor that regulates migration and proliferation of hematopoietic and neuronal progenitor cells [159]. Additionally, Lee et al, have shown that endolyn may promote myogenesis, the process of muscular tissue formation during development, through binding to CXCR4 [160]. Endolyn functions as a regulator of myoblast motility and fusion of myoblast into myotubes [161]. Other literature indicates the role of endolyn on migration in other cell lines including prostate cancer cells through a similar pathway of CXCR4 and its ligand CXCL12 [162].

The differeciated subcellular localization of endolyn in adult and embryonic kidney suggests that endolyn has a funciontal purpose at distinct sites. Endolyn is present intracellularly and at the apical surface in adult rat kidney (Youssef Rbaibi personal communication). Surprisingly, endolyn is localized on the basolateral surface in embryonic rat kidney. Endolyn has been shown to be present in mesenchyme and at the basolateral membrane of the ureteric bud at E13. It is also found on the basolateral membrane of the S-shaped body at E16 [163]. This shift from a basolateral to apical distribution during kidney development suggests a potential role for endolyn at these subcellular locations. To support this hypothesis, an antibody that inhibits nephrogenesis was later found to be directed towards endolyn (Qais Al-Awqati personal communication) [163]. In chapter 4, the role of endolyn in kidney development is investigated using zebrafish as a model system.

1.6 SUMMARY

The major gaps in our understanding of endolyn apical soring include the following: (1) Which step in glycan terminal processing is important for endolyn apical delivery? (2) Is there a receptor mediating endolyn apical sorting? (3) Is the proper sorting of endolyn important for its function? Therefore, a systematic evaluation of the determinant(s) for endolyn apical sorting and a study of endolyn function will further our knowledge in the underlying machinery of carbohydrate apical sorting and its significance on protein function.

To address these questions, it was first necessary to develop an efficient method to knock down specific proteins in polarized epithelial cells without compromising cellular apical-basolateral polarity, as described in Chapter 2. This was essential because introduction of DNA/RNA to polarized cells is always a challenge. Chapter 3 detailed a systematic dissection of the apical sorting signal of endolyn. The goal of this study was to elucidate the mechanism of glycan-dependent apical sorting by evaluating whether terminal processing by polylactosamine and/or sialic acids are critical for endolyn apical delivery. Futher, we investigated whether a receptor is involved in endolyn apical sorting by studying the role of galectin-3,4 and 9 in endolyn apical delivery in Chapter 3. Next, we predicted that the proper sorting and localization of endolyn is important for its function. An animal study with zebrafish was therefore used to examine the role of endolyn during pronephric duct development, as described in Chapter 4. Finally, the conclusions of this body of work, as well as recommended future research directions, are discussed in Chapter 5.

2.0 DEPLETION OF SPECIFIC PROTEIN EXPRESSION IN MDCK CELLS

2.1 ABSTRACT

This work was published at Am J Physiol Renal Physiol. 2010 Nov;299(5):F1178-84.

Here, we compared the effects of nucleofection and lipid-based approaches to introduce siRNA duplexes on the subsequent development of membrane polarity in kidney cells. Nucleofection of Madin-Darby canine kidney (MDCK) cells, even with control siRNA duplexes, disrupted the initial surface polarity as well as the steady-state distribution of membrane proteins. Transfection using lipofectamine yielded slightly less efficient knockdown but did not disrupt membrane polarity. We also demonstrated that galectin-3 is not involved in endolyn apical sorting. Polarized secretion was unaffected by nucleofection, suggesting a selective defect in the development of membrane polarity. Cilia frequency and length were not altered by nucleofection. However, the basolateral appearance of a fluorescent lipid tracer added to the apical surface of nucleofected cells was dramatically enhanced relative to untransfected controls or lipofectamine-treated cells. In contrast, [^{3}H]inulin diffusion and transepithelial electrical resistance were not altered in nucleofected cells compared with untransfected ones. We conclude that lipofectamine mediated transfection is more suitable for polarized MDCK cells.

2.2 INTRODUCTION

The development of methods to introduce heterologous DNA and RNA into cultured cells by transient transfection has revolutionized the study of protein function. Moreover, the recent introduction of RNA silencing technologies has provided a powerful tool to manipulate the spectrum of cellular functions and a potential therapeutic strategy for various diseases. Calcium-phosphate-, cationic lipid-, viral-, and electroporation-based approaches are among the most common methods for this purpose. Inherent in these approaches is the requirement that cell function or morphology is not significantly affected by the experimental manipulation itself. However, the mechanisms by which these approaches enable DNA/RNA passage into cells remain largely obscure.

Polarized cells represent a unique challenge to transfection. The plasma membrane of these cells is delineated by tight junctions (TJs) into two asymmetric compartments: an apical domain and a basolateral domain. The polarized delivery of receptors and ion transporters to these domains is critical for proper function of these cells. Traditionally, polarized epithelial cells have been recalcitrant to transient transfection. Transfection of these cells before polarization generally enhances efficiency; however, expression of the heterologous DNA/RNA may be significantly reduced by the time the cells attain a fully differentiated phenotype. A relatively new approach that has proven useful is nucleofection of DNA and RNA into cells in suspension. Delivery of foreign nucleic acid substrates directly into the nucleus apparently enhances the efficiency of transfection without compromising cellular viability [68,164,165]. This method has been successfully adapted to transfect polarized renal cells and is becoming increasingly popular [166].

In optimizing approaches to transfect cells with siRNA duplexes, I observed that nucleofection of cells, even with control siRNAs, resulted in an unexpected but reproducible decrease in cell polarity of apical membrane proteins in MDCK and other renal eptihelial cells, even when cultured for up to five days on permeable supports after the procedure. Nevertheless, polarized secretion of heterologously expressed and endogenous proteins was unaffected by this maneuver. The decrease in membrane polarity was not due to the absence of TJs as ZO-1 staining patterns were similar in control vs. nucleofected cells. Moreover, cilia length and frequency were indistinguishable in nucleofected vs. control cells. The gate function of TJs was also intact as measured by transepithelial resistance (TER) and paracellular transport of inulin. However, diffusion of an apically added fluorescent lipid probe to the basolateral surface was dramatically enhanced in cells that had been nucleofected before plating. We conclude that nucleofection disrupts the development and function of TJs in MDCK cells that precludes use of this approach to examine polarized trafficking. Conversely, lipofectamine mediated transfection is more suitable for polarized epithelial cells.

2.3 RESULTS

2.3.1 Nucleofection, but not lipofectamine-mediated transfection, disrupts the polarity of membrane proteins in renal epithelial cells

As a prelude to studies on the mechanism of glycan-dependent apical sorting, we tested approaches to efficiently knock down proteins in polarized MDCK cells using siRNA duplexes. Specifically, we were interested in whether knockdown of galectin-3, a protein reported to be

involved in polarized sorting of apical proteins [142], had any effect on the biosynthetic delivery of the sialomucin endolyn. An siRNA duplex targeting canine galectin-3 was designed based on a previously published sequence [142]. As a control, we used a commercially available siRNA duplex targeted against luciferase. SiRNA duplexes were introduced into cells by nucleofection or using lipofectamine. After nucleofection, cells were allowed to recover on plastic overnight, trypsinized and counted, and plated onto permeable supports for 4 days. Lipofectamine-treated cells were plated directly onto filters and analyzed 4 days later. As an additional control for both methods, we plated untransfected MDCK cells on filters in parallel with the siRNA-treated samples.

Nucleofection resulted in very high knockdown efficiency of galectin-3 as assessed by Western blotting (Fig. 6A). Quantitation of galectin-3 expression using a VersaDoc Imager revealed ~85% reduction in samples nucleofected with galectin-3 siRNA vs. luciferase controls. The efficiency of galectin-3 knockdown mediated by lipofectamine assessed by Western blotting was not as high, but approached 80% (Fig. 6B).

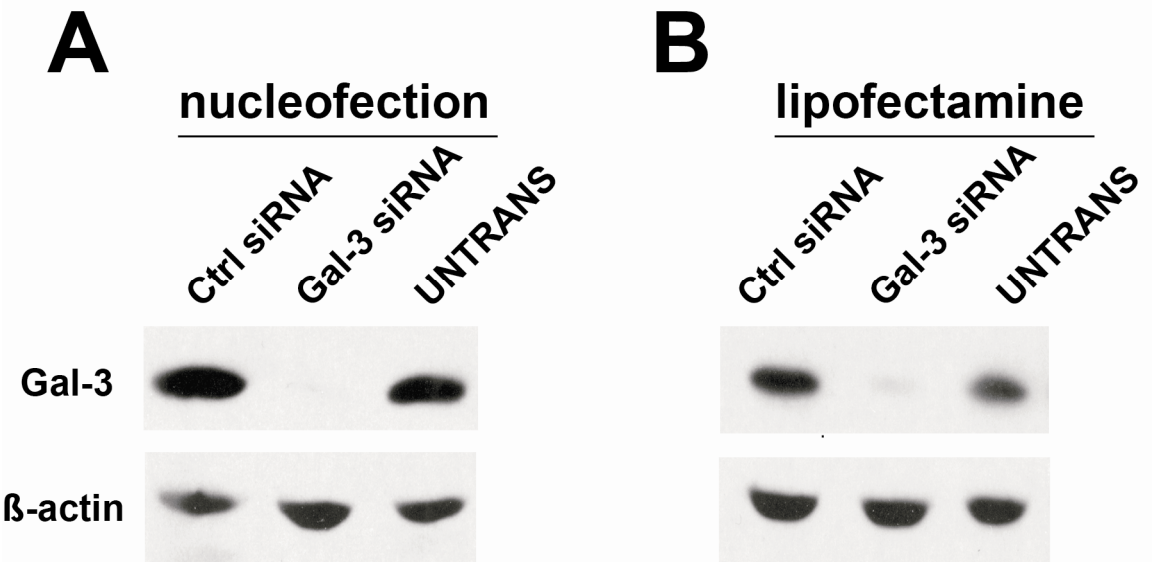

Figure 6. Introduction of siRNA duplexes by nucleofection and lipofectamine-based transfection results in efficient knockdown of galectin-3 in filter-grown MDCK cells [167]

(A) Cells were nucleofected with the indicated siRNAs and plated onto filters the following day. Five days after nucleofection, cells were solubilized and lysates analyzed by Western blotting to detect galectin-3 or ß-actin (as a loading control). Untransfected cells plated under identical conditions were included as an additional control. (B) MDCK cells suspended in MEM were incubated with siRNA duplexes and lipofectamine in the apical chamber of Transwell filter cups. Cells were cultured for 4 days prior to solubilization and Western blotting. Knockdown efficiency was typically >85% in samples nucleofected with galectin-3 siRNA, and slightly lower (~ 80%) in lipofectamine treated cells.

We then assessed the effect of each treatment on polarized delivery of endolyn using a domain-selective biotinylation approach. Three days after being plated, cells were infected with replication-defective recombinant adenovirus-encoding endolyn. In some experiments, stable cell lines expressing endolyn were used, obviating the need for infection. Surprisingly, we routinely observed that endolyn polarity was compromised even in nucleofected cells receiving only

control siRNA. In untransfected controls, the polarity of endolyn surface delivery was 73.9% (Fig. 7A), consistent with our previous observations [100, 171]. In contrast, the apical distribution of endolyn in nucleofected cells was significantly lower (57.6% apical). There was no apparent difference in polarity between cells nucleofected with control vs. galectin-3 siRNA. In contrast, endolyn polarity in lipofectamine-transfected cells was similar to that of untransfected cells (Fig. 7B). Moreover, no effect of galectin-3 knockdown on endolyn polarity was observed, suggesting that this lectin is not required for efficient apical delivery of endolyn. Nucleofection also altered the polarized delivery of two other apical markers: the neurotrophin receptor p75 and influenza HA (data not shown). Whereas endolyn and p75 have glycan-dependent apical targeting information, apical sorting of influenza HA is specified by its transmembrane domain, and this protein takes a distinct route to the apical surface of polarized MDCK cells [109,152,168,169].

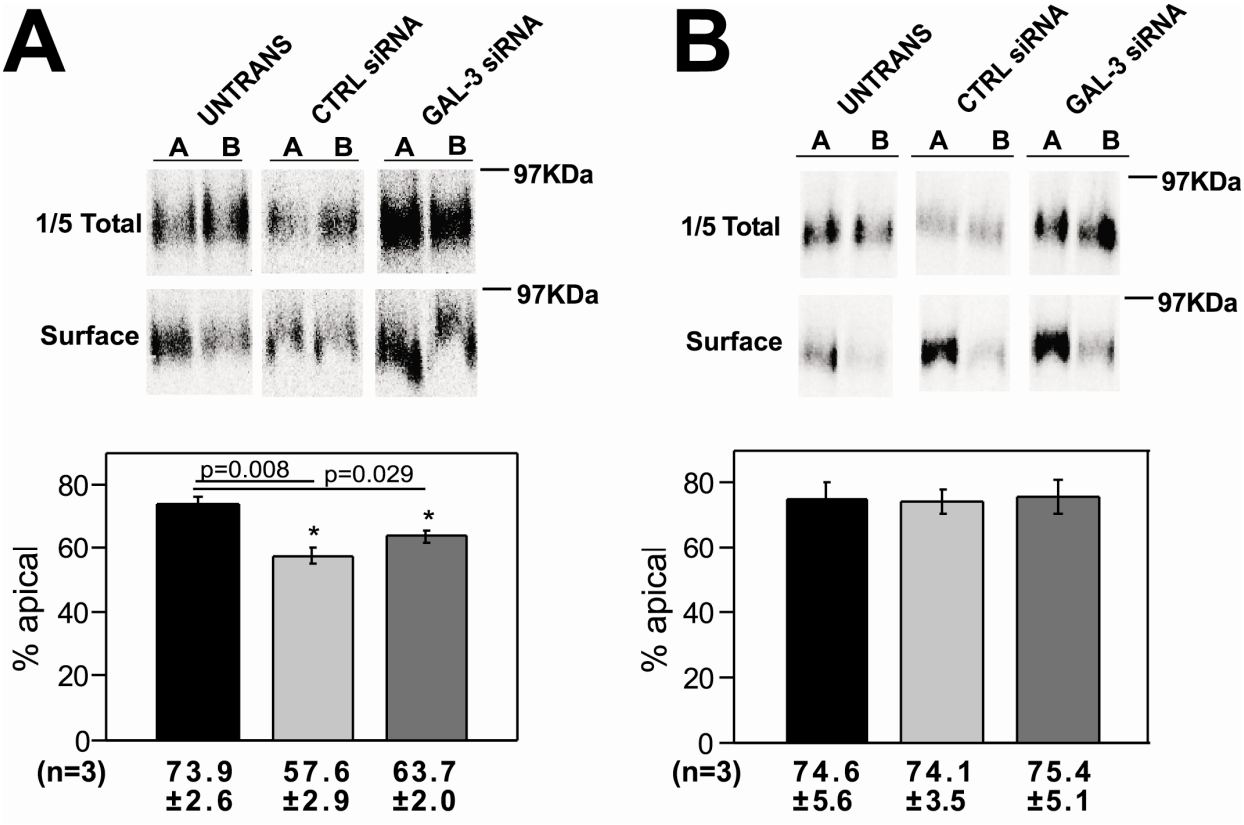

Figure 7. Nucleofection, but not lipofectamine compromises the apical delivery of the transmembrane sialomucin endolyn [167]

(Panel A) Nucleofected or control untransfected endolyn-expressing MDCK cells were starved in cys-free medium for 30 min, radiolabeled with [^{35}S]-cys for 2 h, and chased for 2 h. The apical or basolateral surface of duplicate filters was biotinylated and the polarity of endolyn delivery quantitated as described in Materials and Methods. A representative gel showing total and surface endolyn recovered from apically (A) and basolaterally (B) biotinylated samples is shown. Endolyn polarity in three independent experiments (mean ±SE) each performed in duplicate or triplicate is plotted. *$p<0.05$ versus untransfected cells by ANOVA. (Panel B) The polarity of endolyn cell surface delivery was assessed as described above in filter-grown untransfected or lipofectamine-treated MDCK cells. A representative gel is shown and the results of three experiments, each performed in duplicate or triplicate, is plotted (mean ±SE).

We considered the possibility that altered endolyn polarity was due to our specific nucleofection, recovery, or plating conditions. However, varying the number of cells nucleofected or subsequently plated, the cuvette manufacturer, the Amaxa program used (including the T-20 and L-005 programs recommended for epithelial cells including MDCK), and the postnucleofection recovery conditions did not improve the polarity of endolyn delivery. Substitution of the control (luciferase) siRNA by several other irrelevant siRNA duplexes also disrupted endolyn polarity (data not shown).

Our biochemical experiments suggested that polarized delivery of membrane proteins might be compromised in nucleofected cells. To test whether steady-state distribution of membrane proteins was altered, we used indirect immunofluorescence to examine surface endolyn distribution in nucleofected vs. untransfected MDCK cells. As shown in Fig. 8A, surface endolyn was localized primarily to the apical membrane of untransfected controls. In contrast, endolyn was also clearly visible at the basolateral surface of cells nucleofected with either control or galectin-3 siRNA. Similar results were also observed in MDCK cells expressing p75 and HA. However, the distributions of the endogenous apical protein gp135 and the laterally localized proteins E-cadherin and Na^+-K^+-ATPase were not affected by nucleofection. To confirm that the relocalization is not cell-type specific, endolyn polarity was also examined in nucleofected, lipofectamine-treated, and control (untransfected) mouse CCD cells. As in MDCK cells, endolyn was less apically polarized in nucleofected cells compared with lipofectamine-treated or untransfected cells (Fig. 8B).

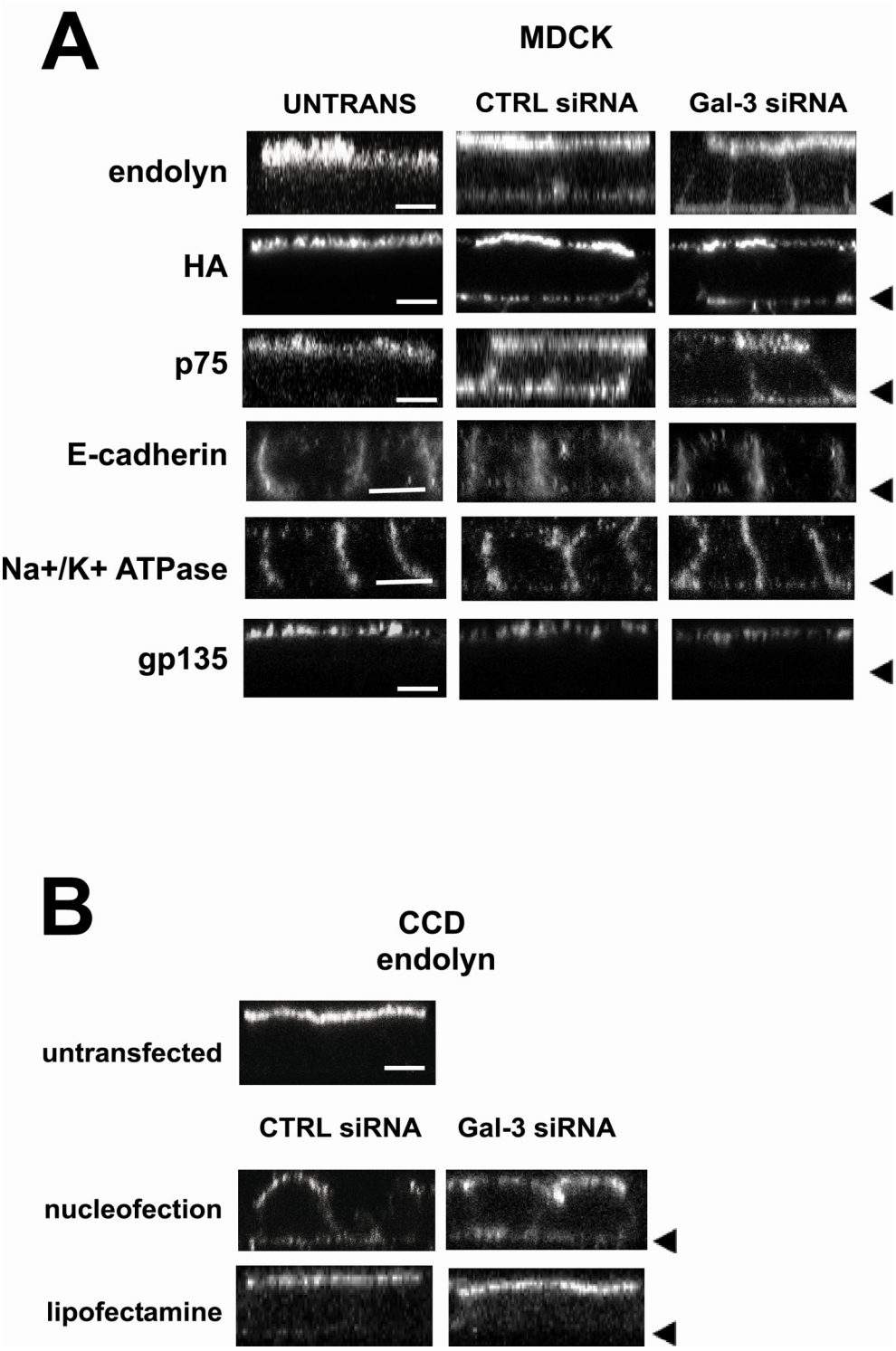

Figure 8. Nucleofection alters the steady-state distribution of transmembrane proteins [167]

A: control (untransfected) or nucleofected MDCK cells plated on 12-well filters for 4 days were incubated on ice with primary antibodies against endolyn, p75, hemagglutinin (HA), or gp135

and Alexa 488-conjugated secondary antibodies before fixation. E-cadherin and Na+-K+-ATPase were detected in cells permeabilized after fixation. Cells were visualized by confocal microscopy and representative XZ sections are shown. Arrowheads mark the position of the filter in each row. B: similar experiments were performed to visualize endolyn distribution in control, nucleofected, and lipofectamine-transfected mouse cortical collecting duct (CCD) cells. Bar = 10 µm.

I next tested whether nucleofection alters the targeting of secreted proteins in polarized cells. To address this, we examined the release of a truncated form of endolyn called ensol. We previously showed that apical secretion of ensol was very efficient (~85%) [100]. Interestingly, nucleofection had no effect on the fidelity of ensol secretion (Fig.9). The polarity of secretion of the endogenous protein complex gp80 was also not affected by nucleofection (data not shown). This suggests that nucleofection selectively alters the polarized distribution of transmembrane but not secreted proteins, and therefore might reflect a postdelivery event rather than a change in biosynthetic sorting efficiency.

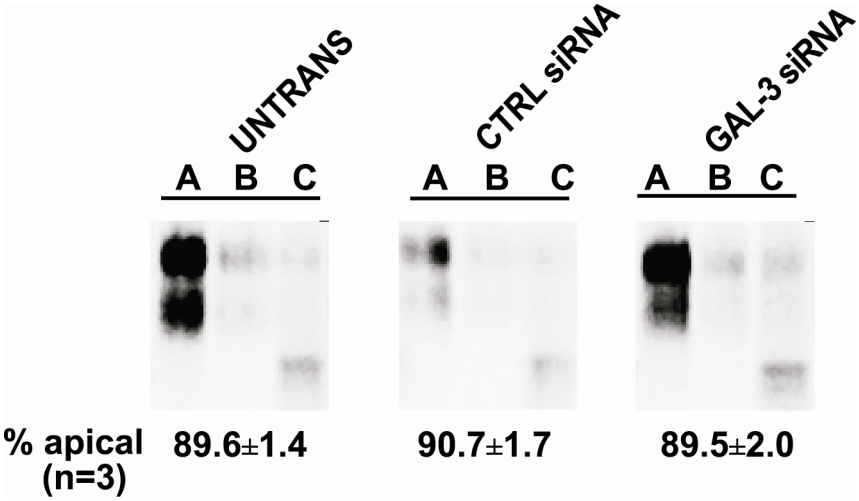

Figure 9. Polarized secretion of a soluble protein is not affected by nucleofection [167]

Filter-grown MDCK cells were subjected to Amaxa nucleofection with the indicated siRNA duplexes. The following day, nucleofected and control (untransfected) cells were plated on filters

and protein secretion of a truncated mutant of endolyn (ensol) tagged with GFP was analyzed four days later. Cells were radiolabeled with [^{35}S]-cys for 30 min, and chased for 1.5 h. The apical and basolateral media were collected separately, and the cells were solubilized. Samples were immunoprecipitated using anti-endolyn antibody and analyzed by SDS-PAGE. Representative samples from one experiment are shown and the quantitation of apically secreted ensol in 3 independent experiments performed in triplicate is noted below each condition. A, apical; B, basolateral; C, cell.

2.3.2 Cilia morphology is unaffected by nucleofection

Primary cilia play an increasingly appreciated role in the development of cell polarity, and defects in ciliary length or formation have been implicated in renal disease [145,147,170,171]. We therefore tested whether nucleofection alters ciliary length in polarized MDCK cells. Cilia in untransfected, nucleofected, or lipofectamine-treated cells were visualized using anti-tubulin antibodies, and their length was assessed using ImageJ software. There was no qualitative difference in the number of cilia observed per field under these different conditions (Fig. 10A). Moreover, we found no variation in ciliary length in nucleofected cells compared with untransfected or lipofectamine-treated cells (Fig.10B).

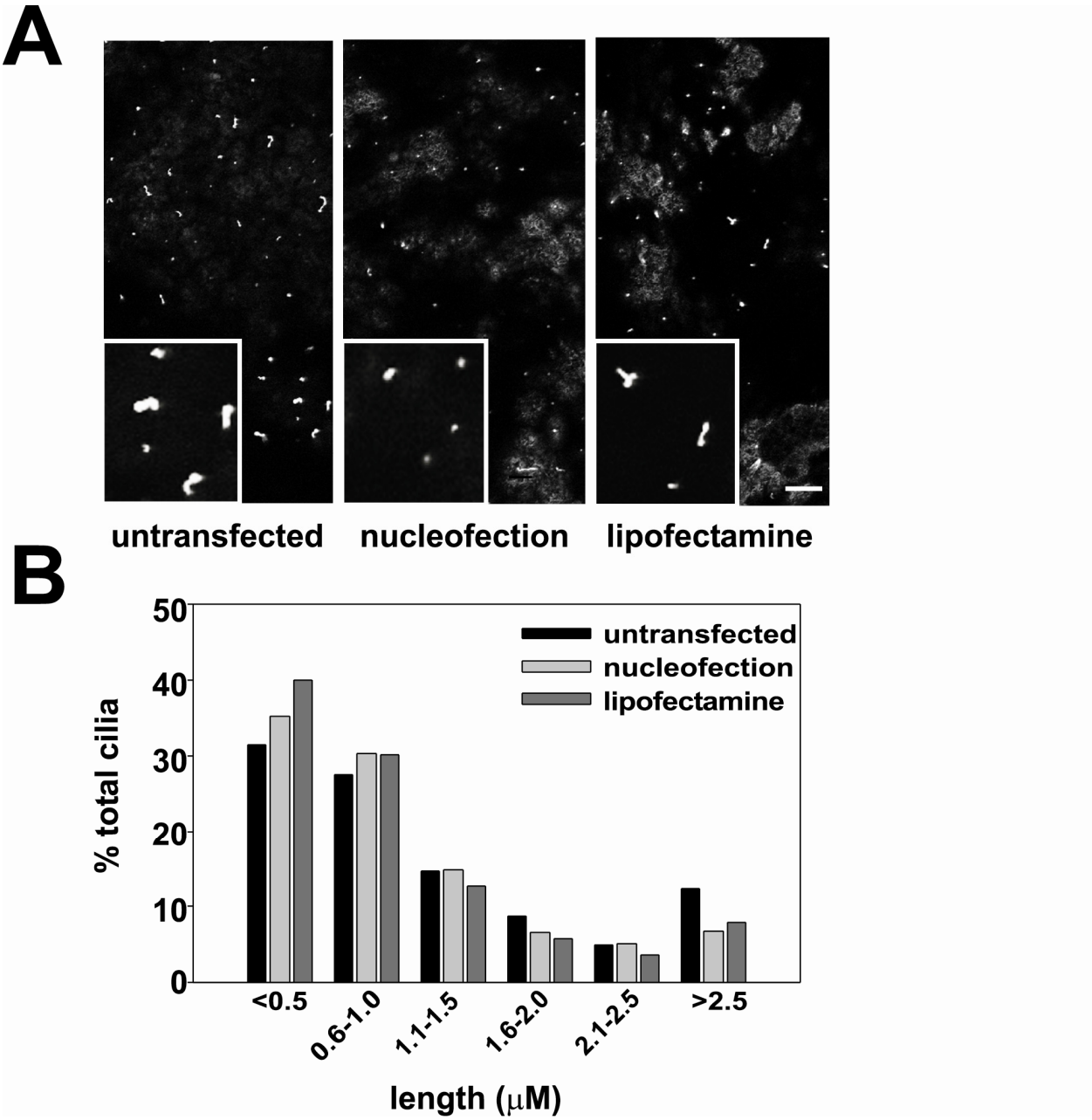

Figure 10. Nucleofection does not alter cilia length [167]

MDCK cells treated as indicated were plated on filters for four days, then fixed and processed for indirect immunofluorescence using monoclonal anti-acetylated β-tubulin antibody. Panel A shows a representative confocal image and inset for each condition. Bar, 10 μm. (Panel B) ImageJ software was used to measure the distribution of cilia lengths from 50 randomly acquired images for each condition.

2.3.3 Fence functions of TJs are disrupted in nucleofected cells

Another possibility to explain the alteration in membrane polarity of nucleofected cells is a defect in TJ formation or function. Nucleofected cells had similar ZO-1 and occludin-staining patterns compared with untransfected controls (Fig. 11), suggesting that the morphology of TJs is not grossly aberrant. We next examined TJ function using several approaches. To assess the gate function of TJs, we monitored the diffusion of the small molecule tracer [^{3}H]inulin. As shown in Fig. 12A, inulin permeability across untransfected, lipofectamine-treated, and nucleofected monolayers was comparable, suggesting that the integrity of the gate function was intact under all conditions. Additionally, we found no significant difference in the TER across filter-grown monolayers (untransfected cells: 101.4 ± 17.4 $\Omega \cdot cm^2$; nucleofected cells: 94.4 ± 6.0 $\Omega \cdot cm^2$; lipofectamine-treated cells: 112.8 ± 9.5 $\Omega \cdot cm^2$).

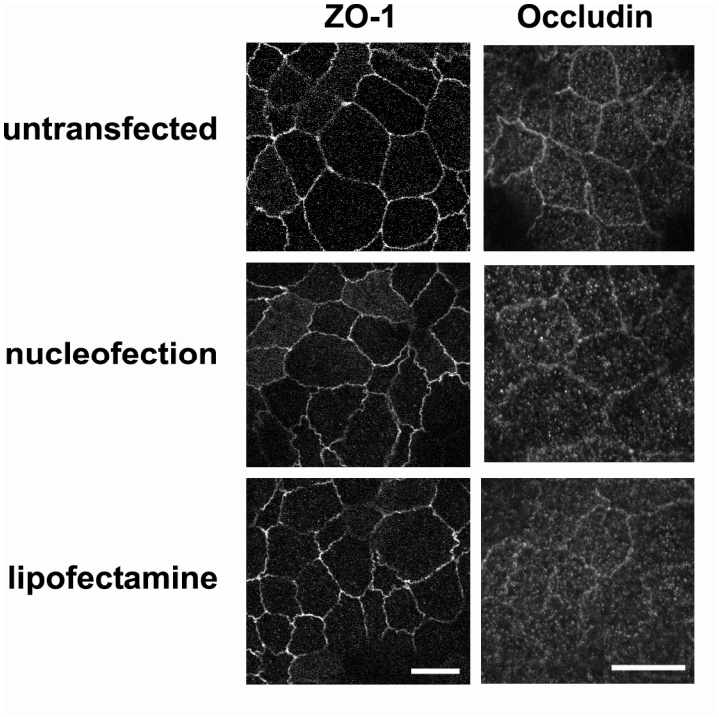

Figure 11. Localization of tight junction markers is not affected in nucleofected cells [167]

Untransfected, nucleofected, and lipofectamine-transfected cells were fixed and processed for indirect immunofluorescence to detect the tight junction markers ZO-1 and occludin. Scale bar = 10 µm.

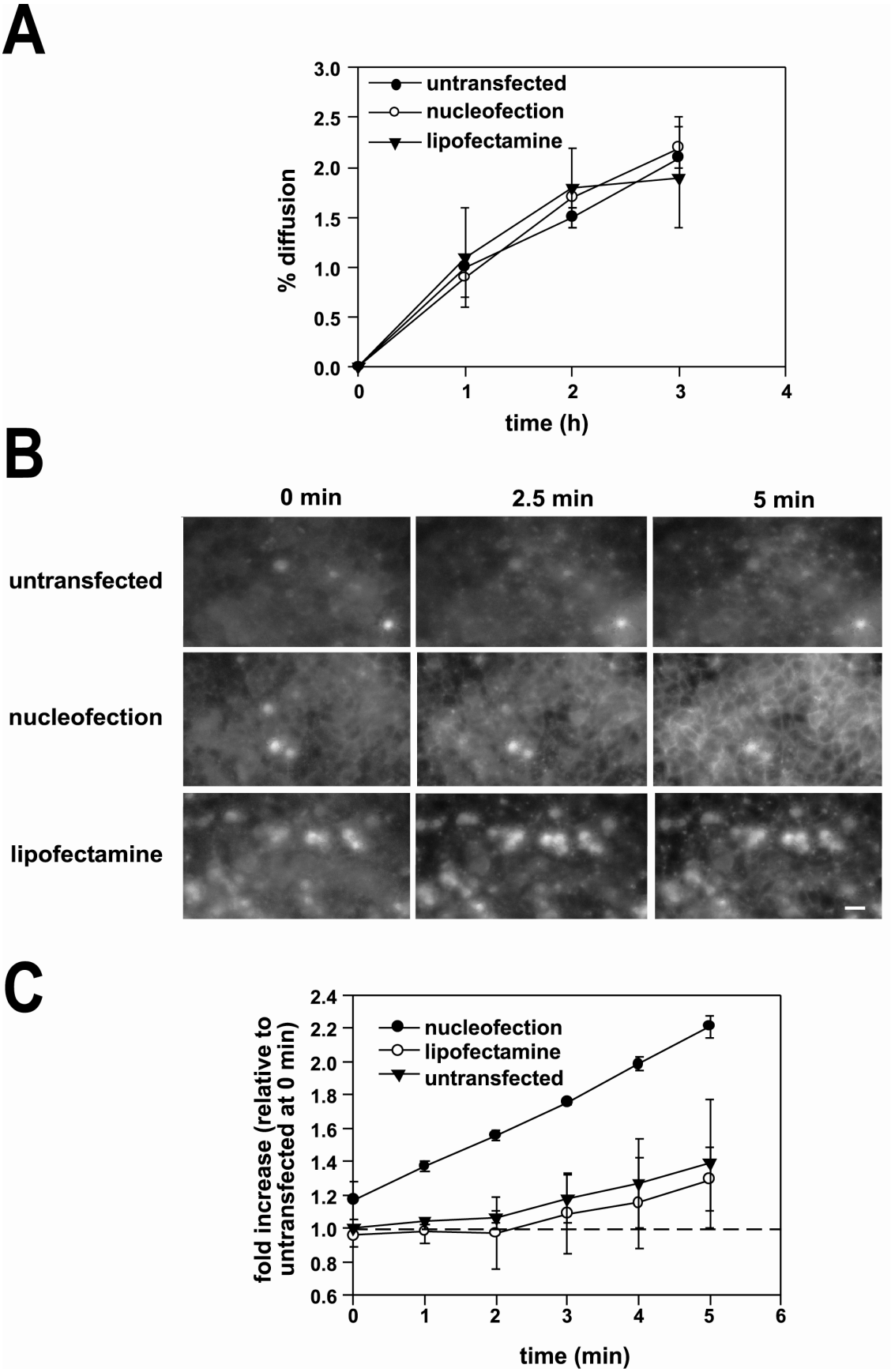
A
3.0
2.5
2.0
1.5
1.0
0.5
0.0
% diffusion
untransfected
nucleofection
lipofectamine
0
1
2
3
4
time (h)
B
0 min
2.5 min
5 min
untransfected
nucleofection
lipofectamine
C
2.4
2.2
2.0
1.8
1.6
1.4
1.2
1.0
0.8
0.6
fold increase (relative to untransfected at 0 min)
nucleofection
lipofectamine
untransfected
0
1
2
3
4
5
6
time (min)

Figure 12. Tight junction fence, but not gate function, is disrupted in nucleofected cells [167]

A: kinetics of transepithelial [3H]inulin diffusion across filter-grown MDCK cells. B: FM4–64FX (100 µM) was added to the apical chamber of filter-grown MDCK cells that had been previously treated as indicated. Cells were imaged every 5 s for 5 min and optical slices collected 2.5 µm above the level of the filters at 0, 2.5, and 5 min after addition of the dye are shown. All images were acquired and processed using identical conditions. The bright spots represent out-of-focus fluorescence from apoptotic cells above the cell monolayer and were especially prominent in lipofectamine-treated samples. Bar = 10 µm. C: change in intensity of FM4–64FX staining at the lateral surface over time was quantified in 2 independent experiments and is plotted relative to the initial intensity measured at time 0 in untransfected cells.

I next examined the diffusion barrier or "fence" function of TJs by testing whether compartmentalization of the lipophilic styryl dye FM4–64FX was compromised in nucleofected cells. Previous studies used this approach to test for defects in TJ fence function [172,173]. FM4–64FX was added to the apical chamber of untransfected, nucleofected, or lipofectamine-treated MDCK cells grown on filters for 4 days, and image stacks were acquired every 5 s for 5 min after addition of the dye. Fig.12 shows the time-dependent accumulation of FM4–64FX fluorescence at the lateral membrane of cells in an optical slice centered at 2.5 µm above the filter for each condition. Strikingly, whereas little to no diffusion of apically added FM4–64FX to the lateral surface was observed in untransfected and lipofectamine-transfected cells, we observed rapid diffusion of the dye in nucleofected cells (Fig. 12B). Quantitation of two independent experiments confirmed an approximately twofold increase in the rate of FM4–64FX diffusion in nucleofected cells vs. untransfected or lipofectamine-treated cells (Fig. 12C). This result indicates that the diffusion barrier between apical and basolateral membranes is disrupted

in nucleofected cells and is consistent with the selective disruption in membrane but not secreted protein polarity that we observed in these cells.

2.4 DISCUSSION

Here, we compared the effects of nucleofection vs. lipofectamine-based transfection methods on the development of polarity in MDCK cells. We found that the distribution of several transmembrane cell surface proteins was disrupted in MDCK and CCD cells that had been nucleofected with control (irrelevant) siRNA duplexes. However, apical sorting of secreted proteins was unaffected by this treatment. Varying numerous facets of the experimental protocol did not rescue the defects in polarity. In contrast, cells transfected using lipofectamine exhibited normal membrane protein polarity, comparable to untransfected cells. Studies to independently test the fence and gate functions of TJs revealed a selective defect in the membrane diffusion barrier in nucleofected cells, whereas transepithelial passage of ions and small molecule tracers was unaffected. These studies have important implications for the design and interpretation of siRNA knockdown experiments in polarized cell lines.

Our studies suggest that biosynthetic sorting of newly synthesized proteins may be unaffected in nucleofected cells and that polarity is lost after surface delivery as a result of compromised TJ fence function. Interestingly, I did not detect any striking changes in the steady-state distribution of three endogenous proteins (gp135, E-cadherin, and Na^+-K^+-ATPase) after nucleofection. The differences we observed between endogenous vs. heterologously expressed proteins might reflect differential assay sensitivity due to the lower abundance of endogenous proteins. Alternatively, endogenous proteins may be better retained at the appropriate plasma

membrane domain as a result of their normal interactions with cytoskeletal or other surface-resident proteins.

TJs are a complex assembly of transmembrane and cytoplasmic proteins that play a role in both the establishment and the maintenance of epithelial cell polarity (reviewed in Refs. [35,174]. The gate function prevents paracellular diffusion of water, ions, and metabolites by regulating movement between adjacent epithelial cells. The fence function prevents the diffusion of transmembrane proteins and outer leaflet lipids. Our results suggest that nucleofection selectively compromises TJ fence but not gate function.

While numerous TJ components have been identified, how gate and fence function are modulated is largely unknown. Inhibiting the function of TJ transmembrane proteins such as occludin, claudins, and junctional adhesion molecules, using antibodies or by overexpression expression or knockdown, generally disrupts the permeability barrier (gate) of polarized epithelial cells without apparently affecting membrane or lipid diffusion across the TJ boundary [175,176,177,178,179,180].

A few studies described maneuvers that disrupt both TJ gate and fence functions. For example, expression of a mutant of occludin lacking its COOH terminus increased paracellular flux as well as lipid diffusion across the TJ of MDCK cells, although the polarity of membrane proteins was unaffected [181]. Similarly, siRNA-mediated knockdown of ZO-2 disrupted both gate and fence functions of TJs [182]. However, only one other report that we are aware of observed a selective defect in TJ fence function with no change in TER. In that study, addition of an antibody directed against the second extracellular loop of occludin resulted in both altered membrane polarity and lipid diffusion in T84 cells [178].

Our results do not address why nucleofection disrupts the establishment of a polarized phenotype. Nucleofection physically creates transient pores in the plasma membrane and nucleus using high-intensity electrical pulses to facilitate the entry of foreign molecules [183]. The pores begin to reseal after the removal of the external field. It is possible that the incubation solutions and/or the electrical pulse itself initiate signal transduction cascades that have long-term consequences on gene expression. Interestingly, whereas most aspects of cell function that we tested are unaffected by this procedure, there appears to be a selective defect in the maintenance of the membrane diffusion barrier. Several possibilities might account for this, including alterations in plasma membrane lipid composition or in the expression of proteins involved in maintaining cell polarity. Regardless of the mechanism, our results suggest that nucleofection of even irrelevant siRNA duplexes compromises the subsequent development of renal epithelial cell polarity, limiting its utility for studies using these cells. In contrast, transfection of siRNA duplexes using lipid-based approaches provides comparable knockdown efficiency without disruption of cell polarity.

2.5 MATERIAL AND METHOD

2.5.1 Cell culture, virus production, and adenoviral infection

MDCK II cells were grown in DMEM (Sigma) with 10% FBS and 1% penicillin/streptomycin. Murine cortical collecting duct (CCD) mpkCCDc14 cells were cultured as previously described [184]. Replication-defective recombinant adenovirus encoding YFP-p75 was originally provided by E. Rodriguez-Boulan. Tetracycline-transactivator-inducible adenoviruses encoding rat endolyn, truncated endolyn (ensol), and influenza hemagglutinin (HA) were generated using the Cre-Lox system or were described previously [185,186]. MDCK cells stably expressing the tetracycline transactivator were infected with recombinant adenoviruses as described in and used for experiments the following day [187].

2.5.2 Nucleofection of siRNA duplexes

MDCK cells in suspension (4 × 106/cuvette) were nucleofected with 10 μg siRNA duplexes using program T23 according to Amaxa Nucleofector instructions in 100 μl Ingenio electroporation solution (Mirus). SiRNA duplexes were purchased from Dharmacon. Unless noted otherwise, cells were then incubated overnight in tissue culture dishes in RPMI medium supplemented with 10% FBS, and then trypsinized, counted, and plated (0.5 × 106 cells/well) on 12-well Transwell filters (Costar) for 4 days. Efficient knockdown of canine galectin-3 was achieved using the siRNA duplex sequence 5′-AUACCAAGCUGGAUAAUAAUU-3′/3′-

GUUAUGGUUCGACCUAUUAUA-5′. Firefly luciferase siRNA was used as a control siRNA (5′-GAAUAUUGUUGCACGAUUUUU-3′/3′-UUCUUAUAACAACGUGCUAAA-5′).

2.5.3 Lipid-based transfection of siRNA duplexes

SiRNA duplexes (1–2 μg) suspended in 500 μl Opti-MEM (GIBCO) were incubated with 5 μl lipofectamine 2000 (Invitrogen) for 30 min at ambient temperature. The transfection mix (125 μl) and 0.5 × 106 MDCK cells in 333 μl of MEM were added to the top chamber of a 12-well Transwell and triturated gently. Experiments were performed 4 days later.

2.5.4 Cell surface biotinylation

Domain-selective biotinylation was performed as previously described [126]. Briefly, MDCK II cells were grown on filters for 4 days after transfection using the indicated methods. Cells were starved with cysteine-free medium for 30 min, radiolabeled for 2 h with [^{35}S]-Cys, then chased in HEPES-buffered MEM for 2 h before apical or basolateral biotinylation. Cells were solubilized and lysates were immunoprecipitated with monoclonal anti-endolyn antibody. After recovery of antibody-antigen complexes, one-fifth of each sample was reserved to calculate the total recovery, and the remainder was incubated with streptavidin to recover biotinylated proteins. Samples were resolved on SDS-PAGE and biotinylation efficiency was quantitated using a phosphorimager (Bio-Rad).

2.5.5 Measurement of polarized secretion

Filter-grown MDCK cells stably expressing GFP-ensol were starved in cysteine-free medium for 30 min, radiolabeled with $^{[35S]}$Cys for 30 min, and incubated in HEPES-buffered MEM for 90 min at 37°C. The apical and basolateral media were collected separately and the cells were solubilized in detergent-containing solution. Ensol was immunoprecipitated from all samples using monoclonal anti-endolyn antibody. The polarity of ensol secretion was quantitated after SDS-PAGE using a phosphorimager. To assess the secretion of gp80, polarized MDCK cells were incubated in Cys/Met-free medium for 30 min, radiolabeled with [^{35}S]-Cys/Met for 2 h, and then incubated in HEPES-buffered MEM for 2 h. Apical and basolateral media were collected from duplicate samples and resolved on SDS-PAGE.

2.5.6 Immunofluorescence microscopy

Mouse antibody 502 against rat endolyn was provided by Dr. G. Ihrke and used at 1:500 dilution. Hybridomas producing anti-p75 and anti-influenza HA antibodies were previously provided by Drs. E. Rodriguez-Boulan and T. Braciale, respectively, and culture supernatants were used at 1:1 dilution. Mouse anti-gp135 was a kind gift of Dr. E. Rodriguez-Boulan and was used at 1:100 dilution. Filter-grown MDCK cells were washed with chilled HEPES-buffered MEM for 15 min and blocked with HEPES-buffered MEM containing BSA for 15 min. To detect surface proteins, cells were incubated with primary antibodies for 1 h on ice, washed extensively, and then incubated with Alexa 488-conjugated goat anti-mouse (Invitrogen; 1:500) for 30 min on ice. Cells were then fixed with 4% paraformaldehyde for 15 min at 37°C and permeabilized with 0.1% (vol/vol) Triton X-100 in PBS-containing glycine and NH4Cl at ambient temperature for 5

min. Permeabilized cells were incubated sequentially with rat anti-ZO-1 hybridoma tissue culture supernatant (gift of Dr. G. Apodaca; 1:1 dilution) for 30 min at 37°C and Alexa 647-conjugated secondary antibody (Invitrogen, 1:500) for 30 min at ambient temperature. E-cadherin, occludin, and Na+-K+-ATPase were detected in fixed and permeabilized cells using mouse anti-E-cadherin antibody (BD Transduction Laboratories), mouse anti-occludin antibody (Invitrogen), and mouse anti-Na^+/K^+-ATPase (abCam), each at 1:100 dilution. To detect cilia, fixed and permeabilized cells were incubated with monoclonal anti-acetylated α-tubulin (Sigma; 1:400) and Alexa 488-conjugated secondary antibody (Invitrogen; 1:500). Confocal images were acquired using a Leica TCS SP microscope equipped with a ×100 HCX PL-APO objective or an Olympus BX61 with a ×100 1.35 NA objective and processed using MetaMorph and Adobe Photoshop software. Cilia length was quantitated from 50 images for each condition using ImageJ software (http://rsb.info.nih.gov/ij/download.html).

2.5.7 Assessment of TJ gate function

TER was determined by applying an EVOM2 epithelial voltohmmeter (WPI). Briefly, control or transfected MDCK cells were cultured on Transwell polycarbonate filters for 4 days. One Transwell chamber was left empty as a control to determine the intrinsic resistance of the filter, which was subtracted from all readings.

To measure paracellular flux, 25 μCi/ml [3H]methoxy-inulin (MP Biomedicals) in 0.5 ml medium were added to the apical chamber of filter-grown MDCK cells (triplicate samples) and the cells were incubated at 37°C. Aliquots (20 μl) of basolateral media were removed at each time point and radioactivity was assessed using a scintillation counter (Wallac).

2.5.8 Integrity of TJ fence function

MDCK cells plated for 4 days after transfection (or not) were mounted in a holder (Bioptechs) on the stage of an Olympus IX81 microscope. FM4–64FX lipophilic styryl dye (100 μM; Invitrogen) was added to the apical chamber of the cells while the basolateral compartment was continuously perfused with PBS supplemented with calcium and magnesium warmed to 37°C. Before image acquisition, the filter membrane was identified and set as the reference plane. During acquisition, images were collected every 5 s at 2.5, 5.0, and 7.5 μm above the reference plane with a ×40 objective (LUCPlanFLN, Olympus). The IX81 was equipped with a xenon lamp (Sutter Instruments) and a wide green filter set (Chroma); exposure time was 300 ms/acquisition. All parameters were controlled using Slidebook 4.2 software (I3). To quantify the average intensity over time under different transfection conditions, a line was drawn across 10 random cell boundaries per field, and the change in average intensity per minute was determined using MetaMorph. Values were normalized to the average intensity measured in untransfected cells at 0 min.

3.0 SIALYLATION OF N-LINKED GLYCANS MEDIATES APICAL DELIVERY OF ENDDOLYN IN RENAL EPITHELIAL CELLS

3.1 ABSTRACT

The sialomucin endolyn is implicated in adhesion, migration, and differentiation of various cell types. Along rat kidney tubules, endolyn is variously localized to the apical surface and endosomal/lysosomal compartments. Apical delivery of newly synthesized rat endolyn predominates over direct lysosomal delivery in polarized Madin-Darby canine kidney (MDCK) cells. Apical sorting depends on terminal processing of a subset of lumenal N-glycans. Here, we dissected the requirements of N-glycan processing for apical targeting and investigated the underlying mechanism. Modulation of glycan branching and subsequent polylactosamine elongation by knockdown of N-acetylglucosaminyltransferase III or V had no effect on apical delivery of endolyn. In contrast, combined but not individual knockdown of sialyltransferases ST3Gal-III, ST3Gal-IV, and ST6Gal-I, which together are responsible for addition of α2,3- and α2,6-linked sialic acids on N-glycans, dramatically decreased endolyn surface polarity. Endolyn synthesized in the presence of kifunensine, which blocks terminal N-glycan processing, reduced its interaction with several recombinant canine galectins, and knockdown of galectin-9 (but not galectins 3, 4 or 8) selectively disrupted endolyn polarity. Our data suggest that sialylation enables recognition of endolyn by galectin-9 to mediate efficient apical sorting. They raise the

intriguing possibility that changes in glycosyltransferase expression patterns and/or galectin-9 distribution may acutely modulate endolyn trafficking in the kidney.

3.2 INTRODUCTION

Proper kidney function requires continuous regulation of protein trafficking and targeting in response to physiological stimuli. Ion transporters and other proteins necessary for renal function must be selectively targeted to the apical or basolateral cell surface of kidney cells and internalized or redistributed on demand to enable tightly controlled recovery of ions and metabolites from the renal filtrate. The polarity of epithelial cells is maintained by active sorting of newly synthesized and recycling proteins to the apical or basolateral membrane domains, which are kept physically separated by tight junctions. The signals and mechanisms that mediate this differential sorting of cargoes are both complex and diverse. Whereas basolateral sorting signals are typically linear peptide motifs, apical sorting signals are less well defined and can be present within the lumenal, transmembrane, or cytosolic regions of the protein [reviewed in [188,189]]. Protein association with glycolipid-enriched lipid rafts has been proposed to mediate apical sorting of some glycosylphosphatidylinositol-anchored proteins as well as the influenza transmembrane proteins hemagglutinin (HA) and neuraminidase. For other proteins, including megalin and several polytopic proteins, cytoplasmic peptide sequences direct apical targeting [188]. Finally, both N- and O-linked glycans within the lumenal domains of some apical cargo have been demonstrated to function as apical targeting signals [reviewed in [118,135]].

Two models have been proposed to mediate glycan-dependent sorting of apically destined cargoes [135]. First, glycans may somehow promote cargo clustering into sorting platforms by providing structural support. Alternatively, some proteins may be segregated for apical delivery upon binding to a sorting receptor that recognizes a carbohydrate-dependent epitope on the cargo. The carbohydrate binding family of galectins (Gal) has been variously suggested to play a role in cargo sorting via both of these mechanisms. Gal-4 binding to sulfated galactosylceramides was shown to cause clustering of lipid rafts [139,140], whereas Gal-3 has been implicated in apical sorting of glycan-dependent cargoes that do not associate with lipid rafts [142,143,148]. MDCK cells express Gal-3 > Gal-9 > Gal-8 > Gal-1 >>> Gal-4 > Gal-7 > Gal-12 [138,190]. However, we found no effect of Gal-3 knockdown on the polarity of several glycan-dependent proteins, including endolyn, in MDCK cells (Chapter 2) [111,167,191].

Endolyn is a sialomucin that modulates cell adhesion, migration and signaling in hematopoietic progenitor cells, myoblasts, and cancerous epithelial cells. Endolyn cycles constitutively from the cell surface to lysosomes and is selectively sorted to the apical surface of polarized kidney cells [152,155,156]. While its function in either renal progenitor or in fully differentiated, polarized cells is currently unknown, we recently found that knockdown of endolyn in zebrafish embryos disrupted pronephric kidney morphology and function (Chapter 4). Moreover, these defects could be fully rescued by expression of rat endolyn but not by endolyn lacking apical membrane or lysosomal sorting determinants.

In polarized MDCK cells, newly synthesized and recycling endolyn is targeted apically via an N-glycan dependent mechanism [126,152,156]. The lumenally exposed portion of endolyn contains two mucin domains linked by a disulfide-bonded compact domain. Rat endolyn contains eight N-glycosylation consensus sequences (Asn-X-Ser/Thr) and 40 predicted O-

glycosylation sites [NetOglyc 3.1 program, [192]]. Previous data from our lab revealed that disruption of two of the N-glycosylation sites within the disulfide-bonded domain (at positions 68 and 74) decreased the initial polarity of endolyn delivery to ~60-65% apical (compared with 75-80% apical for wild type endolyn) [126]. Mutagenesis of all eight N-glycosylation consensus sequences in endolyn resulted in nonpolarized delivery of the protein; however apical sorting was fully rescued when N-glycosylation of Asn68 and Asn74 was restored [126]. Moreover, treatment of MDCK cells with deoxymannojirimycin or kifunensine, drugs that interfere with mannose trimming and subsequent terminal processing, fully disrupted apical delivery [126]. However, the specific glycan structure(s) required for endolyn apical delivery are unknown.

A common penultimate modification of both N- and O-glycans known to play important roles in protein sorting and cellular function is the addition of poly-N-acetyllactosamine (polylactosamine or PL) chains to N- or O-glycans. These chains, consisting of repeating units of N-acetylglucosamine and galactose (GlcNAcß1,4Gal), are added primarily to the ß1,6 branch of multi-antennary N-glycans. Availability of this site for PL addition is regulated by N-acetylglucosaminyltransferases (GlcNAcT) III and V (encoded by the GAT3 and GAT5 genes). These enzymes add or inhibit, respectively, the addition of the 1,6-linked N-acetylglucosamine to which PL is typically added. Consequently, knockdown of GlcNAcT-III leads to enhanced branching and PL addition, whereas knockdown of GlcNAcT-V disrupts PL extension. Elegant studies by Dennis and colleagues have demonstrated that PL addition regulated by these enzymes selectively modulates surface expression levels of a variety of cellular receptors [129,193]. Surface retention is apparently mediated by interaction of PL chains with Gal-3 [129]. Additionally, knockdown of GlcNAcT-III or mutagenesis of N-glycans on the Na,K-ATPase beta subunit was shown to disrupt the permeability barrier in MDCKs and led to alterations in

cell adhesion, suggesting that epithelial cells can regulate the tightness of their cell junctions by modulating N-glycan branching [194].

Instead of PL chain addition, endolyn apical delivery could be modulated by sialylation of its N-glycans. Sialic acids are acidic sugars with a nine-carbon backbone, which can be commonly found on cell surface glycolipids and glycoproteins [195]. The variety of sialic acids is created by diverse α-linkages between the 2-carbon and the underlying sugars. The most common linkages on N-glycans are to the 3- or 6-position of galactose residues, termed α2,3- and α2,6-linkages. Members of a family of at least five different α2,3 sialyltransferases (ST3Gal-I-V) are responsible for synthesis of α2,3-linked sialic acids. The ST3Gal-III and ST3Gal-IV sialyltransferases are responsible for addition of α2,3-linked sialic acids to N-glycans, whereas only one sialyltransferase, ST6Gal-I, adds α2,6-linked sialic acids to N-glycans [Chapter 13 of [196]].

In this study, we have dissected the requirements for endolyn N-glycosylation terminal processing that lead to apical sorting. While we confirmed that endolyn N-glycans are modified by PL extension, modulation of PL addition by knockdown of GlcNAcT-III or -V did not affect the polarity of endolyn delivery. In contrast, we found that addition of both α2,3 and α2,6 linked sialic acids to endolyn N-glycans was essential for efficient apical delivery of endolyn. Knockdown of Gal-9, which bound with reduced affinity to endolyn synthesized in the presence of kifunensine, disrupted endolyn polarity in MDCK cells, suggesting that Gal-9 may selectively recognize sialylated glycans on endolyn to mediate its apical sorting.

3.3 RESULTS

3.3.1 Apical delivery of endolyn is disrupted in ricin-resistant cells

Since endolyn's apical delivery is N-glycan-dependent, differential terminal processing could explain its varied distribution along the renal tubule. To confirm that terminal processing of N-glycans is important for apical delivery of endolyn, we expressed the protein in ricin-resistant MDCK (MDCK-RCA) cells. These cells are deficient in UDP-galactose transport in the Golgi complex and thus lack the ability to add galactose to either N- and O-linked glycans, as well as to glycolipids. Consequently, N- and O-glycans lack terminal processing such as polylactosamine extension or sialylation. Despite these deficiencies, MDCK-RCA cells readily form polarized monolayers [197]. Previous studies demonstrated that apical delivery of gp80 and lipid raft associated proteins were not disrupted in MDCK-RCA cells, whereas the heavily glycosylated protein gp114 was partially mis-sorted to the basolateral surface in these cells [198]. Filter grown MDCK-RCA or control cells were infected with replication-defective recombinant adenovirus expressing rat endolyn, radiolabeled with [^{35}S]-Cys, and subjected to domain selective biotinylation to assess the polarity of endolyn delivery. After biotinylation, cells were solubilized and samples were immunoprecipitated using anti-endolyn antibody. After elution, one fifth of the sample was reserved to quantify total endolyn and the remainder was incubated with streptavidin-agarose to recover the biotinylated (surface) portion. Endolyn recovered from MDCK-RCA cells migrated more rapidly on SDS-PAGE compared with endolyn from control MDCK cells, consistent with altered glycan terminal processing (Fig.13A). As predicted, endolyn polarity was significantly disrupted in the MDCK-RCA cells (36% apical compared with 75% in control cells) (Fig.13B). As a control experiment, we compared the

polarity of influenza HA, a lipid raft associated protein that is apically targeted via a glycan-independent mechanism, in MDCK and MDCK-RCA cells (Fig.13C and D). Apical delivery of newly synthesized HA was similar in both cell lines.

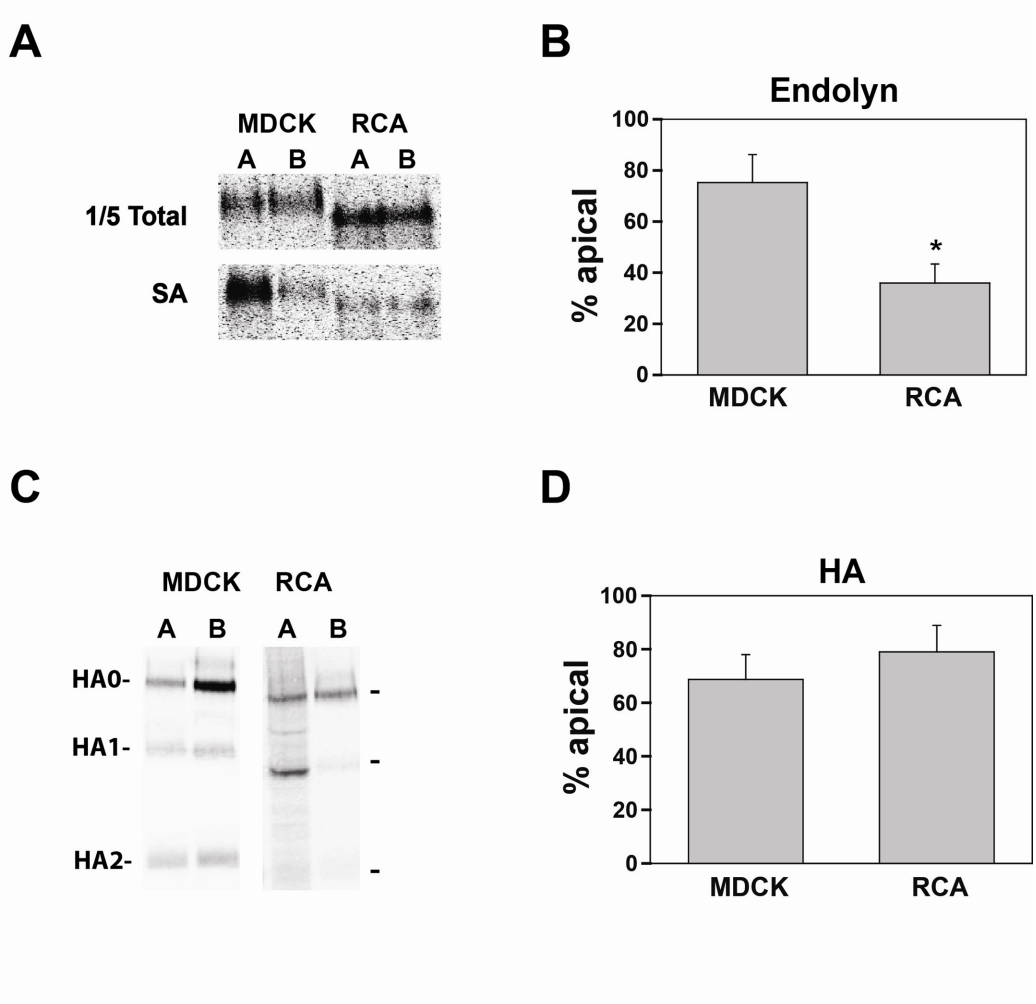

Figure 13. Endolyn polarity is selectively disrupted in ricin-resistant MDCK cells

(A) MDCK or MDCK-RCA cells were starved in cys-free medium for 30 min, radiolabeled with [^{35}S]-Cys for 2 h, and chased for 1 h. The apical or basolateral surface of duplicate filters was biotinylated and the polarity of endolyn delivery was quantitated as described in Methods. A representative gel showing one-fifth of the total sample and streptavidin (SA)-bound (surface) endolyn recovered from apically (A) and basolaterally (B) biotinylated samples is shown. (B) Endolyn polarity quantitated from three independent experiments (means ± SE) each performed in

duplicate or triplicate is plotted. *p<0.001 by Student's t-test. (C) Polarized delivery of influenza HA was assessed by metabolic labeling of either MDCK or MDCK-RCA cells expressing HA for 30 min with [^{35}S]-Met/Cys and chased for 90min, followed by domain selective trypsinization as described in Methods. The migration of full-length HA (HA0) and HA trypsin fragments (HA1 and HA2) are noted. (D) The polarity of HA was quantitated after SDS-PAGE as described in Methods. Data from two experiments are plotted.

3.3.2 Poly-N-acetyllactosamine extensions are not required for apical sorting of endolyn

As described above, extension of N-linked glycans with PL chains is known to modulate glycoprotein surface expression and protein-protein interactions in several systems, and is thus an attractive candidate to consider as a potential apical sorting signal on endolyn. To examine whether PL is important for endolyn sorting, we knocked down N-acetylglucosaminyltransferases GlcNAcT-III and GlcNAcT-V using siRNAs, to enhance or reduce PL addition, respectively (Fig.14A). Knockdown was efficient as determined by RT-PCR for GlcNAcT-III and GlcNAcT-V transcripts (Fig.14B). To test whether knockdown of these enzymes affected endolyn modification with PL, MDCK cells stably expressing endolyn and treated with the indicated siRNAs were radiolabeled with [^{35}S]-Cys for 2 h and endolyn was immunoprecipitated. After recovery of endolyn from the immunoprecipitate, equal aliquots were incubated with either immobilized tomato lectin (*Lycopersicon esculentum agglutinin*, LEA) or wheat germ agglutinin (WGA, *triticum vulgare*) or reserved to calculate total endolyn input. LEA recognizes polylactosamine, whereas WGA binds to the N-glycan chitobiose core structure Manß1,4GlcNAcß1,4GlcNAc as well as to sialic acid. As shown in Fig.14C-E, WGA-conjugated

beads captured approximately 70-80% of the total endolyn added, while only ~8% of endolyn recovered from control cells bound to LEA beads. Whereas the fraction of endolyn recovered by LEA- or WGA-conjugated beads was not increased in GlcNAcT-III knockdown cells, knockdown of GlcNAcT-V significantly reduced recovery of endolyn on LEA beads, and also increased the migration of endolyn on SDS gels (Fig.14C). Because both N- and O-linked glycans can be modified by PL extension, we also examined lectin binding of endolyn recovered from MDCK cells stably overexpressing the sialyltransferase ST6GalNAc-1 (ST6 cells), where PL extension of O-glycans is inhibited by preventing synthesis of all core O-glycans [111]. Approximately 8% of endolyn synthesized in ST6 cells bound to LEA beads, confirming that N-glycans on endolyn receive PL extension (Fig.15). Together, these data demonstrate that GlcNAcT-V knockdown decreases PL extension of N-glycans on endolyn.

To evaluate the effect of GlcNAcT knockdown on endolyn surface delivery, polarized endolyn-expressing cells were radiolabeled and subjected to domain-selective surface biotinylation. As shown in Fig.16, polarized delivery of newly synthesized endolyn was not affected by either GlcNAcT-III or GlcNAcT-V knockdown. Additionally, the total fraction of endolyn biotinylated under each condition was comparable (typically ~20%), suggesting that knockdown did not alter the efficiency of endolyn transit through the biosynthetic pathway. Similarly, no effects were observed on the steady state distribution of endolyn assessed by indirect immunofluorescence (not shown). Thus, PL extension on branched N-glycans is not required for endolyn apical delivery.

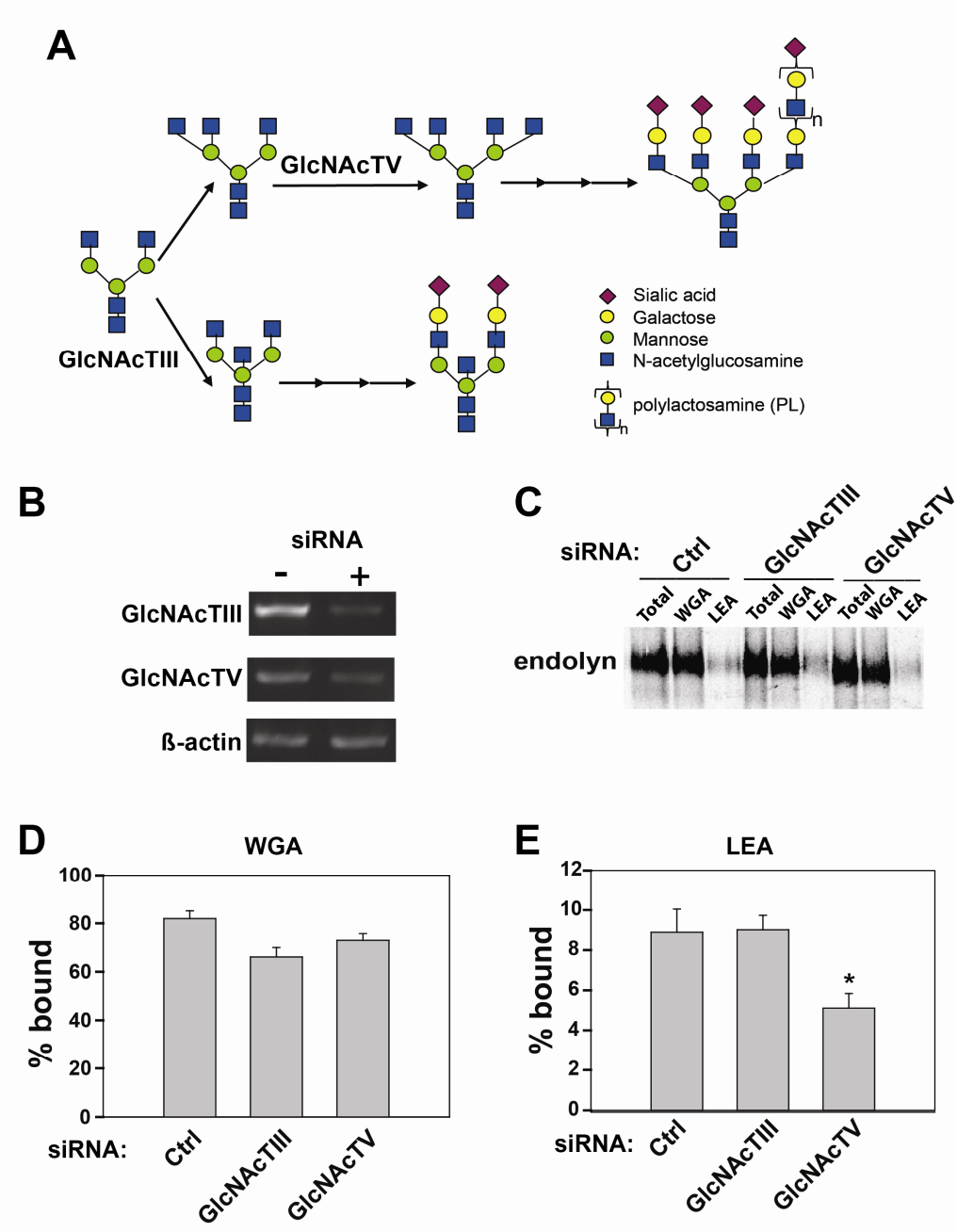

Figure 14. Modulation of N-glycan branching alters polylactosaminylation of endolyn

(A) Schematic showing the effects of GlcNAcT-III and GlcNAcT-V expression on N-glycan branching and subsequent polylactosamine extension. GlcNAcT-III activity adds a bisecting GlcNAc to the ß mannose at the core position that prevents further branching and addition of PL. The competing enzyme GlcNAcT-V adds GlcNAc to the ß1,6 branch that allows polylactosamine extension during later processing steps. (B) Efficient knockdown of GlcNAc transferase enzymes

that modulate N-glycan branching was verified by RT-PCR of MDCK cells transfected with either control siRNA or siRNA targeting GlcNAcT-III or GlcNAcT-V. RT-PCR to detect ß-actin is shown as a control for input RNA levels. (C) Extracts from metabolically labeled filter-grown MDCK cells expressing endolyn and transfected with either control siRNA or siRNA directed against GlcNAcT-III or GlcNAcT-V were immunoprecipitated with anti-endolyn antibodies. Bound fractions were eluted and equal aliquots were incubated overnight with immobilized WGA or LEA or reserved as total before analysis by SDS-PAGE. Quantitation of endolyn binding to WGA- (D) or LEA- (E) conjugated agarose The mean +/- SE of three independent experiments performed in duplicate is plotted. *p<0.05 by Student's t-test.

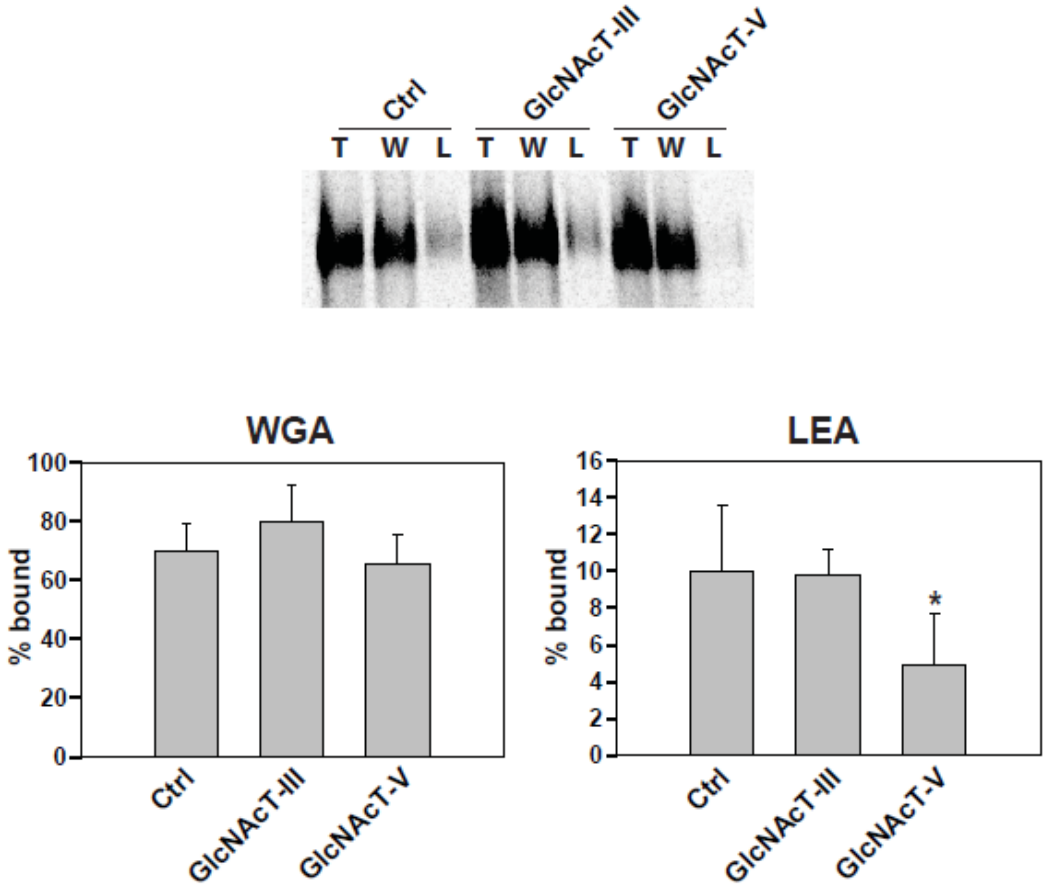

Figure 15 Endolyn N-glycans are modified by PL extension

MDCK cells stably co-expressing CMP-Neu5Ac:GalNAc-Rα2,6-sialyltransferase-1 (ST6) to block synthesis of all O-glycan core structures beyond NeuAcß1,3GalNAc-Ser/Thr and rat endolyn were transfected with either control siRNA or siRNA targeting GlcNAcT-III or GlcNAcT-V. Cells were cultured on permeable supports for three days, radiolabeled with [^{35}S]-Cys, and lysates immunoprecipitated with anti-endolyn antibodies. Binding to lectin-conjugated beads was performed as described in Methods. A representative gel is shown along with quantitation of endolyn binding to WGA- or LEA-conjugated agarose. The mean +/- SE of three independent experiments performed in duplicate is plotted. *p<0.05 by Student's t-test.

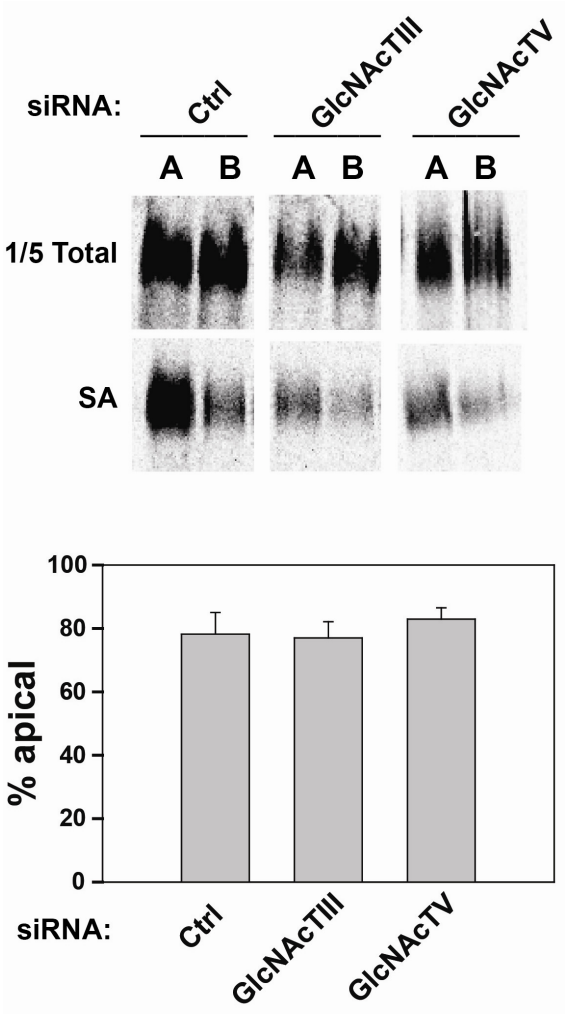

Figure 16. Biosynthetic delivery of endolyn is not affected by knockdown of GlcNAcT-III and GlcNAcT-V

Domain selective biotinylation was performed on MDCK cells stably expressing rat endolyn and transfected with either control siRNA or GlcNAcT-III, GlcNAcT-V siRNAs as described in Methods. A representative gel showing 1/5 total and surface endolyn recovered from apically (A) and basolaterally (B) biotinylated samples is shown (top). Endolyn polarity (mean ± SE) quantitated from 6 independent experiments each performed in duplicate or triplicate is plotted below.

3.3.3 Sialylation of endolyn N-glycans is required for apical delivery

We next examined whether addition of sialic acids to the termini of endolyn N-glycans is important for apical sorting. To test whether endolyn contains α2,3- and/or α2,6-linked sialic acids, we incubated radiolabeled endolyn immunoprecipitated from polarized MDCK cells with the sialic-acid-binding lectins *Maackia amurensis agglutinin* (MAA) and *Sambucus nigra agglutinin* (SNA), which specifically bind to α2,3 and α2,6 linkages, respectively. Whereas 73% of endolyn bound to MAA beads, only 16% was recovered on SNA beads (Fig. 17B and C, Ctrl), suggesting that the sialic acids on endolyn are predominantly in the α2,3 linkage. Additional experiments in which endolyn biotinylated at the apical or basolateral surface was recovered and incubated with lectin beads revealed that the apical and basolateral pools of endolyn had identical SNA and MAA binding profiles (data not shown).

Next, we knocked down ST3Gal-III, ST3Gal-IV, or ST6Gal-I (or various combinations) and examined the effect on sialylation of endolyn. Efficient knockdown of each enzyme was confirmed by RT-PCR analysis of transcript levels (Fig.17A) and the effects on glycan structures evaluated by lectin pull-down assays as described above. Endolyn recovery on MAA beads

tended to be lower when the enzymes responsible for α2,3 sialic acid addition (ST3Gal-III and IV) were knocked down individually, although these values were not significantly different from control. However, knockdown of both enzymes together (with or without concomitant ST6Gal-I knockdown to eliminate O-glycan synthesis) significantly reduced binding (from 73% in control to 35% upon double knockdown). As expected, knockdown of ST6Gal-I alone had no effect on endolyn binding to MAA (Fig.17B and C). Conversely, only knockdown of ST6Gal-I (alone or in combination with knockdown of ST3Gal-III and ST3Gal-IV) significantly reduced binding of endolyn to SNA lectin. This demonstrates that N-glycans on endolyn are sialylated in both α2,3- and α2,6-linkage.

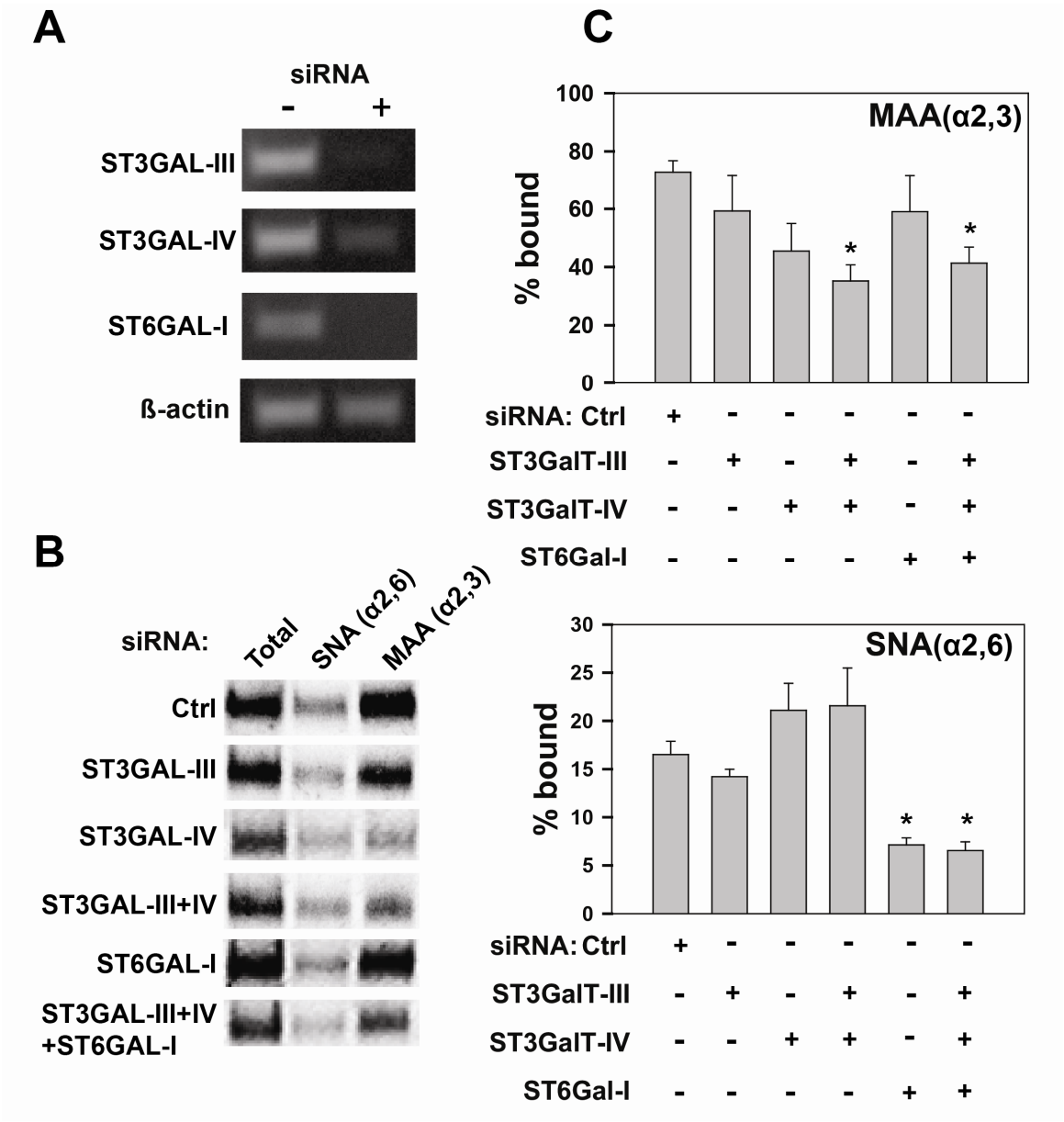

Figure 17. Endolyn contains both α2,3 and α2,6-linked sialic acids

MDCK cells were transfected with control siRNA or siRNA targeting ST3Gal-III, ST3Gal-IV or ST6Gal-I in the indicated combinations. (A) RT-PCR of siRNA-treated MDCK cells demonstrates efficient knockdown of canine sialyltransferases. (B) Immunoprecipitates from endolyn expressing, metabolically labeled MDCK cells transfected with the indicated combinations of siRNAs were incubated overnight with beads conjugated to *Sambucus nigra agglutinin* (SNA) or

***Maackia amurensis agglutinin* (MAA), then washed and bound fractions analyzed by SDS-PAGE (C) Three independent experiments were quantified and plotted. *p<0.05.**

To examine the role of sialylation in endolyn apical sorting, we performed domain selective cell surface biotinylation of endolyn in cells lacking the individual sialyltransferases described above or combinations of all three (Fig. 18). Knockdown of ST3Gal-III or ST3Gal-IV individually or together had no effect on the polarity of endolyn delivery. Similarly, depletion of ST6Gal-I was without effect on endolyn polarity. However, polarized endolyn delivery was significantly disrupted in cells depleted of all three sialyltransferases compared to cells transfected with control siRNA (48% apical in the triple knockdown cells compared with 75% in control cells).

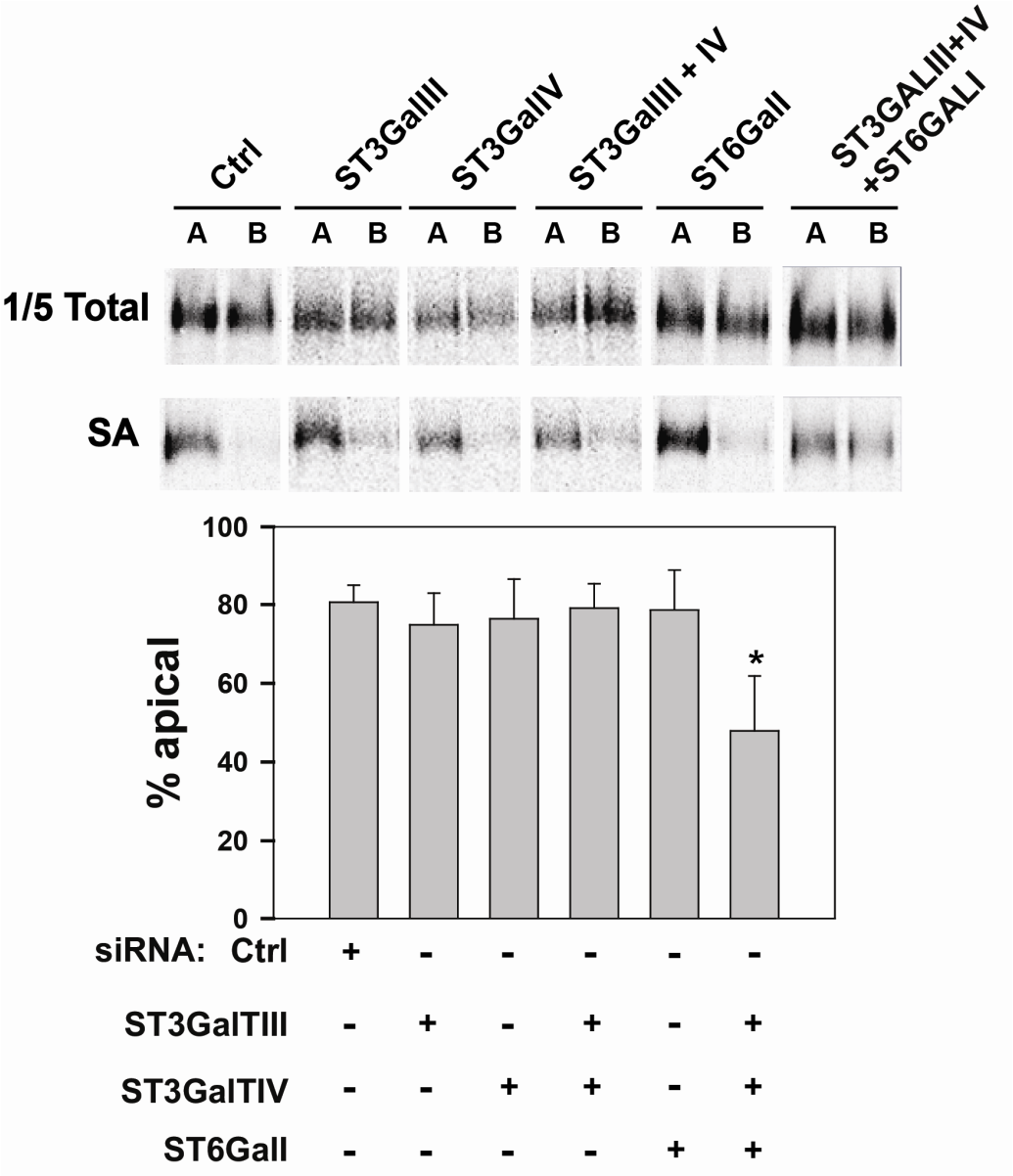

Figure 18. Both α2,3 and α2,6 linked sialic acids are required for efficient apical delivery of endolyn

The polarity of endolyn delivery was assessed in MDCK cells transfected with either control siRNA or siRNA targeting ST3Gal-lII, ST3Gal-IV and ST6Gal-I as indicated Representative gels showing total and surface (SA) endolyn recovered from apically (A) and basolaterally (B) biotinylated samples are shown on the top and endolyn polarity (mean ± SE) in 3 independent experiments each performed in duplicate or triplicate is plotted below. *p=0.033 by Student's t-test.

To examine whether sialyltransferase knockdown caused a generic disruption in apical protein distribution, we examined the surface distribution of endolyn and two additional apical markers (influenza HA and the neurotrophin receptor p75) in control and knockdown cells using indirect immunofluorescence (Fig. 19). Apical delivery of both HA and p75 is independent of N-linked glycosylation [29, 84]. All three proteins were tightly localized to the apical surface in polarized MDCK cells treated with control siRNA. As predicted, endolyn distribution was shifted in cells depleted of all three sialyltransferases, with considerable basolateral staining now evident. Importantly, tight junctions were apparently normal in these cells as demonstrated by ZO-1 staining. In contrast, the apical distributions of HA and p75 were unaffected by sialyltransferase depletion. Overall, these results suggested that sialylation of N-glycans is required for the apical biosynthetic delivery and steady state distribution of endolyn.

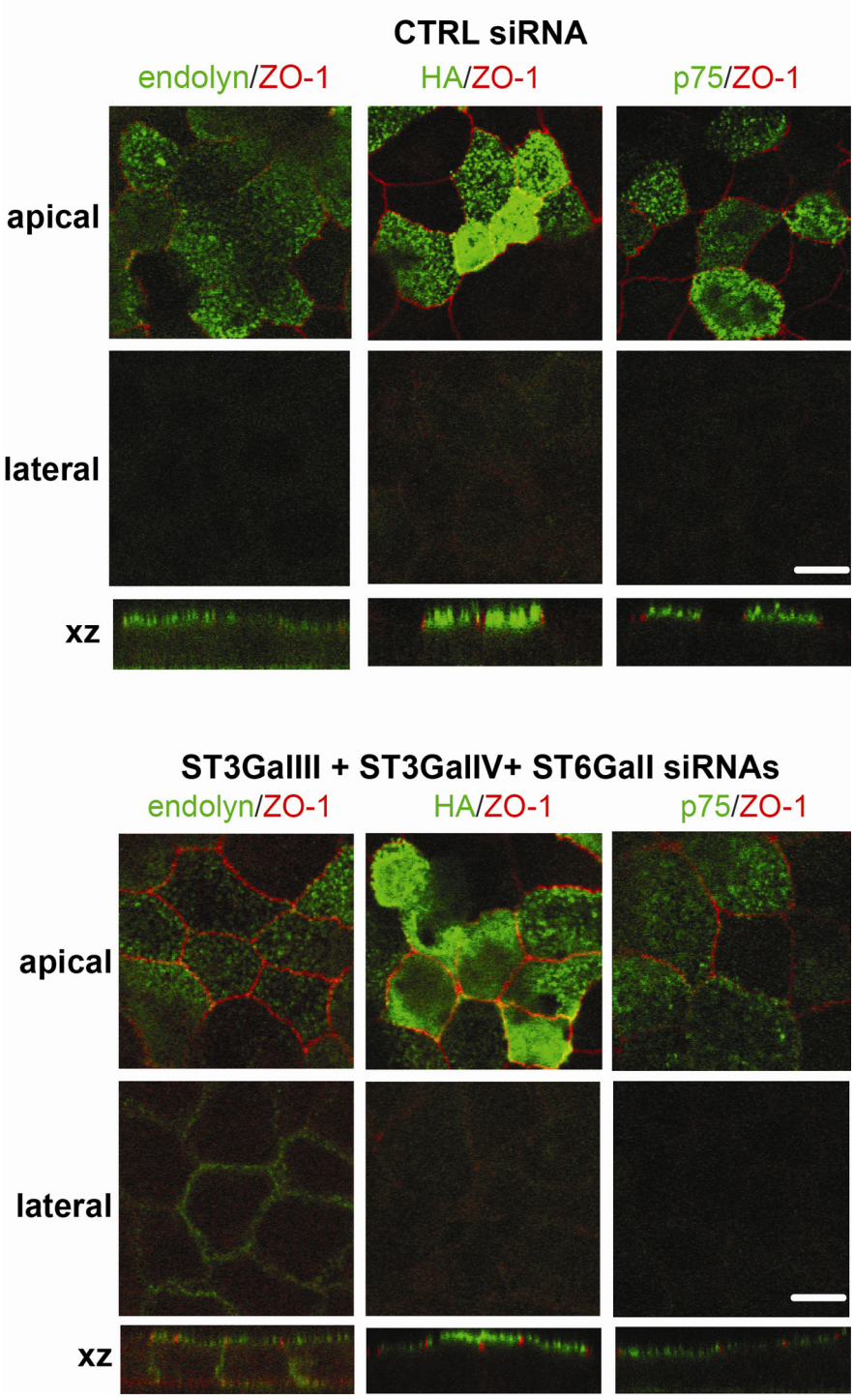

Figure 19. The steady state surface distribution of endolyn is selectively disrupted in sialyltransferase-depleted cells

MDCK cells expressing endolyn, HA, or the neurotrophin receptor p75 were transfected with control siRNA or ST3Gal-III, ST3Gal-IV and ST6Gal-I siRNA combinations as indicated and

processed for surface labeling of the indicated protein (green) as described in Methods. Cells were then fixed and permeabilized and processed to detect the tight junction marker ZO-1 (red). Cells were imaged by confocal microscopy. Single xy sections of overlay images are shown at apical and lateral levels. Xz sections of stacks are shown. Bar = 10 µm.

3.3.4 Galectin-9 plays a role in apical sorting of endolyn

Members of the galectin family have been implicated in cell differentiation and apical protein sorting via several distinct mechanisms [139,148,199,200]. MDCKs express several galectins, including Gal-1, -3, -4, -7, -8, -9, and -12 [138,190]. To see whether galectins might play a role in endolyn sorting, we tested the interaction of radiolabeled endolyn synthesized in the presence or absence of kifunensine (KIF inhibits terminal N-glycan processing) with recombinant GST-tagged canine galectins -1, -3, -4, -7, -8, -9N, and -9C bound to glutathione-conjugated beads as described in Methods. The N-terminal (9N) and C-terminal (9C) carbohydrate recognition domains of Gal-9 were expressed separately due to aggregation of the recombinant full-length canine Gal-9 in bacteria [138]. Interestingly, treatment with KIF dramatically reduced interaction of endolyn with galectins -3, -4, -7, and -9N (Fig. 20).

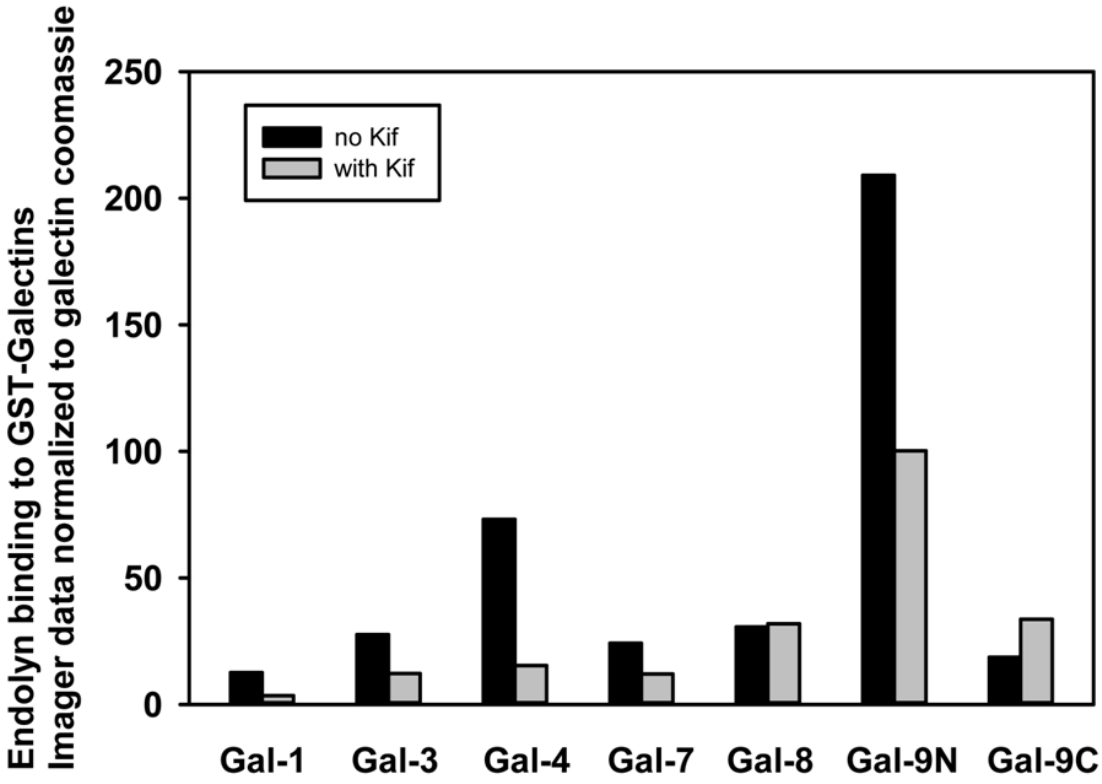

Figure 20. Endolyn synthesized in the presence or absence of kifunensine binds differentially to recombinant canine galectins

Polarized MDCK cells infected with adenovirus encoding rat endolyn were starved for 30 min in cysteine free medium in the presence or absence of 20 µM kifunensine and then radiolabeled with [^{35}S]Cys for 30 min and chased for 90 min in the continued presence of drug. Endolyn was immunoprecipitated from cell extracts and eluted in SDS. The samples were divided into equal aliquots and incubated overnight with recombinant GST-conjugated Gal-1, 3, 4, 7, 8, 9N and 9C prebound to glutathione-beads. The following day beads were washed with buffer, then incubated with sucrose (non-specific binding), and finally with lactose (to elute specifically-bound components). Eluted [^{35}S]-endolyn was analyzed with a BioRad Imager after SDS-PAGE. The beads were incubated with SDS sample buffer to elute GST-Gal for SDS-PAGE and subsequent

staining with Coomassie Blue to quantify bound galectins. Binding of [^{35}S]-endolyn was normalized to the amount of GST-galectin eluted from the beads as previously described [138]. Figure provided by Dr. R Hughey.

We previously showed that Gal-3 is not involved in endolyn delivery (Chapter 2), and Gal-7 has been localized on the primary cilium of polarized kidney epithelial cells where it functions in ciliogenesis and wound healing [201]. We therefore knocked down Gal-4 and -9 and examined their effects on endolyn polarity. Additionally, because Gal-8 selectively binds to sialic acid, we also tested the effect of Gal-8 knockdown on endolyn distribution. Knockdown of Gal-4 or Gal-8 was efficient based on RT-PCR analysis, but had no effect on endolyn polarity monitored by indirect immunofluorescence or by domain selective biotinylation (Fig.21).

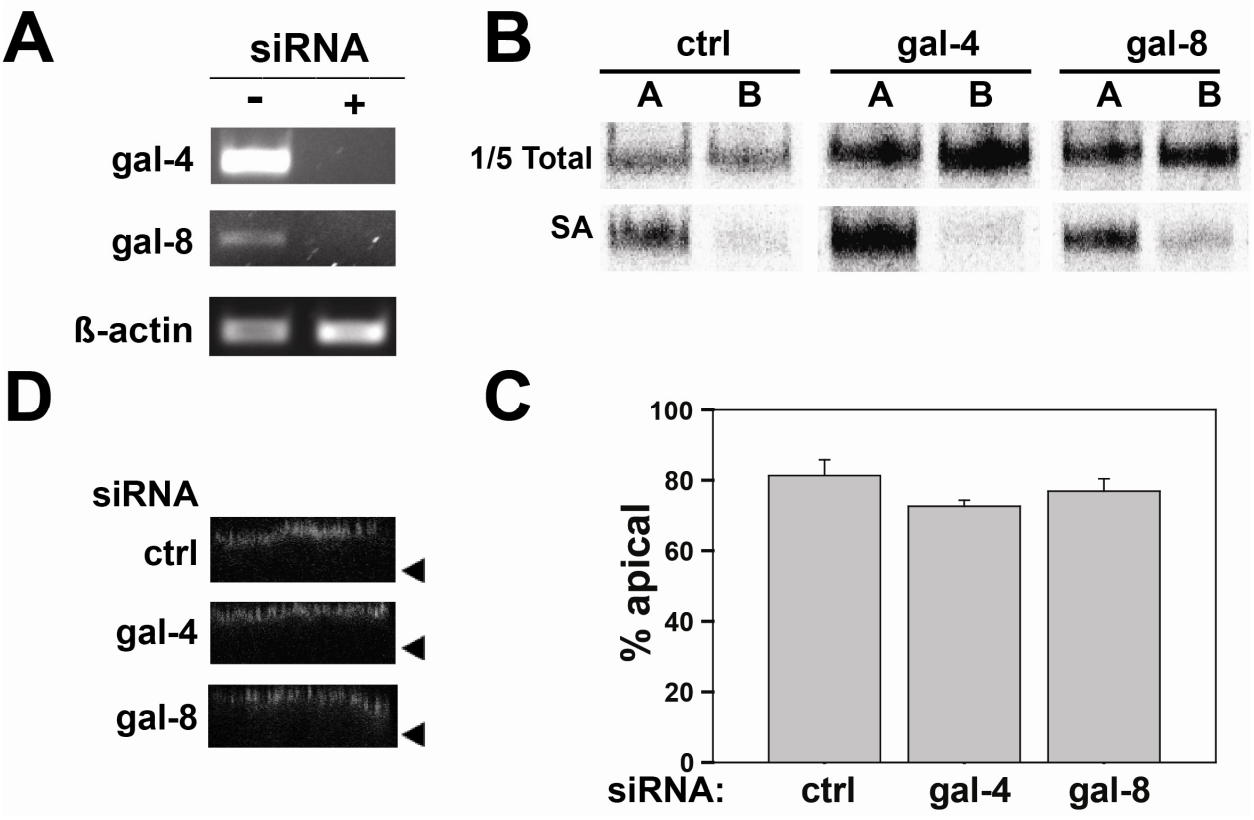

Figure 21. Knockdown of galectins-4 and -8 do not affect endolyn polarity

MDCK cells were transfected with control siRNA or siRNAs targeting galectin-4 and galectin-8. (A) RT-PCR of transfected cells indicates efficient knockdown of canine galectin-4 and galectin-8 after four days. (B) Filter-grown MDCK cells stably expressing endolyn were radiolabeled and endolyn polarity was assessed by domain selective biotinylation. Representative gels are shown. (C) Four independent experiments with duplicate and triplicate samples are plotted (mean ± SE). (D) The steady state surface distribution of endolyn was examined by confocal microscopy. Representative xz sections of stacks of cells treated with the indicated siRNA duplexes are shown. The arrowheads indicate the position of the filter.

Knockdown of Gal-9 was similarly efficient (Fig.22A) but resulted in statistically significant, though modest, redirection of newly synthesized endolyn to the basolateral surface Fig. 22B and C. In contrast, biosynthetic delivery of influenza HA as measured by domain selective trypsinization was unaffected by Gal-9 knockdown (Fig.22D and E). Indirect immunofluorescence confirmed the partial redistribution of endolyn in Gal-9 depleted cells, whereas the steady state localization of HA and p75 were unaffected (Fig.23). Because knockdown of Gal-9 in MDCK cells for five days by induction of lentiviral-expressed shRNA was reported to dramatically affect global cell polarity, we also monitored transepithelial resistance, the distribution of the tight junction marker ZO-1, and the polarity of the endogenously expressed apical protein gp135 (Fig.24). None of these were altered in cells treated with siRNA targeting Gal-9 compared with control siRNA, indicating that the effects of Gal-9 depletion on endolyn delivery and distribution are not due to global perturbations in cell polarity. Thus, Gal-9 has a mechanistic role in the N-glycan dependent apical sorting of endolyn.

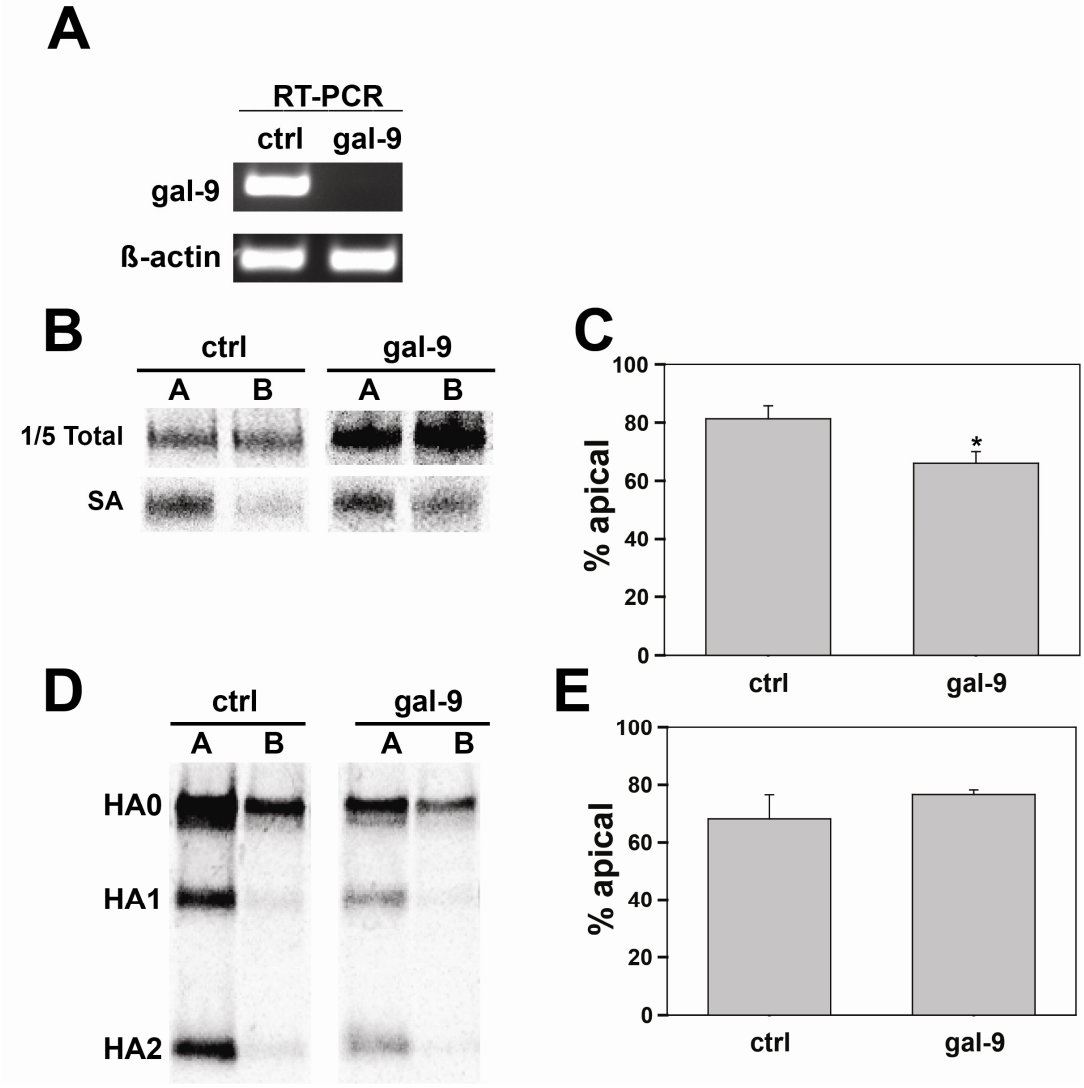

Figure 22. Knockdown of galectin-9 selectively disrupts endolyn polarity

MDCK cells were transfected with control or Gal-9 siRNA duplexes. (A) RT-PCR of siRNA-treated MDCK cells demonstrates efficient knockdown of canine Gal-9. The polarity of endolyn in MDCK cells transfected with either control siRNA or galectin-9 siRNA was assessed using domain selective biotinylation as described in Methods. Representative gels are shown in (B) and five independent experiments with duplicate or triplicate samples are plotted (mean ± SE; *p=0.037 by Student's t-test). (C). Polarized delivery of influenza HA was assessed as described in Methods. The migration of full length (HA0), and HA trypsin fragments (HA1 and HA2) is shown in (D), and HA polarity is plotted in (E).

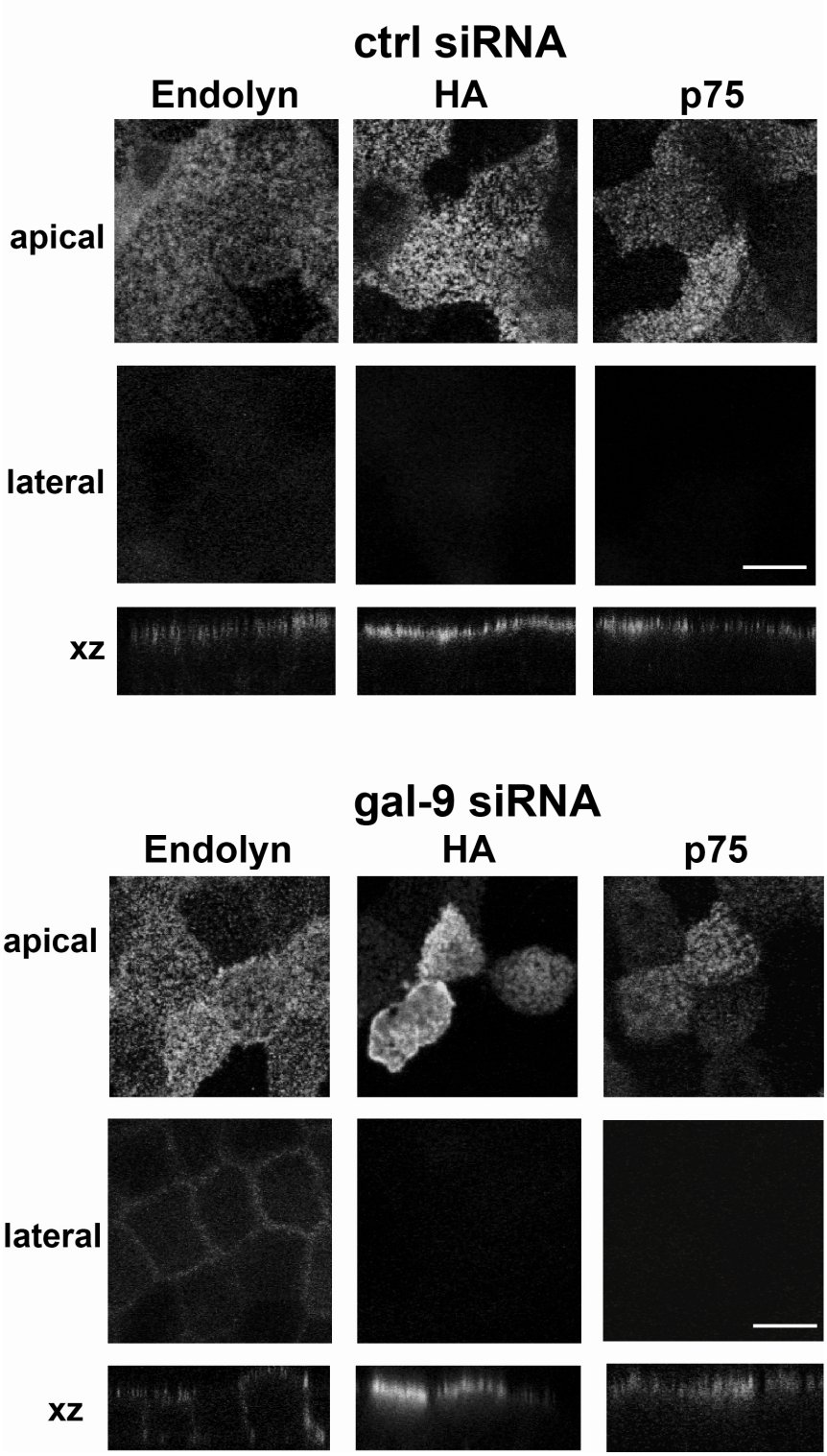

Figure 23. Knockdown of galectin-9 selectively alters the steady state surface distribution of endolyn

MDCK cells transfected with control or Gal-9 siRNA duplexes were grown on filter supports for three days and then infected with replication defective recombinant adenoviruses encoding endolyn, HA, or p75. Cells were processed to detect surface proteins as described in Methods and imaged using confocal microscopy. Representative xy sections through apical and middle ("lateral") planes and xz sections are shown. Bar = 10 µm.

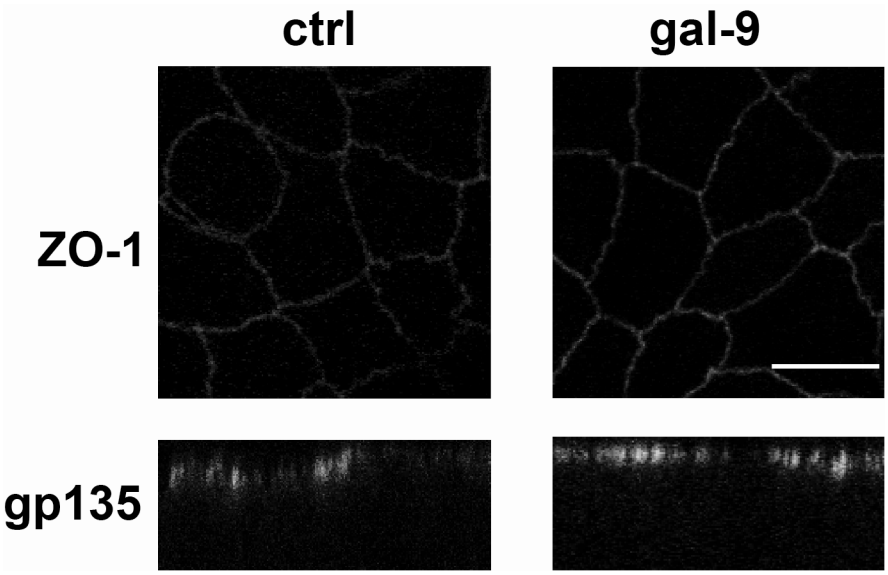

Figure 24. The polarity of MDCK cells is retained in galectin-9-depleted cells

Filter-grown MDCK cells transfected with control or Gal-9 siRNA were fixed and processed for indirect immunofluorescence to detect the tight junction marker ZO-1 and the endogenous apical protein gp135 (antibody used at 1:500 dilution; kind gift of Enrique Rodriguez-Boulan). Representative xy sections at the level of the tight junctions showing ZO-1 staining and xz sections showing gp135 distribution are depicted. Bar = 10 µm.

3.4 DISCUSSION

In this study we have examined the determinants that mediate apical sorting of endolyn in polarized renal epithelial cells. Endolyn was delivered largely to the basolateral surface in ricin-resistant cells, which are unable to add terminal glycan modifications, consistent with our previous demonstration that terminal processing of N-glycans rather than the core N-glycan structures on endolyn are required for apical sorting [126]. While we found that endolyn N-glycans exhibit PL extension, this modification is apparently not required for polarized delivery, as knockdown of the enzymes that modulate N-glycan branching and regulate PL addition had no effect on endolyn sorting. This finding is consistent with our previously reported observation that polarity of endolyn and other glycan-dependent apical proteins is unaffected by knockdown of Gal-3, which efficiently binds to PL chains [111,167,202]. Rather, the presence of both α2,3 and α2,6-linked sialic acids on endolyn N-glycans was required for efficient apical sorting of the protein. Interestingly, inhibition of endolyn terminal processing disrupted its binding to several canine galectins *in vitro*, and knockdown of Gal-9 (but not other galectins examined) selectively disrupted endolyn polarity. We conclude that Gal-9 mediated interaction with sialylated N-glycans on endolyn is important for apical targeting.

3.4.1 Sialic acid as an apical sorting determinant

Efficient apical sorting requires addition of either α2,3 and α2,6 linked sialic acids to endolyn N-glycans, as we observed defects in the polarity of delivery of newly synthesized endolyn, as well as the steady state distribution, only when ST6Gal-I was knocked down in conjunction with ST3Gal-III and –IV. This suggests that a threshold level of sialic acid *per se* rather than the

presence of specific linkages is sufficient to ensure sorting. Our lectin binding studies measure binding to both N- and O-linked sialic acids, so changes in the levels of sialic acids on N-linked glycans cannot be directly assessed. However, knockdown of the sialyltransferases selective for N-linked glycans clearly affected binding to sialic acid-specific lectins and combined prevented polarized sorting of endolyn.

Sialylation of N- and O-glycans has previously been implicated in the sorting of other apical cargoes, including a secreted version of dipeptidylpeptidase IV [117]. Additionally, Real and colleagues have suggested a role for sialylation in apical delivery of glycoproteins in HT-29 and Caco-2 cells [203,204]. This conclusion was based on the observation that long-term treatment of cells with GalNAc-β-O-benzyl inhibits sialylation and causes intracellular retention of apically- but not basolaterally-destined proteins [113,203].

How might sialic acids mediate apical sorting? It has been proposed that clustering of newly synthesized glycoproteins is a universal mechanism to sort apically designated cargos [188]. It is possible that sialic acids facilitate the clustering or crosslinking of proteins into apical sorting platforms, either by enabling interactions between the cargo molecules themselves or through binding to sorting receptors such as galectins. Sialylated N-glycans have previously been shown to be important for oligomerization of the serotonin transporter and its interaction with myosin IIA in CHO cells [205].

3.4.2 Mechanism of galectin-mediated sorting

Galectins may facilitate glycoprotein clustering and segregation as (i) they recognize modified forms of a common structure present on both N- and O-glycans (PL); (ii) form dimers or higher

order oligomers; and (iii) are known to segregate glycoproteins into distinct membrane domains [206].

How and where might binding to Gal-9 mediate endolyn sorting? Galectins are synthesized in the cytosol and exported from the cell via an unconventional and poorly understood secretion pathway. They can then bind to surface glycoconjugates and be internalized into endocytic compartments. Indeed, Gal-9 was found to bind selectively to the apically enriched Forssman glycolipid, and internalization studies following the trafficking of apically added Gal-9 revealed efficient retrograde transport to the TGN as well as to Rab11 positive compartments [199]. As endolyn traffics through the ARE *en route* to the apical surface, it is conceivable that endolyn could bind to Gal-9 at either of these locations [168]. We previously showed that apical recycling of endolyn is disrupted when the apical surface pool of endolyn is desialylated [156]. Thus, Gal-9 might play a role in endolyn sorting in both the biosynthetic and the postendocytic pathway.

In a previously published study, MDCK cells depleted of Gal-9 for 5 days using an inducible shRNA showed dramatic changes in cell morphology, polarity, and transepithelial resistance (TER) [199]. In contrast, under our Gal-9 depletion conditions, we did not observe any changes to cell structure, polarity, or TER other than reduced endolyn polarity. This may reflect a lower efficiency of Gal-9 depletion than that achieved by Mishra et al. [199]. While our RT-PCR analysis confirmed essentially complete depletion of Gal-9 mRNA, we were unable to measure Gal-9 protein levels as available antibodies did not recognize canine Gal-9.

Gal-9 contains two carbohydrate recognition domains (CRDs), and intriguingly, only the N-terminal domain bound to endolyn in our *in vitro* studies. We speculate that differential glycan binding specificities of these domains may allow Gal-9 to be internalized utilizing the C-terminal

CRD (possibly by binding to the Forssman glycolipid) and interacting with cargo to be exported via the N-terminal CRD. Alternatively, the binding of Gal-9 to two distinct cargo proteins that have the intrinsic capacity to form dimers or oligomers could enable their crosslinking into a network able to recruit sorting machinery with high avidity. In support of this idea, there is evidence that endolyn can form dimers [207].

Our findings that endolyn showed clear preference for binding Gal-9N, and that blocking terminal N-glycan processing with KIF specifically reduced binding to Gal-9N, led us to discover a role for Gal-9 in apical targeting of endolyn through knockdown experiments. However, our previous characterization of canine Gal-9N on a synthetic array of glycans did not reveal a preference for sialylated N-glycans. Instead, Gal-9N preferentially bound N-glycans with terminal blood group A and 3-O-sulfated disaccharides [138]. As the array was created with synthetic glycans attached through various linkers to glass slides, it is possible that Gal-9N has additional preferences in a natural setting, such as that created by the two adjacent N-glycans on the disulfide-loop of endolyn that we previously identified as critical for endolyn apical targeting. Alternatively, canine Gal-9N could have preference for a dog-specific sialic acid-dependent N-linked structure expressed in MDCK cells. Future studies using a natural array created from MDCK cells should reveal any unique N-glycan structures [208].

3.5 MATERIAL AND METHOD

3.5.1 Cell line

MDCK II cells stably expressing rat endolyn was previously generated [126]. To maintain the expression, cells were cultured in modified Eagle's medium (Sigma) with 10% FBS and 400 μg/ml G418. Wild type MDCK II cells and ricin-resistant cells (MDCK-RCA were cultured in modified Eagle's medium supplemented with 10% FBS).

3.5.2 Antibodies

Mouse monoclonal antibodies 501 and 502, and rabbit polyclonal antibody 6431 (for immunofluorescence, 1:500 dilution) against rat endolyn were described in [126]. Antibodies 501 and 502 were used interchangeably at the same concentrations and gave similar results (for IP, 1:20,000; for IF, 1:500 dilution). Hybridomas expressing anti-p75 and anti-HA were gifts from Dr. Enrique Rodriguez-Boulan and Dr. Thomas Braciale, respectively, and used at 1:1 dilution for IF). Hybridoma supernatant expressing rat monoclonal anti-ZO-1 was provided by Dr. Gerard Apodaca and used neat.

3.5.3 Replication-defective recombinant adenoviruses and infection

Generation of replication-defective recombinant adenoviruses expressing HA, p75 and endolyn using the Cre-Lox system has been previously described [185,186]. To express HA, p75 and endolyn, MDCK cells stably expressing the tetracycline transactivator were directly

used. Adenovirus expressing this transactivator was used for MDCK-RCA adenoviral infection. Cells were first incubated in calcium-free PBS with 1mM $MgCl_2$ for 5 min at room temperature. Then PBS Magnesium containing adenovirus sufficient for a range of infection of 50 were added to the transwells. Cells were incubated for 1 hr at 37°C. Cells were washed with PBS Magnesium and incubated with MEM media over night at 37°C.

3.5.4 SiRNA knockdown

All siRNA constructs were ordered through Dharmacon. SiRNA duplex sequences for GlcNAcT-III and -V, ST3Gal-III and -IV, ST6Gal-I are listed in Table 1. For GlcNAcT-III and -V knockdown, siRNA duplexes (4-5 µg) suspended in 500 µl Opti-MEM (GIBCO) were incubated with 15 µl lipofectamine 2000 for 30 min at ambient temperature. The transfection mix (125 µl) and $0.5*10^6$ MDCK cells in 333 µl of MEM were added to the top chamber of a 12-well transwell and triturated gently. Experiments were performed 4 days later. For ST3Gal-III, -IV and ST6Gal-I knockdown, 3-4 µg siRNA duplexes and 10 µl lipofectamine 2000 were used. For double and triple knockdown, 1-2 µg of each siRNA were mixed together and 20 µllipofectamine 2000 were used. For knockdown of galectins, 3-4 µg siRNA duplex and 15 µl lipofectamine 2000 was used.

Table 1. Sequences of siRNA duplexes

Name	siRNA duplexes
GlcNAcT-III	5-CGAAGUACCUGCUCAACAAUU-3 3-UUGCUUCAUGGACGAGUUGUU-5
GlcNAcT-V	5-UGAAGAAGGUUGUAGGAAAUU-3 3-UUACUUCUUCCAACAUCCUUU-3
ST3Gal-III	5-UUGCUUGACCUUUGAUCCUU-3 3-UUAACAGAACUGGAAACUAGG-5
ST3Gal-IV	5-AGGGUGAGGCAGAGAGAAAUU-3 3-UUUCCCACUCCGUCUCUCUUU-5
ST6Gal-I	5-UGAGAGGGUGGAGAAACAUU-3 3-UUACUCUCCCGACCUCUUUGU-5
Galectin-4	5-GGGACAAGGUGGUGUUCAAUU-3 3-UUCCCUGUUCCACCACAAGUU-5
Galectin-8	5-GGAAAUUGAUGGAGAUAUUUG-3 3-GUCCUUUAACUACCUCUAUAA-5
Galectin-9	5-GUGGAUAUGUGGUCUGUAAUG-3 3-GUCACCUAUACACCAGACAUU-5

3.5.5 RT-PCR

RNA from MDCK cells treated with the indicated siRNAs was extracted using the RNAqueous phenol-free RNA isolation kit (Ambion) according to the manufacturer's recommendations. Purified RNA (500 ng-1 μg) was incubated with Moloney Murine Leukemia Virus reverse transcriptase (Ambion) at 42°C for 1 h. PCR reactions were set up after inactivation of reverse transcriptase using the GeneAmp High Fidelity PCR system (Applied Biosystems). Primers were designed using PrimerQuest on IDT website and ordered from them. For β-actin, approximately 200bp amplified sequence is expected whereas for the remainder indicated genes, ~600bp amplified sequences is expected. The denaturing temperature was 95°C, the annealing temperature was 55°C and the extension temp was 68°C, with an amplification cycle of 25.

3.5.6 Domain selective biotinylation

Domain-selective biotinylation was performed as previously described [167]. Briefly, MDCK II cells were grown on filters for 4 days after transfection with the indicated siRNA duplexes. Cells were starved with cysteine-free medium for 30 min, radiolabeled for 2 h with [^{35}S]-cysteine (MP Biomedical), then chased in HEPES-buffered MEM for 1 h before apical or basolateral biotinylation. Cells were solubilized and lysates were immunoprecipitated with monoclonal anti-endolyn antibody 501 or 502. After recovery of antibody-antigen complexes, one-fifth of each sample was reserved to calculate the total recovery, and the remainder was incubated with streptavidin to recover biotinylated proteins. Samples were resolved on SDS-PAGE and biotinylation efficiency was quantitated using a phosphorimager (Bio-Rad). Statistical significance was analyzed using Student's t test.

3.5.7 Surface delivery of HA

Wildtype MDCK or MDCK-RCA cells were plated on transwells for 3 days before infected with adenoviruses encoding HA and tetracycline transactivator. The cells were starved for 30min and radiolabeled for 30min with [^{35}S]-Cys/Met, followed by chase for 2 h. The cells were rapidly chilled on ice and rinsed with ice-cold PBS, and then incubated with 100 μg/ml TPCK-trypsin (Sigma) for 30 min, followed by incubation with PBS containing 200 μg/ml soybean trypsin inhibitor (Sigma). Full length HA (HA0) as well as both of its cleavage products (HA1 and HA2) were immunoprecipitated using monoclonal antibody Fc125. Samples were resolved on SDS-PAGE and the percentage of cleaved HA was quantitated.

3.5.8 Immunofluorescence microscopy

Filter-grown MDCK cells were washed with chilled HEPES-buffered MEM for 15 min and blocked with HEPES-buffered MEM containing BSA and 10%FBS for 15 min. To detect surface proteins, cells were incubated with primary antibodies for 1 h on ice, washed extensively, and then incubated with Alexa 488-conjugated goat secondary (Invitrogen; 1:500) for 30 min on ice. After extensive wash, cells were fixed with 4% paraformaldehyde for 15 min at room temperature and permeabilized with 0.1% (vol/vol) Triton X-100 in PBS-containing glycine and NH_4Cl at ambient temperature for 5 min. Permeabilized cells were incubated sequentially with rat anti-ZO-1 hybridoma supernatant for 30 min at 37°C and Alexa 647-conjugated secondary antibody (Invitrogen, 1:500) for 30 min at ambient temperature. Confocal images were acquired using a Leica TCS SP microscope equipped with a100X HCX PL-APO objective and processed using MetaMorph and Adobe Photoshop software.

3.5.9 Lectin binding assays

The protocol is adapted from [111]. Polarized MDCK cells stably expressing endolyn and transfected with the indicated siRNA duplexes were metabolically labeled with [^{35}S]-Cys (MP Biomedical) for 2 h and chased for 1 h. After immunoprecipitation, samples were eluted into 2% SDS, diluted with RIPA buffer and incubated with 50µl of the indicated lectin-agarose beads (EY Laboratories). For LEA and WGA lectin binding, eluted samples were divided into three aliquots, one of which was reserved as "total". For SNA and MAA lectin binding, one-fifth of the samples was reserved to calculate the total IP and the remainder was divided equally for incubation with immobilized lectins as indicated. Samples were incubated with lectin beads overnight at 4^{o}C with end-over-end mixing, washed one time with RIPA and analyzed by SDS-PAGE.

4.0 APICAL TARGETING AND ENDOCYTOSIS OF THE SIALOMUCIN ENDOLYN ARE ESSENTIAL FOR ESTABLISHMENT OF ZEBRAFISH PRONEPHRIC KIDNEY FUNCTION

4.1 ABSTRACT

Kidney function requires the appropriate distribution of membrane proteins between the apical and basolateral surfaces along the kidney tubule. Further, the absolute amount of a protein at the cell surface vs. intracellular compartments must be attuned to specific physiological needs. Endolyn (CD164) is a transmembrane protein that is expressed at the brush border and in apical endosomes of the proximal convoluted tubule and in lysosomes of more distal segments. Endolyn has been shown to regulate CXCR4 signaling in hematopoietic precursor cells and myoblasts; however, little is known about endolyn function in adult or developing kidney. Here we identify endolyn as a novel gene important for zebrafish pronephric kidney function. Zebrafish endolyn lacks the amino terminal mucin-like domain of the mammalian protein, but is otherwise highly conserved. Using in situ hybridization we show that endolyn is expressed early during development in zebrafish brain and pronephric kidney. Embryos injected with a translation inhibiting morpholino targeted against endolyn developed pericardial edema, hydrocephaly, and body curvature. The pronephric kidney appeared normal morphologically, but clearance of fluorescent dextran injected into the common cardinal vein was delayed, consistent with a defect in the regulation of water balance in morphant embryos. Heterologous expression

of rat endolyn rescued the morphant phenotypes. Interestingly, rescue experiments using mutant rat endolyn constructs revealed that both apical sorting and endocytic/lysosomal targeting motifs are required for normal pronephric kidney function. This suggests that both polarized targeting and postendocytic trafficking of endolyn are essential for the protein's proper function in mammalian kidney.

4.2 INTRODUCTION

4.2.1 Zebrafish as a model system to study kidney development

Zebrafish (*Danio rerio*) is a small tropical freshwater fish native to the streams of the southeastern Himalayan region [209]. It serves as a vertebrate model organism that has been extensively used in biomedical research [210]. Some properties of zebrafish, including rapid development of major organs, a sequenced genome and optical clarity of embryos, provide a powerful model system for developmental research [211]. In-situ observation, imaging at cellular resolution and gene expression manipulation all can be adapted in the zebrafish system [212]. For example, a common technique used to knock down endogenous gene expression, morpholino phosphorodiamidate oligonucleotides (morpholinos), can be employed in zebrafish to study gene function during embryonic development [209]. Morpholinos are typically oligomers of 25 morpholine bases each of which contains a phosphorodiamidate backbone, a morpholine ring and a nucleobase complementary to RNA of interest [213]. Morpholinos physically block the interaction between messenger RNA and ribosomal initiation complex or splice-directing small nuclear ribonucleoproteins complexes to interfere with translation or correct splicing [214].

Numerous studies have revealed novel genes and pathways from zebrafish using morpholino as the primary gene-specific knockdown approach [212,215,216].

The zebrafish pronephros provides an ideal model to study kidney development. The zebrafish pronephros is visible and well developed by 48 hpf. Structurally, the zebrafish pronephros can be observed as a simplified stretched mammalian nephron [217]. Functionally, the zebrafish pronephros performs similarly to the mammalian metanephros [11]. From the nephrogenesis standpoint, common signalling pathways like *Pax2* and *Lhx1* are required for both zebrafish pronephros and mesanephros [218]. Ultra-structurally, the zebrafish pronephros contains features shared with mammalian metonephros. For instance, the zebrafish glomerulus contains podocytes with extensive foot processes and fenestrated endothelial cells that organize in a similar fashion as metonephros [11]. Furthermore, the zebrafish pronephros comprises tubular epithelium divided by cell junctions into a well-defined apical brush border and a basolateral membrane [11]. The tubules are also segmented into neck, proximal tubule (convoluted and straight), distal (early and late), and the pronephric duct (Fig.25). The segmentation is defined by segment-specific ion-transport proteins, channels, and genes [217,219].

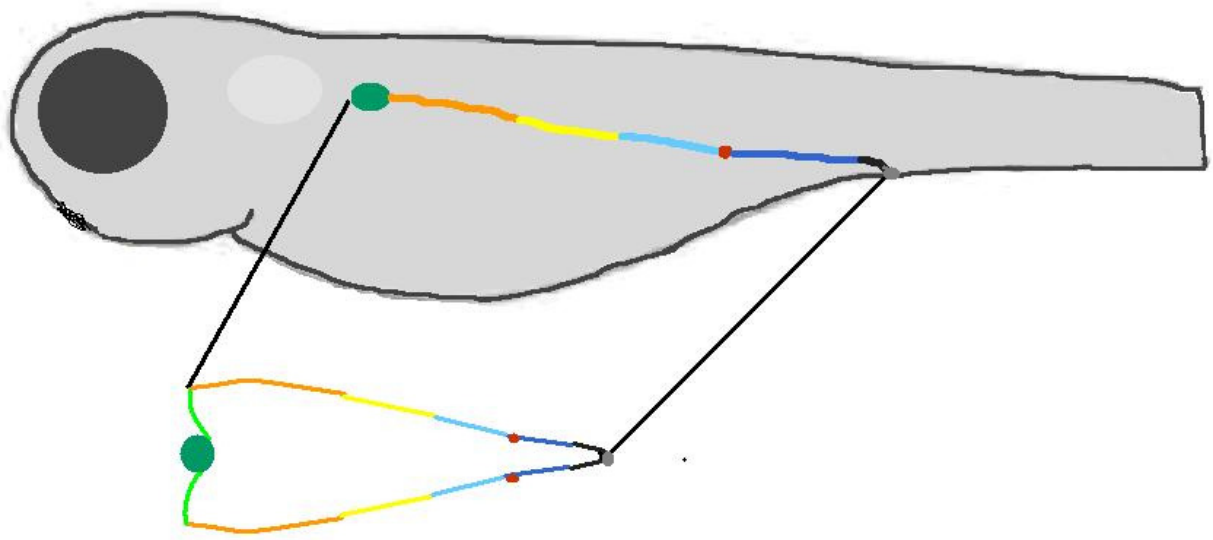

Figure 25. A schematic model of zebrafish

Glomerulus (Dark green), neck (light green), proximal convoluted tubule (orange), proimal straight tubule (yellow), distal early (light blue), corpuscule of Stannius (red), distal late (dark blue), pronephric duct (black), cloaca (grey). Adapted from [211].

Additionally, zebrafish can be exploited for modeling a variety of human diseases including kidney diseases [220]. Genetic analysis and treatment with nephrotoxic chemicals can mimic human diseases of kidney dysfunction such as Joubert Syndrome, polycystic kidney disease, proximal renal tubular acidosis, ciliopathies, proteinuria, and acute renal failure [211]. Evaluation of kidney function can be completed in the laboratory by measuring glomerular filtration rate using fluorescent dyes with various molecular weight [221,222]. To summarize, the zebrafish pronephros is an ideal model to study development, gene function, drug screening, regeneration, and disease modeling because it provides a relevant model of both mammalian nephrogenesis and renal function in a short time period.

4.2.2 Study the function of sialomucin endolyn during kidney development

Morphogenesis and homeostasis of epithelia require the coordination of cell differentiation, proliferation, survival, migration, adhesion, and polarization. Differentiated epithelial cells further respond to changes in their environment by adjusting the compositions of their two different plasma membrane domains to fulfill vectorial transport functions as needed. This is achieved through the appropriate integration of activated signaling pathways upon cues cells receive from their environment. The sialomucin endolyn (CD164) is a highly glycosylated membrane protein that has recently been described as a novel regulator of cell signaling in non-renal tissues. In hematopoietic precursor cells, myoblasts, and various epithelial-derived cancer cells, endolyn associates with the chemokine receptor CXCR4 and regulates downstream signaling and cell behavior, such as collective cell migration [159,160,161,162,223]. Endolyn is highly expressed in mammalian kidney both in embryos and adults, and it is frequently upregulated in renal cell cancer [224]. We have previously shown that the protein is targeted to the apical cell surface in renal epithelial cells and cycles between plasma membrane and lysosomes [152,155,156]; however, little is known about its function in this cell type. CXCR4 is expressed at low or undetectable levels in fully differentiated renal cells suggesting that endolyn may also regulate downstream signaling of other signaling receptors, or operate via completely different mechanisms [225,226].

In this study, we made use of the zebrafish model to begin to shed light on the importance of endolyn function in renal cells. The zebrafish *Danio rerio* has emerged as an attractive model system in which to study vertebrate renal development and function [10,217,227]. The zebrafish pronephric kidney contains only two nephrons with similar tubular segmentation and cell types found in the mammalian kidney[217]. Moreover, filtration and osmoregulation can be measured

in the pronephric kidney by 48 hours post fertilization (hpf), allowing early assessment of kidney function [221,222,228].

Several important domains have been identified in endolyn. The luminal domain contains two mucin-like domains separated by a cysteine-rich domain [153]. We have previously shown that an N-glycan-dependent epitope in the cysteine-rich domain mediates sorting of endolyn to the apical surface of renal epithelial cells [126,152]. Among all vertebrate endolyn proteins the transmembrane and short cytosolic domains are nearly identical and contain a tyrosine-based trafficking motif at their carboxy-terminus that mediates endocytosis and lysosomal sorting [152,153,155]. The N-terminal mucin-like domain of mammalian endolyn, which is thought to be required for adhesion of hematopoietic precursor cells to bone marrow stroma and effect cell proliferation [157,229,230], is absent in lower vertebrate species such as Zebrafish.

Using a translation-blocking morpholinos (MO) we knocked down endolyn expression in zebrafish embryos to interrogate whether acute loss of endolyn interfered with pronephric kidney development or function. We found that endolyn is expressed early during development and localized to the kidney, brain, and digestive tract within several hours after fertilization. Endolyn knockdown revealed a developmental phenotype consistent with a defect in pronephric kidney function. This phenotype was fully rescued by heterologous expression of rat endolyn. However, mutation of either the apical targeting signal or the critical tyrosine residue required for endolyn endocytosis and lysosomal targeting prevented rescue. Our study shows that endolyn expression is needed for normal pronephros function, but its absence does not inhibit pronephros formation *per se*. It further emphasizes the efficacy of the zebrafish model in highlighting essential motifs and domains involved in protein function during development.

4.3 RESULTS

4.3.1 Dual localization of endolyn in mammalian adult kidney

Our previous studies in Madin Darby Canine Kidney (MDCK) type II cells demonstrated that endolyn has an unusual trafficking pattern in that the newly synthesized protein is targeted to the apical surfaces, where it is internalized and transported to lysosomes [152]. It continues to recycle between lysosomes and the cell surface [156,168], but relatively little endolyn is found at the cell surface in this model system at steady state [152]. In rat kidney, endolyn is also found primarily in lysosomes in proximal straight and distal tubules and the collecting system (Fig.26). However, in proximal convoluted tubule a significant fraction of endolyn localizes to the brush border, suggesting differential functions along the kidney tubule.

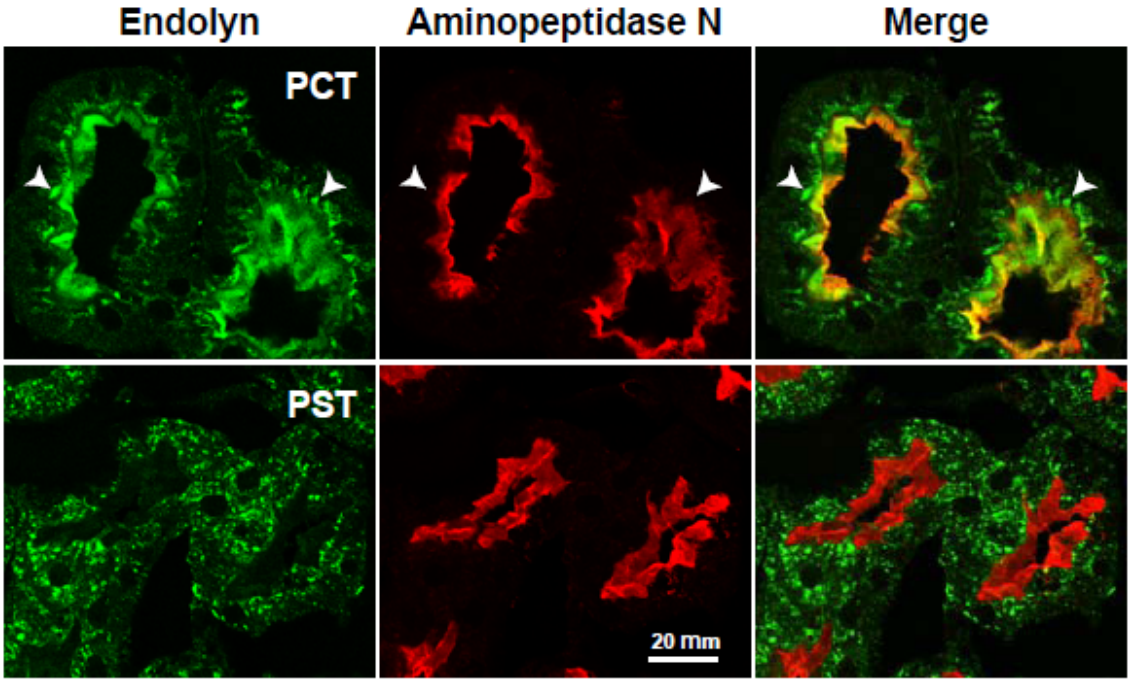

Figure 26. Endolyn is differentially localized along the rat kidney tubule

Adult rat kidney sections were co-labeled with antibodies to endolyn (green) and the proximal tubule marker aminopeptidase N (red), which strongly labels the apical brush border. Endolyn localizes prominently to the brush border of proximal convoluted tubules (PCT, upper panel), but is primarily intracellular in proximal straight tubules (PST, lower panel) and subsequent segments. Figure provided by Dr.G Ihrke.

4.3.2 Expression of Endolyn in zebrafish embryos

Zebrafish endolyn is 43% identical to the rat protein which is shown in Fig.5 in Chpater 1. All domains are highly conserved except the N-terminal mucin-like domain, which is absent. Four of 8-9 potential N-glycosylation sites lie within the cysteine-rich region that contains the N-glycan dependent apical targeting motif characterized in rat endolyn (Fig. 5). The eight cysteines defining the structure of this domain are all conserved between mammals and lower vertebrates. The transmembrane and cytoplasmic sequences are almost identical, with one conservative amino acid change in each domain, and end with the endocytosis motif YHTL.

RT-PCR confirmed the expression of endolyn as early as the 10 somite stage (ss; Fig. 27A) We next conducted whole mount *in situ* hybridization to examine the expression of endolyn at different developmental stages (Fig. 27B). Endolyn was expressed in the brain and the developing pronephric kidney by the 13ss, and strong staining persisted through 72 hpf. At 72 hpf, endolyn was also observed in the digestive system. The localization of endolyn in embryo cross-sections was comparable to that of the pan kidney marker cadherin 17 (cdh17), confirming localization of the transcript to the pronephric kidney at 48 hpf (Fig. 27C).

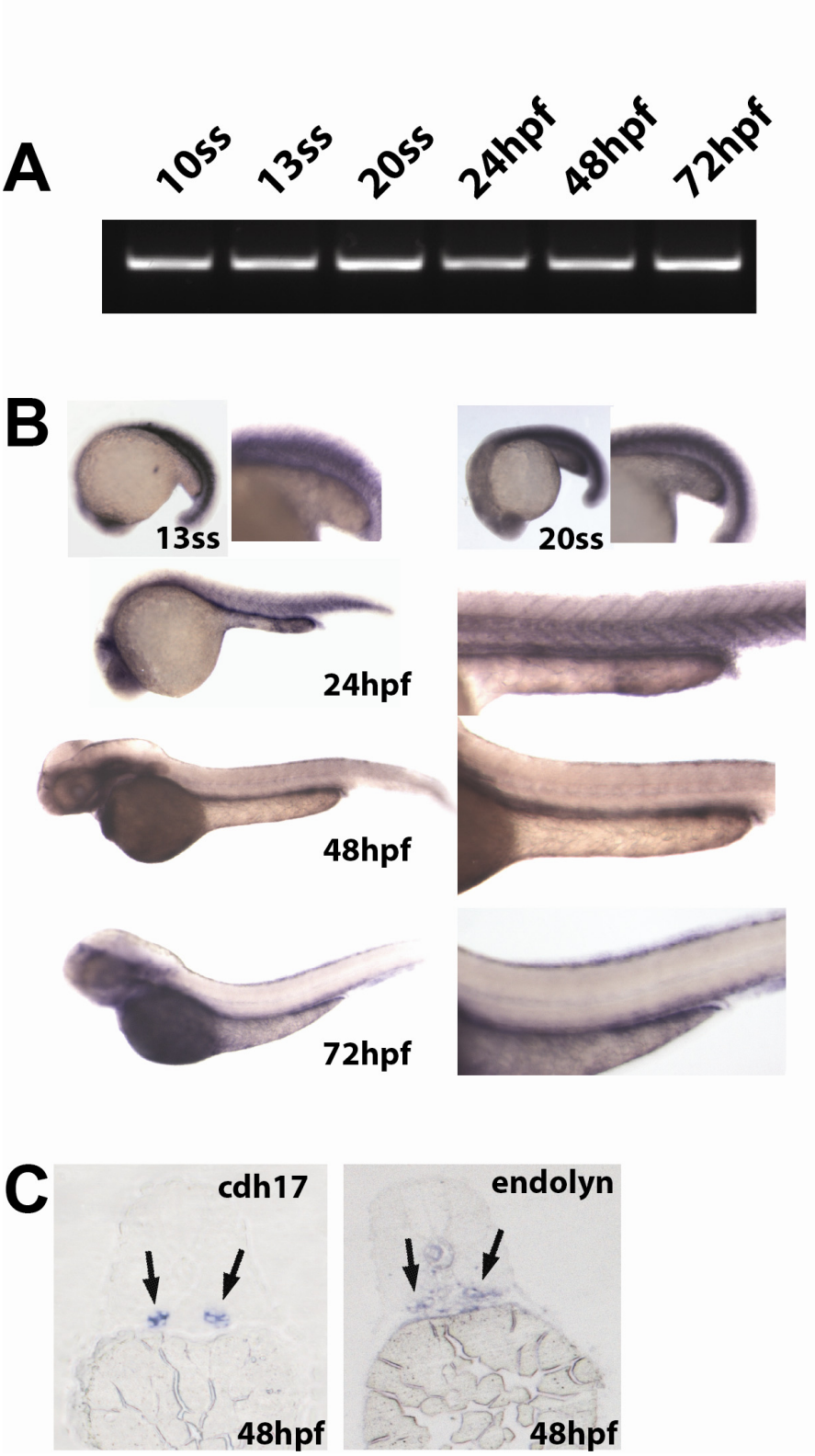

Figure 27. Endolyn is expressed in the zebrafish kidney, brain, and digestive system

(A) RT-PCR analysis of RNA extracted from embryos at the indicated stages was performed using specific primers against endolyn. A ~600 bp band is expected. (B) *In situ* hybridization for endolyn in embryos was performed at 13 ss and 20 ss and at 24, 48, 72 hpf. Kidney (arrowheads) and brain staining are evident by the 13 ss stage and staining of the digestive system appears by 72 hpf. (C) Cross sections through the proximal tubule of zebrafish embryos at 48 hpf. (5 µm) were stained by in-situ hybridization using probes to cadherin 17 (cdh17), a pronephric marker, or endolyn (End). Endolyn staining coincided with that of cadherin 17 in the expected region confirming endolyn localization in the pronephric kidney.

To determine the subcellular distribution of endolyn in zebrafish larvae, we injected mRNA encoding rat endolyn into embryos and fixed at 48 hpf. We used a polyclonal antibody recognizing the luminal domain of rat endolyn for detection by indirect immunofluorescence, which did not cross react with endogenous endolyn (not shown). Some sections were double labeled with the monoclonal antibody 3G8, which labels the apical surface of the pronephric kidney proximal tubule. Rat endolyn colocalized with the 3G8 antigen in the pronephric tubule (Fig. 28), consistent with apical targeting of the protein in zebrafish. Additionally, apical endolyn staining was also detected along the lumen of the gut.

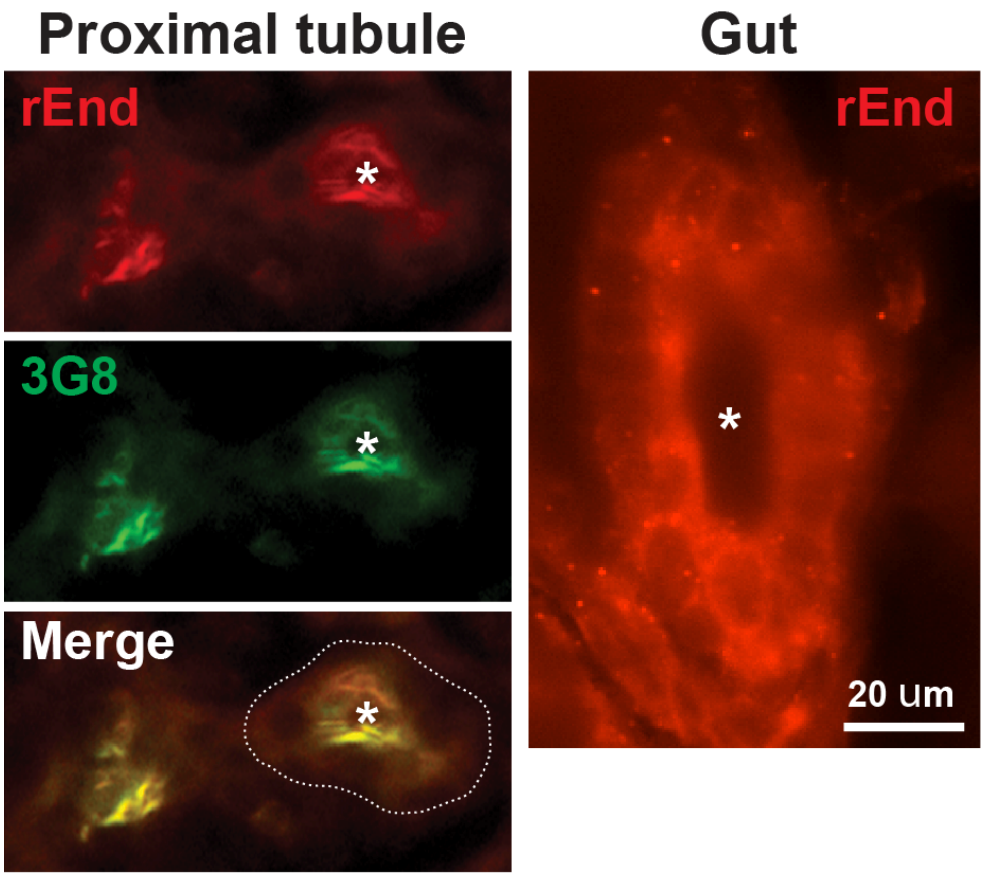

Figure 28. Rat endolyn is targeted to the apical surface of the zebrafish proximal tubule mRNA encoding wild type rat endolyn (200 ng) was injected into zebrafish embryos at the one-cell stage. Embryos were fixed, sectioned and incubated with polyclonal anti-rat endolyn and monoclonal 3G8 antibodies (to mark the apical surface of proximal tubules) as described in Methods. Cross sections through the proximal tubule and gut are shown. The periphery of the proximal tubule is outlined and the lumen is marked by an asterisk.

4.3.3 Knockdown of zfEndolyn disrupts pronephric kidney function

To elucidate the role of endolyn in zebrafish development, we injected a translation blocking MO to knock down endolyn expression. By 48 hpf, the endolyn-depleted embryos were developmentally impaired and exhibited pericardial edema, hydrocephaly, and abnormal body curvature (Fig. 29A). Embryos were classified as wild type, mild-to-moderately affected (class I) and severely affected or dead (class II) based on the extent of body curvature and edema (Fig. 29B). Injection of 5 ng MO resulted in moderate to severe phenotypes in ~70% of embryos by 48 hpf, whereas ~90% of the embryos injected with a scrambled control MO developed normally. The severity of the phenotype was dose dependent. Approximately 10, 30, 70, and 95% of embryos injected with 2.5, 5, 7.5, and 10 ng MO, respectively, were categorized as having severe phenotypes (Fig. 29B). For subsequent experiments, we injected embryos with 5 ng MO and selected mild-to-moderately affected larvae for morphological and functional analysis.

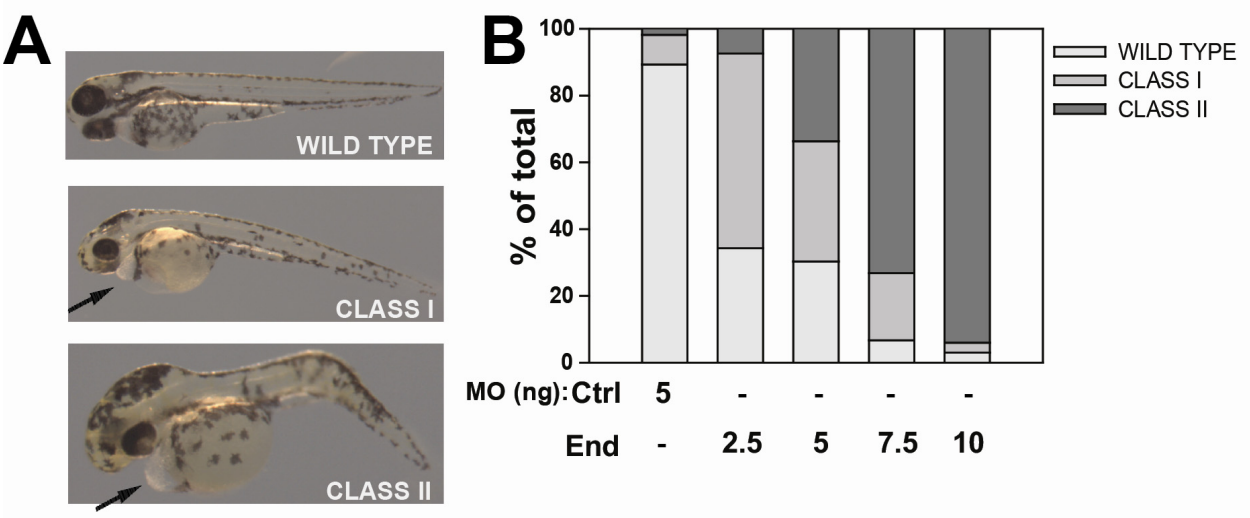

Figure 29. Endolyn morphants develop pericardial edema, hydrocephaly, and body curvature

(A) Zebrafish larvae were imaged 48 hpf after endolyn MO injection and classified as wild type (no visible pericardial edema or body curvature), moderately affected (Class I- frank pericardial edema, visible body curvature, hydrocephaly) and severely affected or dead (Class II- severe pericardial edema, body curvature, severe hydrocephaly). Representative images from each class are shown. (B) The distribution of observed phenotypes at 48 hpf in embryos injected with control MO or the indicated doses of endolyn MOs is graphed. Endolyn knockdown elicits concentration-dependent effects on larval edema and survival. Three independent injections were quantified with 50 or more injected embryos per condition in each experiment.

We next compared the organization of the pronephric kidney in embryos injected with control or endolyn MO. *In situ* hybridization was performed at 48 hpf using the pan pronephric marker cdh17 as well as markers selective for podocytes (wt1a), the proximal tubule (slc4a4), and the distal tubule (slc12a1) [219]. No gross defects in kidney structure were observed in endolyn morphants compared with controls, indicating that endolyn is not required for morphogenesis of the zebrafish pronephros (Fig. 30). We routinely observed dilated tubules and more intense staining in morphants with all probes, but the overall segmental pattern was never changed.

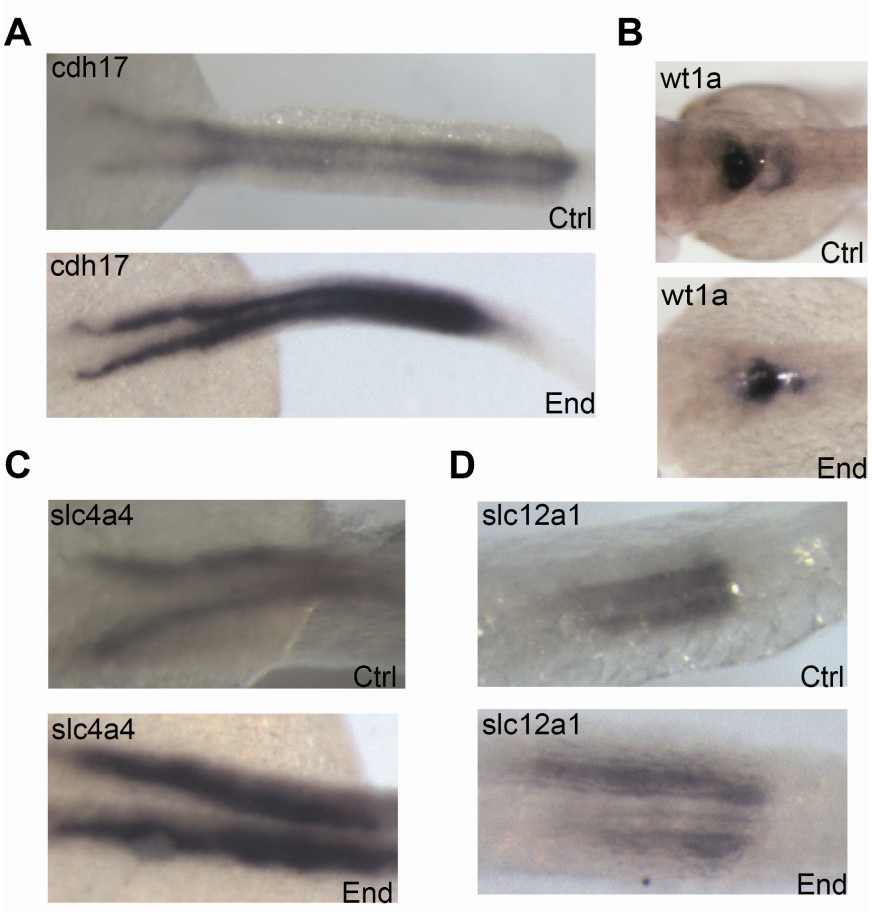

Figure 30. Kidney morphology is intact after zfEndolyn knockdown

(A) In situ hybridization was performed at 48 hpf to detect cdh17 expression in embryos injected with either control or zfEndolyn MOs. (B through D) In situ hybridization was performed at 48 hpf in embryos at 48 hpf injected with either control or zfEndolyn MOs to detect podocyte (wt1a) (B), proximal tubule (slc4a4) (C), and distal tubule (slc12a1) (D) marker distributions. The morphology of the pronephric kidney in morphants is not grossly disrupted. Class I morphants were used in all experiments.

To examine whether pronephric kidney function was compromised by endolyn depletion, we performed a rhodamine-dextran clearance assay. 1 ng of 10 kDa rhodamine-dextran was injected into the common cardinal vein of class I embryos at 48 hpf and depletion of fluorescence at the injection site was monitored over time (1-24 h post injection) as a measure of renal clearance. Rhodamine-dextran was efficiently cleared from larvae injected with control-MO but clearance was significantly slowed in endolyn-MO injected larvae, consistent with a defect in osmoregulation (Fig. 31).

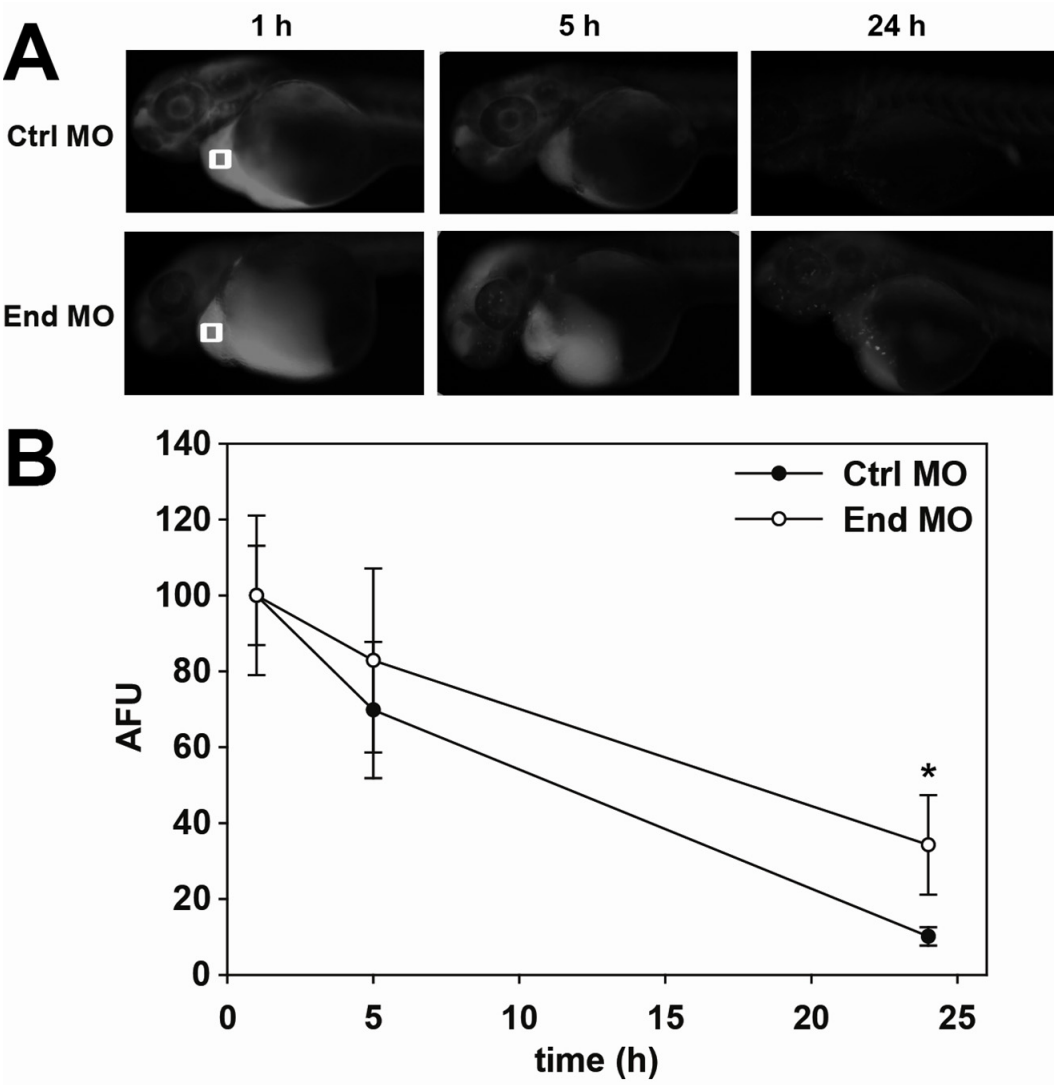

Figure 31. Pronephric kidney function is disrupted in endolyn morphants

(A) 1 ng of 10KDa rhodamine-dextran was injected into the common cardinal vein of control or endolyn morphants at 48phf. Images were acquired under identical conditions at 1, 5, and 24 h post injection. (B) The loss of fluorescence over time near the common cardinal vein (regions marked by white boxes) was quantified, normalized to the initial fluorescence observed at 1 h, and plotted. Three independent injections were quantified with at least 10 Class I and control embryos injected in each experiment. At 24 h, retained fluorescence is significantly greater in endolyn morphants compared with controls (*p=0.001 by Mann-Whitney rank sum test).

4.3.4 Rat endolyn efficiently restores zfEndolyn function during pronephric kidney development

To exclude any off-target effects of the endolyn MO, we asked whether heterologous expression of mRNA encoding rat endolyn could rescue the developmental defects we observed in endolyn MO-injected larvae. First, we tested the effect of injecting rat endolyn mRNA without concomitant MO injection. Delivery of up to 300 pg rat endolyn mRNA into zebrafish larvae did not cause developmental defects, suggesting that overexpression of endolyn is not detrimental to the embryos (Fig. 32). Strikingly, we found that injection of 200 pg mRNA encoding wild type rat endolyn was sufficient to rescue the endolyn MO phenotype. Whereas only ~30% of embryos injected with 5 ng endolyn MO were classified as normal or mildly affected, injection of 200 pg rat endolyn mRNA restored normal development in ~90% of larvae. Injection of 100 pg resulted in ~75% of embryos developing normally (Fig. 33B).

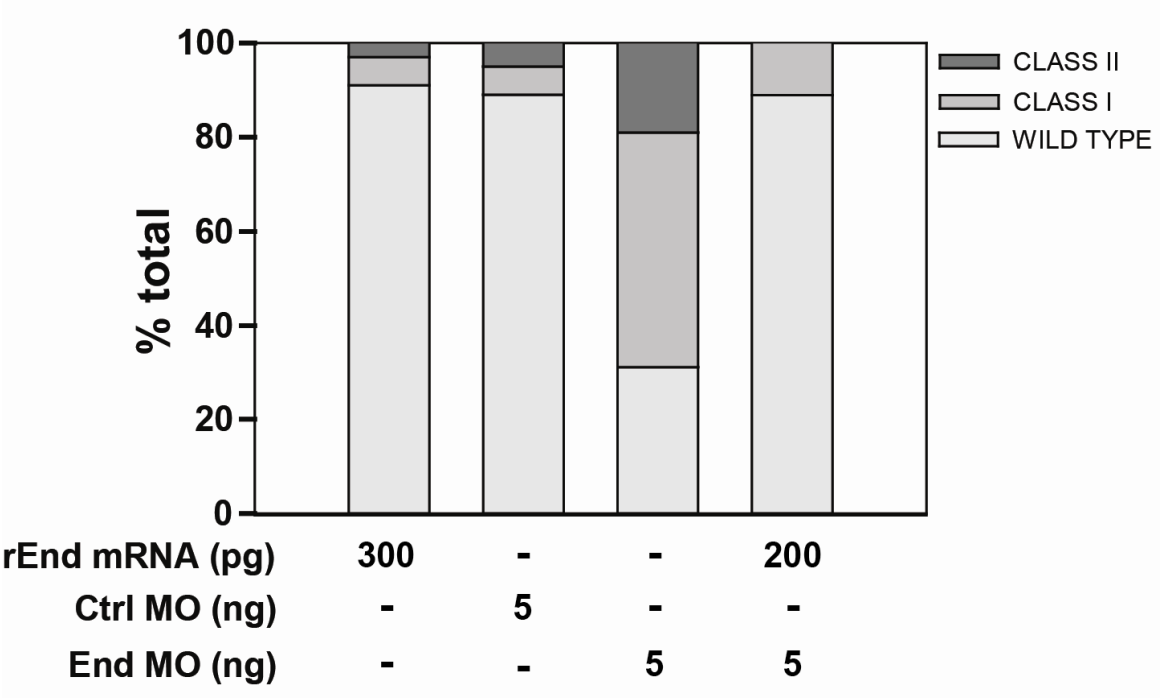

Figure 32. Heterologous expression of rat endolyn restores endolyn function during kidney development

Embryos were injected with 300 pg of mRNA encoding rat endolyn (rEnd) and evaluated at 48phf. For rescue experiments, embryos were injected (or not) with 200 pg rEnd mRNA followed by injection with 5.0 ng control or endolyn MO, and phenotypes were classified at 48 hpf. Data are combined from three experiments with 50 or more embryos per condition.

4.3.5 Lumenal and cytoplasmic regions are required for endolyn function in the pronephric kidney

To identify the critical domain(s) for endolyn function in zebrafish pronephros, we generated rat endolyn constructs containing mutations within the lumenal, transmembrane, or cytoplasmic domains for use in rescue experiments (see schematic in Fig. 33A). To examine the requirement

for apical sorting in endolyn function during zebrafish development, we prevented N-glycosylation of the cysteine-rich domain by mutating the four key asparagine residues to alanine (4NA). We confirmed the polarity of overexpressed proteins in stably transfected MDCK cells. Indirect immunofluorescence labeling showed that wild type endolyn was largely confined to the apical surface at steady state, whereas the 4NA mutant was also observed at the basolateral membrane (Fig. 34A). To verify that newly synthesized 4NA was partially missorted, we performed domain-selective biotinylation of radiolabeled cells (Fig. 34B). Only 63% of the 4NA mutant at the cell surface was delivered apically, compared with 83% of wild type endolyn. This reduction in polarity is consistent with our previous results using similar glycosylation mutants [126].

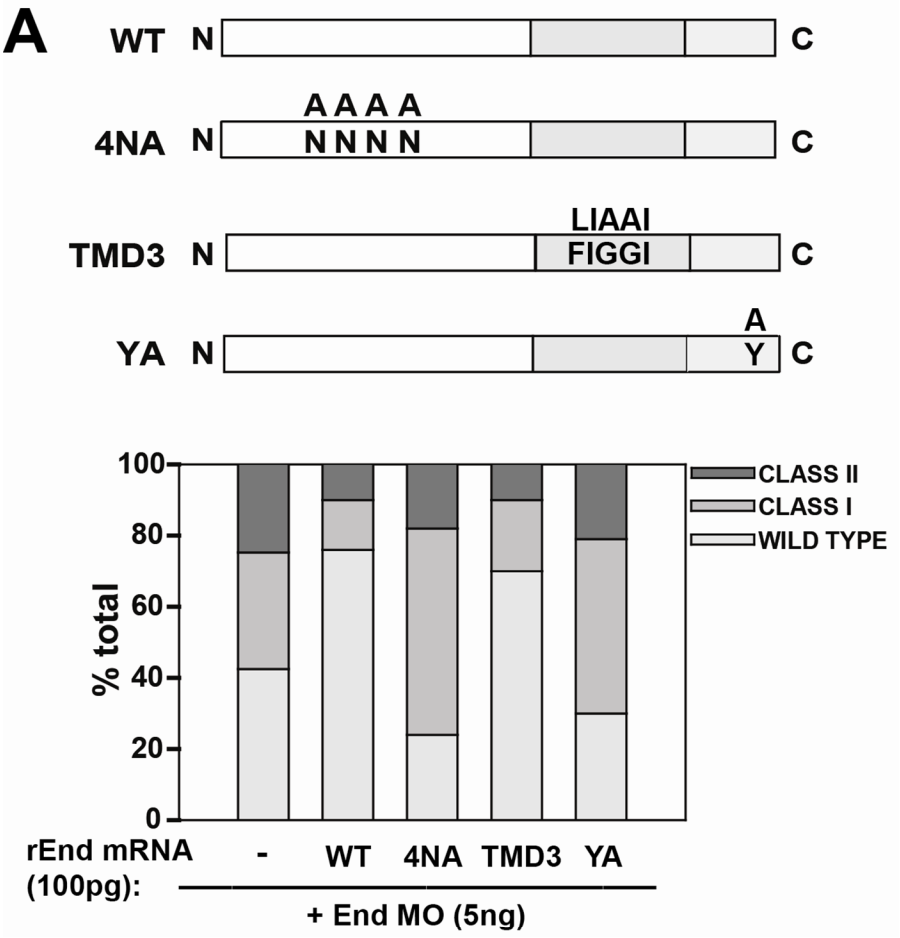

Figure 33. Lumenal and cytoplasmic domains of rat endolyn are required for its function during pronephric development

(A) Schematic of rat endolyn mutants used for rescue studies. The 4NA mutant lacks consensus sites for addition of the four N-glycans within the globular region. TMD3 contains three mutations within the highly conserved FIGGI sequence within the transmembrane region. The YA mutant contains a tyrosine-to-alanine substitution that disrupts the endocytic/lysosomal targeting motif at the carboxy terminus. (B) mRNA encoding wild type or mutant rEnd constructs (100 pg) was injected into embryos at the one-cell stage, followed by injection of 5 ng of zfEndolyn morpholino. Images were acquired at 48 hpf and morphant phenotypes were classified and quantified. Data are combined from three experiments with 50 or more embryos per condition.

Injection of 100 pg of mutant 4NA mRNA failed to restore normal development of morphant zebrafish embryos (Fig. 34B). Essentially identical results were obtained when a mutant construct in which the entire lumenal domain of endolyn was replaced by the corresponding region of CD8 (not shown). These data suggest that endolyn's lumenal domain, and more specifically the glycan-dependent apical targeting information, is critical for its function in zebrafish kidney development. Importantly, even a modest level of endolyn missorting seems to be sufficient to prevent proper functioning.

The transmembrane domain of endolyn contains a five amino acid motif (FIGGI) that is completely conserved among species. To test the role of this sequence in endolyn function, we expressed the mutant TMD3, in which the phenylalanine and two glycine residues were conservatively substituted by leucine and alanines, respectively. This mutant was apically delivered similar to wild type endolyn in MDCK cells as assessed by indirect immunofluorescence and domain selective biotinylation (Figs. 35A and B). The ability of this mutant to rescue endolyn morphants was also comparable to wild type rat endolyn, suggesting that endolyn is fully functional in the absence of the FIGGI motif (Fig. 34B).

Finally, we examined a mutant that lacks the cytoplasmic tyrosine critical for endocytosis and lysosomal sorting of endolyn (YA). Similar to the 4NA mutant, expression of this construct was unable to rescue the morphant phenotype (Fig. 34B). This suggests that apical sorting of endolyn and its distribution between surface and intracellular compartments are similarly important for endolyn function during early development.

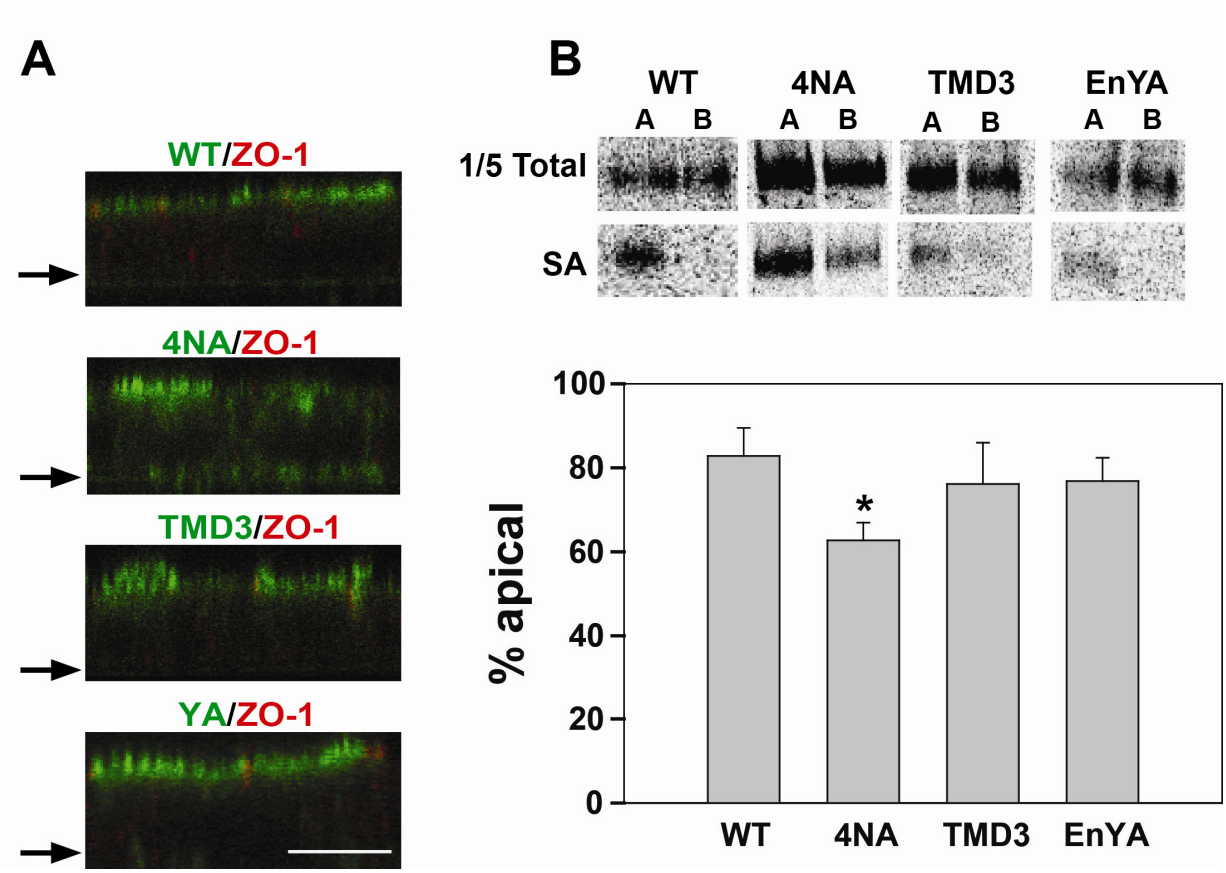

Figure 34. Subcellular localization of rat endolyn mutants in polarized renal epithelial cells

(A) Filter-grown MDCK cells stably expressing either wild type endolyn or different mutants were fixed and processed for indirect immunofluorescence to detect endolyn (green) and the tight junction marker ZO-1 (red). Cells were visualized by confocal microscopy and representative XZ sections are shown. The position of each filter is marked with an arrow. Scale bar: 10 µm. (B) Filter-grown MDCK cells stably expressing wild type or mutant rat endolyn were radiolabeled with $^{[35S]}$-cysteine for 2 h, then chased for 1 h. Cells were biotinylated either apically or basolaterally and cells were solubilized and immunoprecipitation with anti-endolyn antibody. After elution, one-fifth of each sample was reserved as total and the remainder was incubated overnight with streptavidin agarose (SA) to recover surface proteins. Representative gels are shown for each sample and the results from three independent experiments are plotted. The polarity of 4NA is statistically different from wild type (*$p < 0.001$ by Student's t-test) and from YA and TMD3 mutants ($p<0.02$

and p= 0.024, respectively). The polarity of TMD3 and YA were not significantly different from wild type or each other.

4.4 DISCUSSION

In these studies we have identified a novel role for the sialomucin endolyn during zebrafish development and establishment of a functional pronephric kidney. Endolyn is expressed as early as the 10 somite stage in zebrafish embryos and persists in the kidney, brain, and digestive system at least through 72 hpf. Kidney organogenesis and organization were not grossly disrupted upon endolyn knockdown using a translation blocking morpholino. However, morphants exhibited pericardial edema, visible body curvature and hydrocephaly, consistent with a water balance defect indicating a potential kidney malfunction. Moreover, we observed tubular dilation and a reduced rate of clearance of 10 KDa rhodamine-dextran in morphants. The morphant phenotype could be fully rescued by heterologous expression of rat endolyn, which was targeted apically to zebrafish epithelial lumens. However, endolyn mutants lacking the glycan-dependent apical targeting signal or the endocytic/lysosomal targeting motif did not restore normal development and pronephros function. These data suggest that efficient apical delivery and endocytosis are both required for proper endolyn function in the pronephric kidney.

Endolyn has been studied extensively in polarized epithelial cells *in vitro* as an apically targeted glycoprotein with N-glycosylation-dependent sorting information. Apical sorting of endolyn relies on terminal processing of two N-glycans within the cysteine-rich region of the lumenal domain [126]. In polarized MDCK cells, this apical signal is dominant over basolateral sorting information such that newly synthesized endolyn is delivered primarily to the apical

surface. Subsequently, it is internalized and delivered to lysosomes [152]. The proportion of radiolabeled endolyn present at the apical surface remains steady for up to 21 h after labeling, suggesting that endolyn cycles constitutively between lysosomes and the cell membrane [156]. Mutation of the critical tyrosine residue in the endocytic/lysosomal targeting motif prevents binding to adaptor protein complexes and enhances surface expression of the protein [155]. Interestingly, expression of mutants lacking either N-glycosylation consensus sequences required for polarized sorting or an intact endocytic motif could not rescue the endolyn morphant phenotype, whereas heterologous expression of wild type rat endolyn restored the normal morphology. In contrast, disruption of a highly conserved sequence within the transmembrane domain of endolyn did not inhibit efficient rescue by rat endolyn. The fact that both trafficking motifs are indispensable for rescue suggests that proper modulation of endolyn's distribution between the (apical) cell surface and endosomal/lysosomal compartments is a key requirement for endolyn function.

The observation that disrupting the N-glycan-dependent apical sorting motif of endolyn prevented rescue of the morphant phenotype was somewhat unexpected, given that the protein is still delivered to the cell surface with a slight apical preference. Compared with wild type endolyn, where roughly 83% of the newly synthesized protein is delivered apically, we found that 63% of 4NA was present at the apical surface under similar labeling conditions. There are two possible explanations for this observation. First, missorting of a fraction of 4NA to the basolateral surface may be sufficient to disrupt rescue by this mutant. A precedence for the inverse scenario is presented by a disease-causing mutant form of the anion exchanger AE1 lacking a basolateral sorting motif [231]. However, in this case it is clear that any missorting to the wrong surface will disturb the balance of ion transport across the renal epithelium. While it is

conceivable that endolyn effects the distribution of other membrane proteins, it itself is unlikely to have any ion transport activity. However, lowering the effective endolyn concentration at the apical plasma membrane may be sufficient to disrupt its normal physiology. Alternatively, the N-glycans within the cysteine-rich domain may serve another function in addition to their role in apical targeting. These N-glycans may be important for association of endolyn with other protein(s) on the same membrane or extracellular ligands. Given the apparent requirement for endolyn internalization and lysosomal targeting, it is tempting to speculate that endolyn-mediated binding and endocytosis of an associated ligand or *cis*-receptor may be important for its function. Similar to other sialomucins, endolyn is thought to mediate cell-cell (or cell-matrix) adhesion [157,230]; however, no membrane-bound ligand has yet been identified. Noteworthy, the N-terminal mucin-like domain of mammalian endolyn, which has been implicated in cell adhesion [230], is not present in zebrafish endolyn and therefore not expected to be required for rescue of the knockdown phenotype in zebrafish.

Previous studies demonstrated that endolyn associates with CXCR4 after stimulation with CXCL12 and regulates downstream signaling with profound consequences on cell migration [159,161,162,223]. The mechanism by which this regulation occurs remains unclear, although antibody inhibition experiments indicate that the N-terminal mucin-like domain of endolyn—not present in zebrafish endolyn—is required for this function [159]. The CXCL12/CXCR4 axis is involved in cell proliferation, migration, adhesion and differentiation of various cell types, including kidney and other epithelial cells [232,233,234]. Thus, endolyn may have a functional role in metanephric kidney that is mediated via CXCR4, e.g. during development or in renal tubule repair [226,235]. A key step during pronephric kidney morphogenesis in zebrafish is the fluid flow-driven collective cell migration of epithelial cells starting around 30 hpf that is critical

for generation of the proximal convoluted tubule [236,237]; however, endolyn-CXCR4 interaction is unlikely to be critically important for this event. While CXCR4 plays several important roles in zebrafish development, including migration of germ cells and lateral line primordial cells and muscle formation [238,239,240,241], no effects on pronephric kidney function have been reported in CXCR4 morphants. Moreover, the lack of gross morphological changes in the pronephric duct of endolyn morphants is inconsistent with major defects in cell migration, proliferation or apoptosis. Interestingly, Bae et al. found that overexpression of both wild type endolyn and the endocytosis-defective YA mutant promoted myoblast fusion, a CXCR4-mediated function, with the latter having an even stronger promyogenic activity [161]. This suggests that endolyn has different cellular functions, some of which are only dependent on its surface expression, while others require active endocytosis. Future studies will be directed towards identifying additional interaction partners of endolyn and the mechanism(s) by which this protein affects vertebrate kidney function.

4.5 METHODS

4.5.1 Zebrafish husbandry

All animal husbandry adheres to the National Institutes of Health Guide for the Care and Use of Laboratory Animals. Zebrafish were raised and maintained under standard conditions and staged as described previously [242]. Embryos were collected from group matings of wild-type AB adult zebrafish. Embryos were kept in E3 solution at 28.5°C. For *in situ* hybridization, embryos were kept in E3 solution containing 0.003% 1-pheny1-2-thiourea after 24 hpf.

4.5.2 Whole-mount In situ hybridization and immunocytochemistry

In situ hybridization was performed as described previously [242]. Full length zfEndolyn cDNA was purchased from Open Biosystems. The endolyn anti-sense probe was made using the digoxigenin labeling kit (Roche) according to manufacturer's recommendations. T7 RNA polymerase was used for RNA synthesis after linearization of the zfEndolyn cDNA with EcoRI. Embryos fixed in 4% PFA overnight at 4°C were incubated with the endolyn anti-sense probe at 65°C, then washed extensively, incubated in 2% blocking reagent (Roche) with 5% sheep serum in MAB buffer (100 mM maleic acid and 150 mM NaCl), and incubated with anti-digoxigenin alkaline phosphatase antibody (Roche) at 1:15,000 dilution overnight at 4°C. BM purple AP substrate (Roche) was added for staining after extensive washing with PBS+0.1%Tween 20. Stained embryos were photographed using a Leica DMI 6000 CS Trino confocal microscope and images were processed using Adobe Photoshop.

4.5.3 RT-PCR

Dechorionated zebrafish embryos (~30 per stage) were homogenized with a plastic microcentrifuge pestle in 500 µl of TRI reagent (Ambion), and RNA was isolated using the RNeasy Micro Kit (Qiagen) according to the manufacturer's protocol. One µg of RNA was used for the synthesis of cDNA using M-MLV reverse transcriptase (Ambion) according to the manufacturer's recommendations. PCR was performed using the BioRad® icycler and GeneAmp® High Fidelity PCR System (Applied Biosystems). Primer sets against zfEndolyn were designed using PrimerQuest on the IDT website (forward primer: 5'-ATGAGAACCAAACAGCCAACTGCG -3'; reverse primer: 5'-CACACGCTGACAGACACAAACCAA-3'). ~600bp amplified sequence is expected. The denaturing temperature was 95°C, the annealing temperature was 55°C, and the extension temperature was 68°C, with an amplification cycle of 30.

4.5.4 Embryo microinjection

A translational blocking MO against zfEndolyn was designed and ordered from Gene Tools, LLC. (5'-TCACGGCGAAAAGTCTCCAAAACAT-3') and resuspended in nuclease free water (Ambion) at 20 mg/ml and diluted to 1 mg/ml for microinjection. Zebrafish embryos were injected at up to the eight-cell stage either with the indicated doses of zfEndolyn or control (scrambled) MO. Embryos were allowed to develop in E3 solution at 28.5°C. At 48 hpf, images were taken and embryo phenotypes classified. For rat endolyn rescue experiments, zebrafish embryos were injected at the one-cell stage with 100 pg of synthetic wild type or mutant rat

endolyn mRNA. Embryos were photographed and classified at 48 hpf to assess the extent of rescue.

4.5.5 Rhodamine-dextran clearance assay

Renal function was assayed as previously described [221]. Briefly, 1 ng of 10 kDa Rhodamine-dextran was injected into the common cardinal vein of embryos injected with either control or zfEndolyn MOs at 48 hpf. Embryos were imaged under identical conditions sequentially at 1, 5 and 24 h post-injection. The loss of fluorescence near the common cardinal vein area was quantified using Adobe Photoshop. Statistical significance was assessed using the Mann-Whitney rank sum test.

4.5.6 Indirect immunofluorescence of rat endolyn in zebrafish

Embryos were fixed using 4% paraformaldehyde for 4 h at ambient temperature and washed overnight with PBS. Embryos were incubated in increasing concentrations of sucrose up to 30% (w/v), mounted in Tissue Freezing Medium (Ted Pella) and frozen at -80°C. Tissue sections (12 μm thick) were cut using a cryostat (Leica CM1850). Sections were mounted onto slides and dried for 30 min at 37°C. Sections were blocked using 10% Normal Goat Serum and incubated with 3G8 antibody (European Xenopus Resource Centre) (1:100) overnight at 4^{o}C After extensive washing with PBS+0.1%Tween-20, sections were incubated with Alexa-488 conjugated secondary antibodies at 1:500 dilution. Sections were blocked again and incubated with a polyclonal antibody against rat endolyn (1:100; overnight at 4°C) followed by extensive

washing and incubation with Alexa-567 conjugated secondary antibodies (1:500 dilution). Upon dehydration, sections were mounted in Aqua Poly/Mount (Polysciences) . Sections were imaged using a Leica DM6000B microscope with an HCX PL APO 40x/1.25 oil objective and acquired using a QImaging Retiga 4000R camera.

4.5.7 Generation of mutant endolyn constructs

Generation of the rat endolyn YA mutant was previously described13. The 4NA and TMD3 mutant constructs were generated using PCR. These constructs were subcloned into the pCB6 vector28 and verified by DNA sequencing. To obtain mRNA for rescue experiments, constructs were subcloned into pCS2+ vector behind the SP6 promoter by PCR. The mMESSAGE mMACHINE SP6 Kit (Ambion) was used to make mRNA from linearized cDNA.

4.5.8 Generation of MDCK stable cell lines

Stably transfected cell lines were generated in MDCK II cells as previously described29 and cultured in MEM with 10% fetal bovine serum and 400 μg/ml G418. For domain selective biotinylation and immunofluorescence experiments, cells were cultured on permeable supports for three days and then incubated with 2 mM butyrate for 18-21 h to induce endolyn expression.

4.5.9 Domain selective biotinylation

Polarized MDCK cells were starved and pulse-labeled for 2 h with [^{35}S]-cysteine, then chased for 1 h. Biotinylation was performed essentially as described previously [126]. After cell lysis

and immunoprecipitation with anti-endolyn antibody, samples were eluted. Four-fifths of the eluate was incubated overnight with streptavidin agarose (Pierce) to recover biotinylated proteins; the remainder was used to determine total endolyn. All samples were resolved on SDS-PAGE. Polarity was quantitated after exposure of dried gels to PhosphorImager screens.

4.5.10 Indirect immunofluorescence in MDCK cells

Filter grown cells were fixed by adding 4% paraformaldehyde at 37.C. Cells were permeabilized with 0.1% TX-100 in PBS for 10 min, blocked with 1% fish gelatin (Sigma), and incubated with mouse monoclonal antibody against endolyn (1:500 dilution) and rat monoclonal antibody against ZO-1 (hybridoma supernatant from G. Apodaca, used neat) for 1 h. After extensive washing with PBS, filters were incubated with Alexa 488- and 647-conjugated secondary antibodies (1:500 dilution) for 30 min (Invitrogen), washed, mounted, and imaged. Confocal stacks were collected and XZ images were generated and processed using MetaMorph.

5.0 CONCLUSIONS AND FUTURE DIRECTIONS

The polarity established in epithelial cells allows these cells to interact with and between internal and external environments [29]. Maintenance of this polarity requires sustained proper sorting of proteins and lipids to either apical or basolateral membranes using distinct sorting signals [188]. The apical sorting signals present a unique challenge for research caused by their diversity and heterogeneity whereas basolateral sorting signals are more unified. Association with lipid rafts and carbohydrates are the two most characterized apical sorting signals [188]. To further dissect the exact determinant on glycans which is responsible for mediating apical sorting is difficult due to the complex and distinct nature of these moieties. In this dissertation, I used the sialomucin endolyn as a model protein to study the N-glycan-dependent apical sorting in detail. The objective of the work carried out in this dissertation was to characterize the N-glycan dependent apical sorting of endolyn and the relationship between endolyn sorting and function during pronephric kidney development. This was investigated by: (i) optimization of an efficient approach to knock down genes of interest in polarized epithelial cells without compromising their polarity, (ii) conducting a systematic study to dissect the exact determinant on N-glycans structure that is responsible for endolyn apical delivery, (iii) identifying potential receptor(s) for endolyn apical sorting, (iv) exploring the function of endolyn during pronephric kidney development using the zebrafish *Danio rerio* as a model system, (v) determining the conserved

region(s) that is critical for endolyn function, and (vi) analyzing the requirement for endolyn trafficking in its function.

In search of the determinant for endolyn's apical sorting signal, I first developed an efficient approach to knock down genes of interest in polarized MDCK cells. I compared two commonly used transfection methods and evaluated their efficiency and effect on cell integrity and polarity. I found that nucleofection disrupts the fence function of the tight junction and thus, compromises the overall polarity of MDCK cells. Conversely, I developed a lipofectamine based transfection approach, which achieved reasonable knockdown and maintained normal membrane protein polarity comparable to untransfected cells.

In the second part of the study, I conducted a systematic study to dissect the specific requirement(s) for N-glycan dependent apical sorting of endolyn. Previous data from our lab indicate that terminal processing of N-glycosylation is important for endolyn apical delivery [126]. Therefore, I knocked down specific glycosyltransferases that are responsible for glycan branching and sialylation to determine whether polylactosamine extension or addition of sialic acids are required for endolyn apical delivery. The results revealed that both α2,3- and α2,6-linked sialic acids are required for apical sorting of endolyn. Conversely, polylactosamine extension of glycan chains is not required for endolyn apical sorting. My results are significant in the sense that I have clearly demonstrated that a specific step of N-glycan terminal processing is required for carbohydrate-dependent apical sorting. However, our study didn't conclude whether sialylation is required for apical expression of all N-glycan apical targeted proteins. The apical delivery of other N-glycan dependent proteins needs to be tested in sialyltransferase(s)-depleted cells, (e.g. glycosylated growth hormone). Apical secretion of glycosylated growth hormone in sialyltransferases-depleted cells should be measured to assess if sialylation is required.

One question that arises from these results is: What are the mechanisms for N-glycan apical sorting? Two models have been proposed so far (Fig. 35) [135]. The first model proposes that a family of receptors exist to recognize glycans and subsequently sort apical glycoproteins (Fig. 35A). Growing evidence suggest that members of the galectin family may be involved in both raft-dependent and glycan-dependent apical sorting pathways. Galectin-3 is reported to mediate raft-independent apical sorting of p75 and gp114 whereas galectin-4 is suggested to regulate raft-dependent apical sorting [139,142,148]. Furthermore, galectin-9 plays a role in the establishment of apical-basolateral polarity of MDCK cells [146]. Therefore, I specifically knocked down galectins-3, 4, and 9 in polarized MDCK cells and evaluated their effect on endolyn apical sorting. Results from surface biotinylation and indirect immunofluorescence suggest that apical delivery of endolyn is modestly but statistically significanlly disrupted in galectin-9 depleted cells whereas it remains unchanged in galectin-3 and 4 depleted cells (Fig.7, 21,22,23). However, due to the sequence similarity in the carbohydrate recognition domain, different galectins may bind to similar carbohydrates [138]. It's worth investigating whether the apical devlivery of endolyn is disrupted more severely when we knock down galectin-3, 4, and 9 together. A broader question raised from these results is whether galectins is involved in other N- and O-glycan dependent apical sorting events. A thorough screen of endogenous galectins in MDCK cells has been performed by Hughey and coworkers [138]. Galectins differentially bound to specific glycan structures. This study revealed that MUC1, an O-glycan dependent apical protein, preferably binds to galectin-3 and 9. It is possible that galectins may be involved in MUC1 apical sorting. One limitation of this study is that we only used MDCK cells as a representative of epithelial cells. However, growing evidence suggests that different epithelial cells develop distinct mechanisms and routes to sort cargo proteins [54,243,244,245]. To test if

sialylation and galectin-9 are exploited by apical proteins in other epithelial cell lines, similar experiments should be performed for various cell lines including Caco-2, a human intestinal epithelium and WIF-B, derived from hepatocytes [98,246].

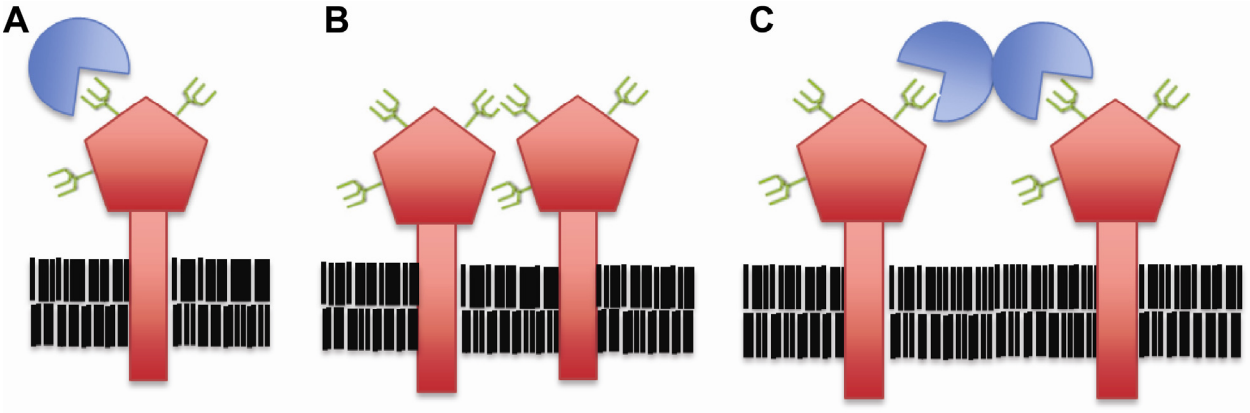

Figure 35. Proposed model for N-glycan dependent apical sorting

(A) A group of receptors exist to recognize specific glycan structures and sort glycoproteins. (B) Glycans interact with each other to present a transport-competent conformation. (C) Clustering is required for glycan dependent apical sorting. This process may be mediated by oligomerization of receptors.

The second model proposes that a specific transport-competent confirmation is required for apical sorting (Fig. 35B). In support of this model, I expect that endolyn would be retained in TGN when sialylation is perturbed. However, my data does not agree with this possibility for endolyn apical delivery. Retention of endolyn in TGN was not observed in sialyltransferases-depleted cells by both domain selective biotinylation and indirect immunofluorescence.

Alternatively, clustering of apical sorting proteins may be required for both raft-dependent and independent pathways (Fig. 35C). This mechanism has already been demonstrated to be exploited by raft-associated proteins [76,89]. Some evidence indicates that O-

glycan dependent apical proteins may require clustering for their apical delivery. For example, galectin-3 is reported to form high molecular weight cluster with p75 to mediate its apical sorting [148,247]. However, it has never been examined whether N-glycan dependent apical sorting requires clustering. To test this hypothesis, we attempted to measure the mobility of endolyn-containing vesicles leaving the TGN by fluorescence recovery after photobleaching (FRAP) in sialyltransferases-depleted cells. However, we didn't observe a difference in endolyn mobility between cells treated with control or sialyltransferases siRNAs, suggesting that endolyn may not require clustering for its apical delivery. There are two possible explanations for this result. First, clustering may not be required for endolyn to exit the TGN, rather, it may operate at the level of endosomal compartments. One piece of evidence to support this is that galectin-3 is enriched in Rab11-positive apical recycling endosomes rather than in the TGN, suggesting that the cross-linking between galectin-3 and p75 may take place in endosomes instead of TGN [144]. Data from our lab suggest that endolyn traverses to the apical recycling endosomes before arrival at the apical surface [168]. Thus, additional experiments should be performed to track endolyn-containing vesicles leaving the apical recycling endosomes. Second, the level of sensitivity may not be sufficient for FRAP to detect clusters as we were not able to detect p75 clustering in MDCK cells using FRAP (Robert Youker personal communication). Therefore, a more sensitive approach should be explored. For example, fluorescence correlation spectroscopy (FCS) and photon counting histogram (PCH) analysis are complementary techniques that can be used to measure dynamics and oligomeric status of fluorescent molecules in living intact cells (for a brief review, [248]). In FCS, the fluorescenc fluctuations created by the movement of a labeled molecule (eg. GFP-tagged protein) through the focal volume of a microscope are recorded and the diffusion rate and concentration of the protein can be determined. FCS is an exquisitely

sensitive technique allowing measurements on the microsecond timescale on only a few molecules. Satistical methods have been developed that allow fluctuation data collected by FCS to be analyzed to determine the number of photons emitted per second per molecule or molecular brightness, a readout for the oligoeric status of a protein, which is the basis of PCH analysis [249].

In the last part of my study, I characterized the function of endolyn in kidney development using zebrafish as a model system. I showed that zfEndolyn is expressed early during development in the brain and pronephric kidney of zebrafish. Embryos injected with a translation inhibiting morpholino targeted against zfEndolyn developed pericardial edema, hydrocephaly, and body curvature, suggesting a potential kidney developmental defect. The pronephric kidney appeared normal morphologically, but its clearance of fluorescent dextran injected into the common cardinal vein function was delayed, consistent with a defect in the regulation of water balance in morphant embryos. In addition, rescue experiments suggested that both lumenal and cytoplasmic regions are required for endolyn function. Furthermore, proper sorting of endolyn to both the apical surface and lysosomes are critical for its function.

Our study for the first time demonstrates that endolyn is involved in kidney development. One question that arises from this study is: What exactly the function of endolyn in kidney development? Given the apparent requirement for endolyn proper localization on either the apical surface or lysosomes, it is tempting to speculate that endolyn-mediated binding and endocytosis of an associated ligand may be important for its function. One possible candidate is CXCR4. It has been reported that endolyn is a coreceptor for CXCR4 to regulate cell proliferation, adhesion and differentiation of various cell lines including hematopoietic cells and prostate cancer cells [159,162]. However, no evidence suggests a role of CXCR4 in pronephric

kidney development in zebrafish. Future studies to determine if CXCR4 is involved in pronephric kidney development and to identify additional interaction partners for endolyn are warranted. However, identification of potential endolyn binding partners in zebrafish may not be a straightforward prospect due to the limited availability of reagents and techniques for the zebrafish system. A polarized embryonic kidney cell line would be valuable to address this problem. We obtained a rat embryonic kidney cell line in our laboratory recently; however, more effort to characterize it is required. Once a cell line is established, we are able to knock in or knock out endolyn to evaluate possible defects and identify interaction partners. For example, we are able to evaluate cell proliferation using bromodeoxyuridine (BrdU) incorporation assay [250]. We can measure apoptosis by performing TUNEL assay [251]. Additionally, we can measure cell migration by carrying out wound-healing assay [252]. Furthermore, an unbiased screen for endolyn binding partners should be warranted using mass spectrometry-based proteomics [253]. Further, although the zebrafish pronephros serves as an ideal model to study kidney development, it is unknown how precisely it reflects the development of the mammalian metonephros, a much more complex organ containing millions of nephrons. Further study to characterize endolyn function in a more advance animal model will address this concern. An endolyn knock-out mice model should be reasonably considered.

To summarize this body of work, we demonstrated that apical delivery of endolyn can be modulated by posttranslational N-glycan processing in MDCK cells. Futher, we found that the proper sorting of endolyn is relevant to its function during kidney development. As shown in Fig.26, endolyn localization varies along the renal tubule between apical and lysosomal compartments. The remaining questions are how endolyn localization is differentially regulated in the kidney tubules and how endolyn localization affects its function in the developing and

adult kidney. One possible explaination is that endolyn localization can be regulated by altering the expression or activity of enzymes involved in the synthesis or degradation of N-glycans. Indeed, a previous report documented differential recognition of human endolyn in various tissues using monoclonal antibodies directed towards distinct glycan-dependent epitopes on endolyn [254]. In the absence of a dominant apical sorting signal, endolyn would recycle more between lysosomes and the basolateral cell surface due to the presence of a cytosolic tyrosine-based motif [153,155], and this could act in concert with a potentially reduced retention of endolyn at the apical surface. Alternatively, changes in Gal-9 expression might play a role in controlling the steady state distribution of endolyn along the renal tubule; however, this is less likely as Gal-9 is expressed throughout the cortex of adult mouse kidney [255]. To date, the expression patterns of sialyltransferases ST3GalT-III, ST3GalT-IV, and ST6Gal-I in the kidney have not been carefully examined. One previous report describes sialoconjugate distribution along the rat renal tubule assessed using SNA and MAA lectins [256]. Interestingly, this study found that only the α2,6-selective lectin SNA bound to the proximal convoluted tubule (S1 and S2 segments), whereas both SNA and MAA bound to the proximal straight tubule (S3). However, this approach cannot distinguish between sialic acids on N- vs. O-linked glycans or on glycolipids, and thus provides little information about sialyltransferase expression in these segments. Future studies using in situ hybridization or specific antibodies staining will reveal the expression patten of specific enzymes that involved in regulation of N-glycans. This will provide clues to determine how endolyn localization is regulated in kidney tubules and what exactly the role of endolyn is in kidney.

BIBLIOGRAPHY

1. Ross MH PW, Barnash TA (2009) Atlas of Descriptive Histology.
2. Ovalle WK NP (2008) Netter's essential histology.
3. Campbell MF WA, Kavoussi LR (2012) Wein: Campbell-Walsh Urology, 10th. ed.
4. Quaggin SE, Kreidberg JA (2008) Development of the renal glomerulus: good neighbors and good fences. Development 135: 609-620.
5. Brenner BM, Hostetter TH, Humes HD (1978) Glomerular permselectivity: barrier function based on discrimination of molecular size and charge. Am J Physiol 234: F455-460.
6. Davidson AJ (2008) StemBook [Internet]. Harvard Stem Cell Institue.
7. Zhou W, Boucher RC, Bollig F, Englert C, Hildebrandt F (2010) Characterization of mesonephric development and regeneration using transgenic zebrafish. Am J Physiol Renal Physiol 299: F1040-1047.
8. Sawle A (2009) Development of embryonic nephrons. Wikimedia Commons.
9. Jones EA (2005) Xenopus: a prince among models for pronephric kidney development. J Am Soc Nephrol 16: 313-321.
10. Drummond IA (2005) Kidney development and disease in the zebrafish. J Am Soc Nephrol 16: 299-304.
11. Drummond I (2003) Making a zebrafish kidney: a tale of two tubes. Trends Cell Biol 13: 357-365.
12. Pole RJ, Qi BQ, Beasley SW (2002) Patterns of apoptosis during degeneration of the pronephros and mesonephros. J Urol 167: 269-271.
13. Smith C, Mackay S (1991) Morphological development and fate of the mouse mesonephros. J Anat 174: 171-184.
14. Saxen L, Lehtonen E (1987) Embryonic kidney in organ culture. Differentiation 36: 2-11.
15. Sainio K, Hellstedt P, Kreidberg JA, Saxen L, Sariola H (1997) Differential regulation of two sets of mesonephric tubules by WT-1. Development 124: 1293-1299.
16. Zhou W, Boucher RC, Bollig F, Englert C, Hildebrandt F Characterization of mesonephric development and regeneration using transgenic zebrafish. Am J Physiol Renal Physiol 299: F1040-1047.
17. Vize PD WA, Bard JBL (2003) The kidney: from normal development to congenital disease.
18. Davies JA, Bard JB (1998) The development of the kidney. Curr Top Dev Biol 39: 245-301.
19. Bard JB, Gordon A, Sharp L, Sellers WI (2001) Early nephron formation in the developing mouse kidney. J Anat 199: 385-392.
20. Bard JB (2002) Growth and death in the developing mammalian kidney: signals, receptors and conversations. Bioessays 24: 72-82.

21. Kispert A, Vainio S, McMahon AP (1998) Wnt-4 is a mesenchymal signal for epithelial transformation of metanephric mesenchyme in the developing kidney. Development 125: 4225-4234.
22. Dressler GR, Deutsch U, Chowdhury K, Nornes HO, Gruss P (1990) Pax2, a new murine paired-box-containing gene and its expression in the developing excretory system. Development 109: 787-795.
23. Dressler GR, Douglass EC (1992) Pax-2 is a DNA-binding protein expressed in embryonic kidney and Wilms tumor. Proc Natl Acad Sci U S A 89: 1179-1183.
24. Benigni A, Morigi M, Remuzzi G (2010) Kidney regeneration. Lancet 375: 1310-1317.
25. Simons K, Wandinger-Ness A (1990) Polarized sorting in epithelia. Cell 62: 207-210.
26. St Johnston D, Ahringer J Cell polarity in eggs and epithelia: parallels and diversity. Cell 141: 757-774.
27. Mellman I, Nelson WJ (2008) Coordinated protein sorting, targeting and distribution in polarized cells. Nat Rev Mol Cell Biol 9: 833-845.
28. Zegers MM, Hoekstra D (1998) Mechanisms and functional features of polarized membrane traffic in epithelial and hepatic cells. Biochem J 336 (Pt 2): 257-269.
29. Bornens M (2008) Organelle positioning and cell polarity. Nat Rev Mol Cell Biol 9: 874-886.
30. Welling PA, Weisz OA Sorting it out in endosomes: an emerging concept in renal epithelial cell transport regulation. Physiology (Bethesda) 25: 280-292.
31. Martin-Belmonte F, Perez-Moreno M (2012) Epithelial cell polarity, stem cells and cancer. Nat Rev Cancer 12: 23-38.
32. Perez-Moreno M, Jamora C, Fuchs E (2003) Sticky business: orchestrating cellular signals at adherens junctions. Cell 112: 535-548.
33. Martin-Belmonte F, Mostov K (2008) Regulation of cell polarity during epithelial morphogenesis. Curr Opin Cell Biol 20: 227-234.
34. Niessen CM, Gottardi CJ (2008) Molecular components of the adherens junction. Biochim Biophys Acta 1778: 562-571.
35. Cereijido M, Contreras RG, Shoshani L, Flores-Benitez D, Larre I (2008) Tight junction and polarity interaction in the transporting epithelial phenotype. Biochim Biophys Acta 1778: 770-793.
36. Tsukita S, Yamazaki Y, Katsuno T, Tamura A (2008) Tight junction-based epithelial microenvironment and cell proliferation. Oncogene 27: 6930-6938.
37. Lee M, Vasioukhin V (2008) Cell polarity and cancer--cell and tissue polarity as a non-canonical tumor suppressor. J Cell Sci 121: 1141-1150.
38. Weber GF, Bjerke MA, DeSimone DW Integrins and cadherins join forces to form adhesive networks. J Cell Sci 124: 1183-1193.
39. Ooshio T, Fujita N, Yamada A, Sato T, Kitagawa Y, et al. (2007) Cooperative roles of Par-3 and afadin in the formation of adherens and tight junctions. J Cell Sci 120: 2352-2365.
40. Sakisaka T, Ikeda W, Ogita H, Fujita N, Takai Y (2007) The roles of nectins in cell adhesions: cooperation with other cell adhesion molecules and growth factor receptors. Curr Opin Cell Biol 19: 593-602.
41. Mege RM, Gavard J, Lambert M (2006) Regulation of cell-cell junctions by the cytoskeleton. Curr Opin Cell Biol 18: 541-548.

42. Horikoshi Y, Suzuki A, Yamanaka T, Sasaki K, Mizuno K, et al. (2009) Interaction between PAR-3 and the aPKC-PAR-6 complex is indispensable for apical domain development of epithelial cells. J Cell Sci 122: 1595-1606.
43. Laprise P, Viel A, Rivard N (2004) Human homolog of disc-large is required for adherens junction assembly and differentiation of human intestinal epithelial cells. J Biol Chem 279: 10157-10166.
44. Navarro C, Nola S, Audebert S, Santoni MJ, Arsanto JP, et al. (2005) Junctional recruitment of mammalian Scribble relies on E-cadherin engagement. Oncogene 24: 4330-4339.
45. Birchmeier W, Behrens J (1994) Cadherin expression in carcinomas: role in the formation of cell junctions and the prevention of invasiveness. Biochim Biophys Acta 1198: 11-26.
46. Gonzalez-Mariscal L, Lechuga S, Garay E (2007) Role of tight junctions in cell proliferation and cancer. Prog Histochem Cytochem 42: 1-57.
47. Stein M, Wandinger-Ness A, Roitbak T (2002) Altered trafficking and epithelial cell polarity in disease. Trends Cell Biol 12: 374-381.
48. Naim HY, Roth J, Sterchi EE, Lentze M, Milla P, et al. (1988) Sucrase-isomaltase deficiency in humans. Different mutations disrupt intracellular transport, processing, and function of an intestinal brush border enzyme. J Clin Invest 82: 667-679.
49. Musch A, Xu H, Shields D, Rodriguez-Boulan E (1996) Transport of vesicular stomatitis virus G protein to the cell surface is signal mediated in polarized and nonpolarized cells. J Cell Biol 133: 543-558.
50. Simmons NL (1982) Cultured monolayers of MDCK cells: a novel model system for the study of epithelial development and function. Gen Pharmacol 13: 287-291.
51. Rindler MJ, Ivanov IE, Plesken H, Sabatini DD (1985) Polarized delivery of viral glycoproteins to the apical and basolateral plasma membranes of Madin-Darby canine kidney cells infected with temperature-sensitive viruses. J Cell Biol 100: 136-151.
52. Keller P, Toomre D, Diaz E, White J, Simons K (2001) Multicolour imaging of post-Golgi sorting and trafficking in live cells. Nat Cell Biol 3: 140-149.
53. Cereijido M, Robbins ES, Dolan WJ, Rotunno CA, Sabatini DD (1978) Polarized monolayers formed by epithelial cells on a permeable and translucent support. J Cell Biol 77: 853-880.
54. Ellis MA, Potter BA, Cresawn KO, Weisz OA (2006) Polarized biosynthetic traffic in renal epithelial cells: sorting, sorting, everywhere. Am J Physiol Renal Physiol 291: F707-713.
55. Carmosino M, Valenti G, Caplan M, Svelto M Polarized traffic towards the cell surface: how to find the route. Biol Cell 102: 75-91.
56. Mostov KE, de Bruyn Kops A, Deitcher DL (1986) Deletion of the cytoplasmic domain of the polymeric immunoglobulin receptor prevents basolateral localization and endocytosis. Cell 47: 359-364.
57. Casanova JE, Apodaca G, Mostov KE (1991) An autonomous signal for basolateral sorting in the cytoplasmic domain of the polymeric immunoglobulin receptor. Cell 66: 65-75.
58. Matter K, Hunziker W, Mellman I (1992) Basolateral sorting of LDL receptor in MDCK cells: the cytoplasmic domain contains two tyrosine-dependent targeting determinants. Cell 71: 741-753.
59. Thomas DC, Brewer CB, Roth MG (1993) Vesicular stomatitis virus glycoprotein contains a dominant cytoplasmic basolateral sorting signal critically dependent upon a tyrosine. J Biol Chem 268: 3313-3320.

60. Hunziker W, Geuze HJ (1996) Intracellular trafficking of lysosomal membrane proteins. Bioessays 18: 379-389.
61. Hunziker W, Fumey C (1994) A di-leucine motif mediates endocytosis and basolateral sorting of macrophage IgG Fc receptors in MDCK cells. EMBO J 13: 2963-2969.
62. Miranda KC, Khromykh T, Christy P, Le TL, Gottardi CJ, et al. (2001) A dileucine motif targets E-cadherin to the basolateral cell surface in Madin-Darby canine kidney and LLC-PK1 epithelial cells. J Biol Chem 276: 22565-22572.
63. Guezguez B, Vigneron P, Alais S, Jaffredo T, Gavard J, et al. (2006) A dileucine motif targets MCAM-l cell adhesion molecule to the basolateral membrane in MDCK cells. FEBS Lett 580: 3649-3656.
64. Folsch H (2005) The building blocks for basolateral vesicles in polarized epithelial cells. Trends Cell Biol 15: 222-228.
65. Hirst J, Barlow LD, Francisco GC, Sahlender DA, Seaman MN, et al. (2011) The fifth adaptor protein complex. PLoS Biol 9: e1001170.
66. Robinson MS, Bonifacino JS (2001) Adaptor-related proteins. Curr Opin Cell Biol 13: 444-453.
67. Ohno H, Tomemori T, Nakatsu F, Okazaki Y, Aguilar RC, et al. (1999) Mu1B, a novel adaptor medium chain expressed in polarized epithelial cells. FEBS Lett 449: 215-220.
68. Ang AL, Folsch H, Koivisto UM, Pypaert M, Mellman I (2003) The Rab8 GTPase selectively regulates AP-1B-dependent basolateral transport in polarized Madin-Darby canine kidney cells. J Cell Biol 163: 339-350.
69. Simmen T, Honing S, Icking A, Tikkanen R, Hunziker W (2002) AP-4 binds basolateral signals and participates in basolateral sorting in epithelial MDCK cells. Nat Cell Biol 4: 154-159.
70. Straight SW, Karnak D, Borg JP, Kamberov E, Dare H, et al. (2000) mLin-7 is localized to the basolateral surface of renal epithelia via its NH(2) terminus. Am J Physiol Renal Physiol 278: F464-475.
71. Olsen O, Liu H, Wade JB, Merot J, Welling PA (2002) Basolateral membrane expression of the Kir 2.3 channel is coordinated by PDZ interaction with Lin-7/CASK complex. Am J Physiol Cell Physiol 282: C183-195.
72. Lisanti MP, Caras IW, Davitz MA, Rodriguez-Boulan E (1989) A glycophospholipid membrane anchor acts as an apical targeting signal in polarized epithelial cells. J Cell Biol 109: 2145-2156.
73. Brown DA, Crise B, Rose JK (1989) Mechanism of membrane anchoring affects polarized expression of two proteins in MDCK cells. Science 245: 1499-1501.
74. Brown D, Waneck GL (1992) Glycosyl-phosphatidylinositol-anchored membrane proteins. J Am Soc Nephrol 3: 895-906.
75. Schroeder RJ, Ahmed SN, Zhu Y, London E, Brown DA (1998) Cholesterol and sphingolipid enhance the Triton X-100 insolubility of glycosylphosphatidylinositol-anchored proteins by promoting the formation of detergent-insoluble ordered membrane domains. J Biol Chem 273: 1150-1157.
76. Brown DA, Rose JK (1992) Sorting of GPI-anchored proteins to glycolipid-enriched membrane subdomains during transport to the apical cell surface. Cell 68: 533-544.
77. Skibbens JE, Roth MG, Matlin KS (1989) Differential extractability of influenza virus hemagglutinin during intracellular transport in polarized epithelial cells and nonpolar fibroblasts. J Cell Biol 108: 821-832.

78. Scheiffele P, Roth MG, Simons K (1997) Interaction of influenza virus haemagglutinin with sphingolipid-cholesterol membrane domains via its transmembrane domain. EMBO J 16: 5501-5508.
79. Tall RD, Alonso MA, Roth MG (2003) Features of influenza HA required for apical sorting differ from those required for association with DRMs or MAL. Traffic 4: 838-849.
80. Takeda M, Leser GP, Russell CJ, Lamb RA (2003) Influenza virus hemagglutinin concentrates in lipid raft microdomains for efficient viral fusion. Proc Natl Acad Sci U S A 100: 14610-14617.
81. Engel S, de Vries M, Herrmann A, Veit M (2012) Mutation of a raft-targeting signal in the transmembrane region retards transport of influenza virus hemagglutinin through the Golgi. FEBS Lett 586: 277-282.
82. Veit M, Kretzschmar E, Kuroda K, Garten W, Schmidt MF, et al. (1991) Site-specific mutagenesis identifies three cysteine residues in the cytoplasmic tail as acylation sites of influenza virus hemagglutinin. J Virol 65: 2491-2500.
83. Wagner R, Herwig A, Azzouz N, Klenk HD (2005) Acylation-mediated membrane anchoring of avian influenza virus hemagglutinin is essential for fusion pore formation and virus infectivity. J Virol 79: 6449-6458.
84. van Meer G, Simons K (1988) Lipid polarity and sorting in epithelial cells. J Cell Biochem 36: 51-58.
85. Simons K, Ikonen E (1997) Functional rafts in cell membranes. Nature 387: 569-572.
86. Paladino S, Sarnataro D, Pillich R, Tivodar S, Nitsch L, et al. (2004) Protein oligomerization modulates raft partitioning and apical sorting of GPI-anchored proteins. J Cell Biol 167: 699-709.
87. Zurzolo C, Lisanti MP, Caras IW, Nitsch L, Rodriguez-Boulan E (1993) Glycosylphosphatidylinositol-anchored proteins are preferentially targeted to the basolateral surface in Fischer rat thyroid epithelial cells. J Cell Biol 121: 1031-1039.
88. Meiss HK, Green RF, Rodriguez-Boulan EJ (1982) Lectin-resistant mutants of polarized epithelial cells. Mol Cell Biol 2: 1287-1294.
89. Hannan LA, Lisanti MP, Rodriguez-Boulan E, Edidin M (1993) Correctly sorted molecules of a GPI-anchored protein are clustered and immobile when they arrive at the apical surface of MDCK cells. J Cell Biol 120: 353-358.
90. Maeda Y, Tashima Y, Houjou T, Fujita M, Yoko-o T, et al. (2007) Fatty acid remodeling of GPI-anchored proteins is required for their raft association. Mol Biol Cell 18: 1497-1506.
91. Kinoshita T, Fujita M, Maeda Y (2008) Biosynthesis, remodelling and functions of mammalian GPI-anchored proteins: recent progress. J Biochem 144: 287-294.
92. Frank M (2000) MAL, a proteolipid in glycosphingolipid enriched domains: functional implications in myelin and beyond. Prog Neurobiol 60: 531-544.
93. Puertollano R, Alonso MA (1999) MAL, an integral element of the apical sorting machinery, is an itinerant protein that cycles between the trans-Golgi network and the plasma membrane. Mol Biol Cell 10: 3435-3447.
94. Cheong KH, Zacchetti D, Schneeberger EE, Simons K (1999) VIP17/MAL, a lipid raft-associated protein, is involved in apical transport in MDCK cells. Proc Natl Acad Sci U S A 96: 6241-6248.
95. Puertollano R, Alonso MA (1999) Targeting of MAL, a putative element of the apical sorting machinery, to glycolipid-enriched membranes requires a pre-golgi sorting event. Biochem Biophys Res Commun 254: 689-692.

96. de Marco MC, Puertollano R, Martinez-Menarguez JA, Alonso MA (2006) Dynamics of MAL2 during glycosylphosphatidylinositol-anchored protein transcytotic transport to the apical surface of hepatoma HepG2 cells. Traffic 7: 61-73.
97. Marazuela M, Acevedo A, Garcia-Lopez MA, Adrados M, de Marco MC, et al. (2004) Expression of MAL2, an integral protein component of the machinery for basolateral-to-apical transcytosis, in human epithelia. J Histochem Cytochem 52: 243-252.
98. Ramnarayanan SP, Cheng CA, Bastaki M, Tuma PL (2007) Exogenous MAL reroutes selected hepatic apical proteins into the direct pathway in WIF-B cells. Mol Biol Cell 18: 2707-2715.
99. Vieira OV, Verkade P, Manninen A, Simons K (2005) FAPP2 is involved in the transport of apical cargo in polarized MDCK cells. J Cell Biol 170: 521-526.
100. Vieira OV, Gaus K, Verkade P, Fullekrug J, Vaz WL, et al. (2006) FAPP2, cilium formation, and compartmentalization of the apical membrane in polarized Madin-Darby canine kidney (MDCK) cells. Proc Natl Acad Sci U S A 103: 18556-18561.
101. Chuang JZ, Sung CH (1998) The cytoplasmic tail of rhodopsin acts as a novel apical sorting signal in polarized MDCK cells. J Cell Biol 142: 1245-1256.
102. Tai AW, Chuang JZ, Bode C, Wolfrum U, Sung CH (1999) Rhodopsin's carboxy-terminal cytoplasmic tail acts as a membrane receptor for cytoplasmic dynein by binding to the dynein light chain Tctex-1. Cell 97: 877-887.
103. Marzolo MP, Yuseff MI, Retamal C, Donoso M, Ezquer F, et al. (2003) Differential distribution of low-density lipoprotein-receptor-related protein (LRP) and megalin in polarized epithelial cells is determined by their cytoplasmic domains. Traffic 4: 273-288.
104. Takeda T, Yamazaki H, Farquhar MG (2003) Identification of an apical sorting determinant in the cytoplasmic tail of megalin. Am J Physiol Cell Physiol 284: C1105-1113.
105. Chmelar RS, Nathanson NM (2006) Identification of a novel apical sorting motif and mechanism of targeting of the M2 muscarinic acetylcholine receptor. J Biol Chem 281: 35381-35396.
106. Dunbar LA, Aronson P, Caplan MJ (2000) A transmembrane segment determines the steady-state localization of an ion-transporting adenosine triphosphatase. J Cell Biol 148: 769-778.
107. Carmosino M, Gimenez I, Caplan M, Forbush B (2008) Exon loss accounts for differential sorting of Na-K-Cl cotransporters in polarized epithelial cells. Mol Biol Cell 19: 4341-4351.
108. Edited by Ajit Varki RDC, Jeffrey D Esko, Hudson H Freeze, Pamela Stanley, Carolyn R Bertozzi, Gerald W Hart, and Marilynn E Etzler. (2009) Essentials of Glycobiology, 2nd edition.
109. Yeaman C, Le Gall AH, Baldwin AN, Monlauzeur L, Le Bivic A, et al. (1997) The O-glycosylated stalk domain is required for apical sorting of neurotrophin receptors in polarized MDCK cells. J Cell Biol 139: 929-940.
110. Jacob R, Alfalah M, Grunberg J, Obendorf M, Naim HY (2000) Structural determinants required for apical sorting of an intestinal brush-border membrane protein. J Biol Chem 275: 6566-6572.
111. Kinlough CL, Poland PA, Gendler SJ, Mattila PE, Mo D, et al. (2011) Core-glycosylated mucin-like repeats from MUC1 are an apical targeting signal. J Biol Chem 286: 39072-39081.

112. Spodsberg N, Alfalah M, Naim HY (2001) Characteristics and structural requirements of apical sorting of the rat growth hormone through the O-glycosylated stalk region of intestinal sucrase-isomaltase. J Biol Chem 276: 46597-46604.
113. Delacour D, Gouyer V, Leteurtre E, Ait-Slimane T, Drobecq H, et al. (2003) 1-benzyl-2-acetamido-2-deoxy-alpha-D-galactopyranoside blocks the apical biosynthetic pathway in polarized HT-29 cells. J Biol Chem 278: 37799-37809.
114. Gouyer V, Leteurtre E, Zanetta JP, Lesuffleur T, Delannoy P, et al. (2001) Inhibition of the glycosylation and alteration in the intracellular trafficking of mucins and other glycoproteins by GalNAcalpha-O-bn in mucosal cell lines: an effect mediated through the intracellular synthesis of complex GalNAcalpha-O-bn oligosaccharides. Front Biosci 6: D1235-1244.
115. Leteurtre E, Gouyer V, Delacour D, Hemon B, Pons A, et al. (2003) Induction of a storage phenotype and abnormal intracellular localization of apical glycoproteins are two independent responses to GalNAcalpha-O-bn. J Histochem Cytochem 51: 349-361.
116. Gouyer V, Leteurtre E, Delmotte P, Steelant WF, Krzewinski-Recchi MA, et al. (2001) Differential effect of GalNAcalpha-O-bn on intracellular trafficking in enterocytic HT-29 and Caco-2 cells: correlation with the glycosyltransferase expression pattern. J Cell Sci 114: 1455-1471.
117. Slimane TA, Lenoir C, Sapin C, Maurice M, Trugnan G (2000) Apical secretion and sialylation of soluble dipeptidyl peptidase IV are two related events. Exp Cell Res 258: 184-194.
118. Potter BA, Hughey RP, Weisz OA (2006) Role of N- and O-glycans in polarized biosynthetic sorting. Am J Physiol Cell Physiol 290: C1-C10.
119. Kornfeld R, Kornfeld S (1985) Assembly of asparagine-linked oligosaccharides. Annu Rev Biochem 54: 631-664.
120. Varki A (1992) Diversity in the sialic acids. Glycobiology 2: 25-40.
121. Tsuji S (1996) Molecular cloning and functional analysis of sialyltransferases. J Biochem 120: 1-13.
122. Scheiffele P, Peranen J, Simons K (1995) N-glycans as apical sorting signals in epithelial cells. Nature 378: 96-98.
123. Urban J, Parczyk K, Leutz A, Kayne M, Kondor-Koch C (1987) Constitutive apical secretion of an 80-kD sulfated glycoprotein complex in the polarized epithelial Madin-Darby canine kidney cell line. J Cell Biol 105: 2735-2743.
124. Vagin O, Turdikulova S, Sachs G (2004) The H,K-ATPase beta subunit as a model to study the role of N-glycosylation in membrane trafficking and apical sorting. J Biol Chem 279: 39026-39034.
125. Gut A, Kappeler F, Hyka N, Balda MS, Hauri HP, et al. (1998) Carbohydrate-mediated Golgi to cell surface transport and apical targeting of membrane proteins. EMBO J 17: 1919-1929.
126. Potter BA, Ihrke G, Bruns JR, Weixel KM, Weisz OA (2004) Specific N-glycans direct apical delivery of transmembrane, but not soluble or glycosylphosphatidylinositol-anchored forms of endolyn in Madin-Darby canine kidney cells. Mol Biol Cell 15: 1407-1416.
127. Kitagawa Y, Sano Y, Ueda M, Higashio K, Narita H, et al. (1994) N-glycosylation of erythropoietin is critical for apical secretion by Madin-Darby canine kidney cells. Exp Cell Res 213: 449-457.

128. Martinez-Maza R, Poyatos I, Lopez-Corcuera B, E Nu, Gimenez C, et al. (2001) The role of N-glycosylation in transport to the plasma membrane and sorting of the neuronal glycine transporter GLYT2. J Biol Chem 276: 2168-2173.
129. Lau KS, Partridge EA, Grigorian A, Silvescu CI, Reinhold VN, et al. (2007) Complex N-glycan number and degree of branching cooperate to regulate cell proliferation and differentiation. Cell 129: 123-134.
130. An HJ, Gip P, Kim J, Wu S, Park KW, et al. (2012) Extensive determination of glycan heterogeneity reveals an unusual abundance of high-mannose glycans in enriched plasma membranes of human embryonic stem cells. Mol Cell Proteomics.
131. Comelli EM, Head SR, Gilmartin T, Whisenant T, Haslam SM, et al. (2006) A focused microarray approach to functional glycomics: transcriptional regulation of the glycome. Glycobiology 16: 117-131.
132. Ohtsubo K, Marth JD (2006) Glycosylation in cellular mechanisms of health and disease. Cell 126: 855-867.
133. Ito H, Kuno A, Sawaki H, Sogabe M, Ozaki H, et al. (2009) Strategy for glycoproteomics: identification of glyco-alteration using multiple glycan profiling tools. J Proteome Res 8: 1358-1367.
134. Wearne KA, Winter HC, O'Shea K, Goldstein IJ (2006) Use of lectins for probing differentiated human embryonic stem cells for carbohydrates. Glycobiology 16: 981-990.
135. Rodriguez-Boulan E, Gonzalez A (1999) Glycans in post-Golgi apical targeting: sorting signals or structural props? Trends Cell Biol 9: 291-294.
136. Fiedler K, Parton RG, Kellner R, Etzold T, Simons K (1994) VIP36, a novel component of glycolipid rafts and exocytic carrier vesicles in epithelial cells. EMBO J 13: 1729-1740.
137. Fullekrug J, Scheiffele P, Simons K (1999) VIP36 localisation to the early secretory pathway. J Cell Sci 112 (Pt 17): 2813-2821.
138. Poland PA, Rondanino C, Kinlough CL, Heimburg-Molinaro J, Arthur CM, et al. (2011) Identification and characterization of endogenous galectins expressed in Madin Darby canine kidney cells. J Biol Chem 286: 6780-6790.
139. Delacour D, Gouyer V, Zanetta JP, Drobecq H, Leteurtre E, et al. (2005) Galectin-4 and sulfatides in apical membrane trafficking in enterocyte-like cells. J Cell Biol 169: 491-501.
140. Stechly L, Morelle W, Dessein AF, Andre S, Grard G, et al. (2009) Galectin-4-regulated delivery of glycoproteins to the brush border membrane of enterocyte-like cells. Traffic 10: 438-450.
141. Morelle W, Stechly L, Andre S, Van Seuningen I, Porchet N, et al. (2009) Glycosylation pattern of brush border-associated glycoproteins in enterocyte-like cells: involvement of complex-type N-glycans in apical trafficking. Biol Chem 390: 529-544.
142. Delacour D, Cramm-Behrens CI, Drobecq H, Le Bivic A, Naim HY, et al. (2006) Requirement for galectin-3 in apical protein sorting. Curr Biol 16: 408-414.
143. Delacour D, Koch A, Ackermann W, Eude-Le Parco I, Elsasser HP, et al. (2008) Loss of galectin-3 impairs membrane polarisation of mouse enterocytes in vivo. J Cell Sci 121: 458-465.
144. Schneider D, Greb C, Koch A, Straube T, Elli A, et al. (2010) Trafficking of galectin-3 through endosomal organelles of polarized and non-polarized cells. Eur J Cell Biol 89: 788-798.

145. Koch A, Poirier F, Jacob R, Delacour D (2010) Galectin-3, a novel centrosome-associated protein, required for epithelial morphogenesis. Mol Biol Cell 21: 219-231.
146. Mishra R, Grzybek M, Niki T, Hirashima M, Simons K (2010) Galectin-9 trafficking regulates apical-basal polarity in Madin-Darby canine kidney epithelial cells. Proc Natl Acad Sci U S A 107: 17633-17638.
147. Chiu MG, Johnson TM, Woolf AS, Dahm-Vicker EM, Long DA, et al. (2006) Galectin-3 associates with the primary cilium and modulates cyst growth in congenital polycystic kidney disease. Am J Pathol 169: 1925-1938.
148. Delacour D, Greb C, Koch A, Salomonsson E, Leffler H, et al. (2007) Apical sorting by galectin-3-dependent glycoprotein clustering. Traffic 8: 379-388.
149. Ihrke G, Martin GV, Shanks MR, Schrader M, Schroer TA, et al. (1998) Apical plasma membrane proteins and endolyn-78 travel through a subapical compartment in polarized WIF-B hepatocytes. J Cell Biol 141: 115-133.
150. Akasaki K, Michihara A, Fujiwara Y, Mibuka K, Tsuji H (1996) Biosynthetic transport of a major lysosome-associated membrane glycoprotein 2, lamp-2: a significant fraction of newly synthesized lamp-2 is delivered to lysosomes by way of early endosomes. J Biochem 120: 1088-1094.
151. Carlsson SR, Fukuda M (1992) The lysosomal membrane glycoprotein lamp-1 is transported to lysosomes by two alternative pathways. Arch Biochem Biophys 296: 630-639.
152. Ihrke G, Bruns JR, Luzio JP, Weisz OA (2001) Competing sorting signals guide endolyn along a novel route to lysosomes in MDCK cells. EMBO J 20: 6256-6264.
153. Ihrke G, Gray SR, Luzio JP (2000) Endolyn is a mucin-like type I membrane protein targeted to lysosomes by its cytoplasmic tail. Biochem J 345 Pt 2: 287-296.
154. Harter C, Mellman I (1992) Transport of the lysosomal membrane glycoprotein lgp120 (lgp-A) to lysosomes does not require appearance on the plasma membrane. J Cell Biol 117: 311-325.
155. Ihrke G, Kyttala A, Russell MR, Rous BA, Luzio JP (2004) Differential use of two AP-3-mediated pathways by lysosomal membrane proteins. Traffic 5: 946-962.
156. Potter BA, Weixel KM, Bruns JR, Ihrke G, Weisz OA (2006) N-glycans mediate apical recycling of the sialomucin endolyn in polarized MDCK cells. Traffic 7: 146-154.
157. Zannettino AC, Buhring HJ, Niutta S, Watt SM, Benton MA, et al. (1998) The sialomucin CD164 (MGC-24v) is an adhesive glycoprotein expressed by human hematopoietic progenitors and bone marrow stromal cells that serves as a potent negative regulator of hematopoiesis. Blood 92: 2613-2628.
158. Watt SM, Buhring HJ, Rappold I, Chan JY, Lee-Prudhoe J, et al. (1998) CD164, a novel sialomucin on CD34(+) and erythroid subsets, is located on human chromosome 6q21. Blood 92: 849-866.
159. Forde S, Tye BJ, Newey SE, Roubelakis M, Smythe J, et al. (2007) Endolyn (CD164) modulates the CXCL12-mediated migration of umbilical cord blood CD133+ cells. Blood 109: 1825-1833.
160. Lee YN, Kang JS, Krauss RS (2001) Identification of a role for the sialomucin CD164 in myogenic differentiation by signal sequence trapping in yeast. Mol Cell Biol 21: 7696-7706.
161. Bae GU, Gaio U, Yang YJ, Lee HJ, Kang JS, et al. (2008) Regulation of myoblast motility and fusion by the CXCR4-associated sialomucin, CD164. J Biol Chem 283: 8301-8309.

162. Havens AM, Jung Y, Sun YX, Wang J, Shah RB, et al. (2006) The role of sialomucin CD164 (MGC-24v or endolyn) in prostate cancer metastasis. BMC Cancer 6: 195.
163. Goldberg MR, Barasch J, Shifteh A, D'Agati V, Oliver JA, et al. (1997) Spatial and temporal expression of cell surface molecules during nephrogenesis. Am J Physiol 272: F79-86.
164. Gresch O, Engel FB, Nesic D, Tran TT, England HM, et al. (2004) New non-viral method for gene transfer into primary cells. Methods 33: 151-163.
165. Hamm A, Krott N, Breibach I, Blindt R, Bosserhoff AK (2002) Efficient transfection method for primary cells. Tissue Eng 8: 235-245.
166. Chen X, Macara IG (2006) RNA interference techniques to study epithelial cell adhesion and polarity. Methods Enzymol 406: 362-374.
167. Mo D, Potter BA, Bertrand CA, Hildebrand JD, Bruns JR, et al. (2010) Nucleofection disrupts tight junction fence function to alter membrane polarity of renal epithelial cells. Am J Physiol Renal Physiol 299: F1178-1184.
168. Cresawn KO, Potter BA, Oztan A, Guerriero CJ, Ihrke G, et al. (2007) Differential involvement of endocytic compartments in the biosynthetic traffic of apical proteins. EMBO J 26: 3737-3748.
169. Lin S, Naim HY, Rodriguez AC, Roth MG (1998) Mutations in the middle of the transmembrane domain reverse the polarity of transport of the influenza virus hemagglutinin in MDCK epithelial cells. J Cell Biol 142: 51-57.
170. Overgaard CE, Sanzone KM, Spiczka KS, Sheff DR, Sandra A, et al. (2009) Deciliation is associated with dramatic remodeling of epithelial cell junctions and surface domains. Mol Biol Cell 20: 102-113.
171. Verghese E, Ricardo SD, Weidenfeld R, Zhuang J, Hill PA, et al. (2009) Renal primary cilia lengthen after acute tubular necrosis. J Am Soc Nephrol 20: 2147-2153.
172. Rojas R, Ruiz WG, Leung SM, Jou TS, Apodaca G (2001) Cdc42-dependent modulation of tight junctions and membrane protein traffic in polarized Madin-Darby canine kidney cells. Mol Biol Cell 12: 2257-2274.
173. Wakabayashi Y, Chua J, Larkin JM, Lippincott-Schwartz J, Arias IM (2007) Four-dimensional imaging of filter-grown polarized epithelial cells. Histochem Cell Biol 127: 463-472.
174. Shin K, Fogg VC, Margolis B (2006) Tight junctions and cell polarity. Annu Rev Cell Dev Biol 22: 207-235.
175. Balda MS, Anderson JM, Matter K (1996) The SH3 domain of the tight junction protein ZO-1 binds to a serine protein kinase that phosphorylates a region C-terminal to this domain. FEBS Lett 399: 326-332.
176. Furuse M, Hata M, Furuse K, Yoshida Y, Haratake A, et al. (2002) Claudin-based tight junctions are crucial for the mammalian epidermal barrier: a lesson from claudin-1-deficient mice. J Cell Biol 156: 1099-1111.
177. Liu Y, Nusrat A, Schnell FJ, Reaves TA, Walsh S, et al. (2000) Human junction adhesion molecule regulates tight junction resealing in epithelia. J Cell Sci 113 (Pt 13): 2363-2374.
178. Tokunaga Y, Kojima T, Osanai M, Murata M, Chiba H, et al. (2007) A novel monoclonal antibody against the second extracellular loop of occludin disrupts epithelial cell polarity. J Histochem Cytochem 55: 735-744.

179. Van Itallie CM, Anderson JM (2006) Claudins and epithelial paracellular transport. Annu Rev Physiol 68: 403-429.
180. Yu AS, McCarthy KM, Francis SA, McCormack JM, Lai J, et al. (2005) Knockdown of occludin expression leads to diverse phenotypic alterations in epithelial cells. Am J Physiol Cell Physiol 288: C1231-1241.
181. Balda MS, Whitney JA, Flores C, Gonzalez S, Cereijido M, et al. (1996) Functional dissociation of paracellular permeability and transepithelial electrical resistance and disruption of the apical-basolateral intramembrane diffusion barrier by expression of a mutant tight junction membrane protein. J Cell Biol 134: 1031-1049.
182. Hernandez S, Chavez Munguia B, Gonzalez-Mariscal L (2007) ZO-2 silencing in epithelial cells perturbs the gate and fence function of tight junctions and leads to an atypical monolayer architecture. Exp Cell Res 313: 1533-1547.
183. Rols MP (2008) Mechanism by which electroporation mediates DNA migration and entry into cells and targeted tissues. Methods Mol Biol 423: 19-33.
184. Bens M, Vallet V, Cluzeaud F, Pascual-Letallec L, Kahn A, et al. (1999) Corticosteroid-dependent sodium transport in a novel immortalized mouse collecting duct principal cell line. J Am Soc Nephrol 10: 923-934.
185. Hardy S, Kitamura M, Harris-Stansil T, Dai Y, Phipps ML (1997) Construction of adenovirus vectors through Cre-lox recombination. J Virol 71: 1842-1849.
186. Henkel JR, Apodaca G, Altschuler Y, Hardy S, Weisz OA (1998) Selective perturbation of apical membrane traffic by expression of influenza M2, an acid-activated ion channel, in polarized madin-darby canine kidney cells. Mol Biol Cell 9: 2477-2490.
187. Henkel JR, Weisz OA (1998) Influenza virus M2 protein slows traffic along the secretory pathway. pH perturbation of acidified compartments affects early Golgi transport steps. J Biol Chem 273: 6518-6524.
188. Weisz OA, Rodriguez-Boulan E (2009) Apical trafficking in epithelial cells: signals, clusters and motors. J Cell Sci 122: 4253-4266.
189. Folsch H, Mattila PE, Weisz OA (2009) Taking the scenic route: biosynthetic traffic to the plasma membrane in polarized epithelial cells. Traffic 10: 972-981.
190. Friedrichs J, Torkko JM, Helenius J, Teravainen TP, Fullekrug J, et al. (2007) Contributions of galectin-3 and -9 to epithelial cell adhesion analyzed by single cell force spectroscopy. J Biol Chem 282: 29375-29383.
191. Mattila PE, Youker RT, Mo D, Bruns JR, Cresawn KO, et al. (2012) Multiple biosynthetic trafficking routes for apically secreted proteins in MDCK cells. Traffic 13: 433-442.
192. Julenius K, Molgaard A, Gupta R, Brunak S (2005) Prediction, conservation analysis, and structural characterization of mammalian mucin-type O-glycosylation sites. Glycobiology 15: 153-164.
193. Dennis JW, Lau KS, Demetriou M, Nabi IR (2009) Adaptive regulation at the cell surface by N-glycosylation. Traffic 10: 1569-1578.
194. Vagin O, Tokhtaeva E, Yakubov I, Shevchenko E, Sachs G (2008) Inverse correlation between the extent of N-glycan branching and intercellular adhesion in epithelia. Contribution of the Na,K-ATPase beta1 subunit. J Biol Chem 283: 2192-2202.
195. Schauer R (2000) Achievements and challenges of sialic acid research. Glycoconj J 17: 485-499.
196. Varki A (2009) Essentials of glycobiology. Cold Spring Harbor, N.Y.: Cold Spring Harbor Laboratory Press. xxix, 784 p. p.

197. Brandli AW, Hansson GC, Rodriguez-Boulan E, Simons K (1988) A polarized epithelial cell mutant deficient in translocation of UDP-galactose into the Golgi complex. J Biol Chem 263: 16283-16290.
198. Le Bivic A, Garcia M, Rodriguez-Boulan E (1993) Ricin-resistant Madin-Darby canine kidney cells missort a major endogenous apical sialoglycoprotein. J Biol Chem 268: 6909-6916.
199. Mishra R, Grzybek M, Niki T, Hirashima M, Simons K (2010) Galectin-9 trafficking regulates apical-basal polarity in Madin-Darby canine kidney epithelial cells. Proceedings of the National Academy of Sciences of the United States of America 107: 17633-17638.
200. Hikita C, Vijayakumar S, Takito J, Erdjument-Bromage H, Tempst P, et al. (2000) Induction of terminal differentiation in epithelial cells requires polymerization of hensin by galectin 3. J Cell Biol 151: 1235-1246.
201. Rondanino C, Poland PA, Kinlough CL, Li H, Rbaibi Y, et al. (2011) Galectin-7 modulates the length of the primary cilia and wound repair in polarized kidney epithelial cells. Am J Physiol Renal Physiol 301: F622-633.
202. Mattila PE, Kinlough CL, Bruns JR, Weisz OA, Hughey RP (2009) MUC1 traverses apical recycling endosomes along the biosynthetic pathway in polarized MDCK cells. Biol Chem 390: 551-556.
203. Ulloa F, Franci C, Real FX (2000) GalNAc-alpha -O-benzyl inhibits sialylation of de Novo synthesized apical but not basolateral sialoglycoproteins and blocks lysosomal enzyme processing in a post-trans-Golgi network compartment. J Biol Chem 275: 18785-18793.
204. Huet G, Hennebicq-Reig S, de Bolos C, Ulloa F, Lesuffleur T, et al. (1998) GalNAc-alpha-O-benzyl inhibits NeuAcalpha2-3 glycosylation and blocks the intracellular transport of apical glycoproteins and mucus in differentiated HT-29 cells. J Cell Biol 141: 1311-1322.
205. Ozaslan D, Wang S, Ahmed BA, Kocabas AM, McCastlain JC, et al. (2003) Glycosyl modification facilitates homo- and hetero-oligomerization of the serotonin transporter. A specific role for sialic acid residues. J Biol Chem 278: 43991-44000.
206. Pace KE, Lee C, Stewart PL, Baum LG (1999) Restricted receptor segregation into membrane microdomains occurs on human T cells during apoptosis induced by galectin-1. J Immunol 163: 3801-3811.
207. Croze E, Ivanov IE, Kreibich G, Adesnik M, Sabatini DD, et al. (1989) Endolyn-78, a Membrane Glycoprotein Present in Morphologically Diverse Components of the Endosomal and Lysosomal Compartments - Implications for Lysosome Biogenesis. Journal of Cell Biology 108: 1597-1613.
208. Song X, Heimburg-Molinaro J, Smith DF, Cummings RD (2011) Derivatization of free natural glycans for incorporation onto glycan arrays: derivatizing glycans on the microscale for microarray and other applications (ms# CP-10-0194). Curr Protoc Chem Biol 3: 53-63.
209. Ingham PW (2009) The power of the zebrafish for disease analysis. Hum Mol Genet 18: R107-112.
210. Spence R, Gerlach G, Lawrence C, Smith C (2008) The behaviour and ecology of the zebrafish, Danio rerio. Biol Rev Camb Philos Soc 83: 13-34.
211. Ebarasi L, Oddsson A, Hultenby K, Betsholtz C, Tryggvason K (2011) Zebrafish: a model system for the study of vertebrate renal development, function, and pathophysiology. Curr Opin Nephrol Hypertens 20: 416-424.

212. Amsterdam A, Hopkins N (2006) Mutagenesis strategies in zebrafish for identifying genes involved in development and disease. Trends Genet 22: 473-478.
213. Summerton J, Weller D (1997) Morpholino antisense oligomers: design, preparation, and properties. Antisense Nucleic Acid Drug Dev 7: 187-195.
214. Bedell VM, Westcot SE, Ekker SC (2011) Lessons from morpholino-based screening in zebrafish. Brief Funct Genomics 10: 181-188.
215. Bill BR, Petzold AM, Clark KJ, Schimmenti LA, Ekker SC (2009) A primer for morpholino use in zebrafish. Zebrafish 6: 69-77.
216. Hardy S, Legagneux V, Audic Y, Paillard L (2010) Reverse genetics in eukaryotes. Biol Cell 102: 561-580.
217. Wingert RA, Davidson AJ (2008) The zebrafish pronephros: a model to study nephron segmentation. Kidney Int 73: 1120-1127.
218. Drummond IA (2000) The zebrafish pronephros: a genetic system for studies of kidney development. Pediatr Nephrol 14: 428-435.
219. Wingert RA, Selleck R, Yu J, Song HD, Chen Z, et al. (2007) The cdx genes and retinoic acid control the positioning and segmentation of the zebrafish pronephros. PLoS Genet 3: 1922-1938.
220. Lieschke GJ, Currie PD (2007) Animal models of human disease: zebrafish swim into view. Nat Rev Genet 8: 353-367.
221. Cianciolo Cosentino C, Roman BL, Drummond IA, Hukriede NA (2010) Intravenous microinjections of zebrafish larvae to study acute kidney injury. J Vis Exp.
222. Hentschel DM, Park KM, Cilenti L, Zervos AS, Drummond I, et al. (2005) Acute renal failure in zebrafish: a novel system to study a complex disease. Am J Physiol Renal Physiol 288: F923-929.
223. Tang J, Zhang L, She X, Zhou G, Yu F, et al. (2012) Inhibiting CD164 Expression in Colon Cancer Cell Line HCT116 Leads to Reduced Cancer Cell Proliferation, Mobility, and Metastasis in vitro and in vivo. Cancer Invest.
224. Jones J, Otu H, Spentzos D, Kolia S, Inan M, et al. (2005) Gene signatures of progression and metastasis in renal cell cancer. Clin Cancer Res 11: 5730-5739.
225. Eitner F, Cui Y, Hudkins KL, Alpers CE (1998) Chemokine receptor (CXCR4) mRNA-expressing leukocytes are increased in human renal allograft rejection. Transplantation 66: 1551-1557.
226. Togel F, Isaac J, Hu Z, Weiss K, Westenfelder C (2005) Renal SDF-1 signals mobilization and homing of CXCR4-positive cells to the kidney after ischemic injury. Kidney Int 67: 1772-1784.
227. Swanhart LM, Cosentino CC, Diep CQ, Davidson AJ, de Caestecker M, et al. (2011) Zebrafish kidney development: basic science to translational research. Birth Defects Res C Embryo Today 93: 141-156.
228. Drummond IA, Davidson AJ (2010) Zebrafish kidney development. Methods Cell Biol 100: 233-260.
229. Altschuler Y, Kinlough CL, Poland PA, Bruns JB, Apodaca G, et al. (2000) Clathrin-mediated endocytosis of MUC1 is modulated by its glycosylation state. Mol Biol Cell 11: 819-831.
230. Doyonnas R, Yi-Hsin Chan J, Butler LH, Rappold I, Lee-Prudhoe JE, et al. (2000) CD164 monoclonal antibodies that block hemopoietic progenitor cell adhesion and proliferation interact with the first mucin domain of the CD164 receptor. J Immunol 165: 840-851.

231. Devonald MA, Smith AN, Poon JP, Ihrke G, Karet FE (2003) Non-polarized targeting of AE1 causes autosomal dominant distal renal tubular acidosis. Nat Genet 33: 125-127.
232. Miller RJ, Banisadr G, Bhattacharyya BJ (2008) CXCR4 signaling in the regulation of stem cell migration and development. J Neuroimmunol 198: 31-38.
233. Floege J, Smeets B, Moeller MJ (2009) The SDF-1/CXCR4 axis is a novel driver of vascular development of the glomerulus. J Am Soc Nephrol 20: 1659-1661.
234. Lu BC, Cebrian C, Chi X, Kuure S, Kuo R, et al. (2009) Etv4 and Etv5 are required downstream of GDNF and Ret for kidney branching morphogenesis. Nat Genet 41: 1295-1302.
235. Ueland J, Yuan A, Marlier A, Gallagher AR, Karihaloo A (2009) A novel role for the chemokine receptor Cxcr4 in kidney morphogenesis: an in vitro study. Dev Dyn 238: 1083-1091.
236. Vasilyev A, Drummond IA (2010) Fluid flow and guidance of collective cell migration. Cell Adh Migr 4: 353-357.
237. Vasilyev A, Liu Y, Mudumana S, Mangos S, Lam PY, et al. (2009) Collective cell migration drives morphogenesis of the kidney nephron. PLoS Biol 7: e9.
238. Perlin JR, Talbot WS (2007) Signals on the move: chemokine receptors and organogenesis in zebrafish. Sci STKE 2007: pe45.
239. Knaut H, Werz C, Geisler R, Nusslein-Volhard C, Tubingen Screen C (2003) A zebrafish homologue of the chemokine receptor Cxcr4 is a germ-cell guidance receptor. Nature 421: 279-282.
240. Valentin G, Haas P, Gilmour D (2007) The chemokine SDF1a coordinates tissue migration through the spatially restricted activation of Cxcr7 and Cxcr4b. Curr Biol 17: 1026-1031.
241. Chong SW, Nguyet LM, Jiang YJ, Korzh V (2007) The chemokine Sdf-1 and its receptor Cxcr4 are required for formation of muscle in zebrafish. BMC Dev Biol 7: 54.
242. de Groh ED, Swanhart LM, Cosentino CC, Jackson RL, Dai W, et al. (2010) Inhibition of histone deacetylase expands the renal progenitor cell population. J Am Soc Nephrol 21: 794-802.
243. Rodriguez-Boulan E, Musch A (2005) Protein sorting in the Golgi complex: shifting paradigms. Biochim Biophys Acta 1744: 455-464.
244. Bonilha VL, Marmorstein AD, Cohen-Gould L, Rodriguez-Boulan E (1997) Apical sorting of influenza hemagglutinin by transcytosis in retinal pigment epithelium. J Cell Sci 110 (Pt 15): 1717-1727.
245. Matter K, Brauchbar M, Bucher K, Hauri HP (1990) Sorting of endogenous plasma membrane proteins occurs from two sites in cultured human intestinal epithelial cells (Caco-2). Cell 60: 429-437.
246. Le Bivic A, Quaroni A, Nichols B, Rodriguez-Boulan E (1990) Biogenetic pathways of plasma membrane proteins in Caco-2, a human intestinal epithelial cell line. J Cell Biol 111: 1351-1361.
247. Breuza L, Monlauzeur L, Arsanto JP, Le Bivic A (1999) [Identification of signals and mechanisms of sorting of plasma membrane proteins in intestinal epithelial cells]. J Soc Biol 193: 131-134.
248. Slaughter BD, Li R (2010) Toward quantitative "in vivo biochemistry" with fluorescence fluctuation spectroscopy. Mol Biol Cell 21: 4306-4311.
249. Chen Y, Muller JD, So PT, Gratton E (1999) The photon counting histogram in fluorescence fluctuation spectroscopy. Biophys J 77: 553-567.

250. Ormerod MG (1997) Analysis of cell proliferation using the bromodeoxyuridine/Hoechst-ethidium bromide method. Methods Mol Biol 75: 357-365.
251. Watanabe M, Hitomi M, van der Wee K, Rothenberg F, Fisher SA, et al. (2002) The pros and cons of apoptosis assays for use in the study of cells, tissues, and organs. Microsc Microanal 8: 375-391.
252. Rodriguez LG, Wu X, Guan JL (2005) Wound-healing assay. Methods Mol Biol 294: 23-29.
253. Han X, Aslanian A, Yates JR, 3rd (2008) Mass spectrometry for proteomics. Curr Opin Chem Biol 12: 483-490.
254. Watt SM, Butler LH, Tavian M, Buhring HJ, Rappold I, et al. (2000) Functionally defined CD164 epitopes are expressed on CD34(+) cells throughout ontogeny but display distinct distribution patterns in adult hematopoietic and nonhematopoietic tissues. Blood 95: 3113-3124.
255. Wada J, Ota K, Kumar A, Wallner EI, Kanwar YS (1997) Developmental regulation, expression, and apoptotic potential of galectin-9, a beta-galactoside binding lectin. J Clin Invest 99: 2452-2461.
256. Zuber C, Paulson JC, Toma V, Winter HC, Goldstein IJ, et al. (2003) Spatiotemporal expression patterns of sialoglycoconjugates during nephron morphogenesis and their regional and cell type-specific distribution in adult rat kidney. Histochem Cell Biol 120: 143-160.